Application of high-resolution membrane capacitance measurements in the study of exocytosis and endocytosis in *Saccharomyces cerevisiae*

TECHNISCHE UNIVERSITÄT DARMSTADT

Vom Fachbereich Biologie der Technischen Universität Darmstadt
zur Erlangung des akademischen Grades
eines Doctorum rerum naturalium
genehmigte Dissertation von
Diplom-Biologin Lucia Carrillo
aus Freiburg im Breisgau

Berichterstatter: Prof. Dr. Adam Bertl
Mitberichterstatter: Prof. Dr. Gerhard Thiel

Eingereicht am: 02.09.2015
Mündliche Prüfung am: 27.11.2015

Darmstadt 2015

D17

„Nur wenige wissen, wie viel man wissen muss, um zu wissen, wie wenig man weiß.“

Werner Heisenberg (1901-1976)

1. Table of contents

1.....Table of contents i

2.....Abstract 1

3.....Zusammenfassung 2

4.....Introduction 4

4.1. Secretory pathway in yeast 4

4.2. Mechanism of vesicle targeting and fusion: the final steps of exocytosis 6

4.3. Fusion pores 9

4.4. Endocytosis in yeast 10

4.5. Fission mechanism of endocytotic vesicles 12

4.6. Plasma membrane of yeast cells 13

4.7. Capacitance measurements in the study exo- and endocytotic events 14

4.8. Aim of the research: application of capacitance measurements in the study of vesicle fission and fusion in yeast cells 15

5.....Material and methods 17

5.1. Yeast strain and culture conditions 17

5.2. Protoplast preparation 17

5.3. Growth of isolated protoplasts 17

5.4. Uptake of fluorescent beads 18

5.5. Uptake of FM4-64 18

5.6. Growth assay 18

5.7. Localization of Tok1-GFP 19

5.8. Evaluation of CLSM data 19

5.9. Electron microscopy 20

5.10. Electrophysiology 21

5.10.1. The fundamental principles of capacity measurements 21

5.10.2. Whole-cell vs. cell-attached configuration: 25

5.10.3. Fusion pores analysis: the equivalent circuit of fusion pores 27

5.10.4. Experimental conditions 30

5.10.5. Data analysis 30

6.....Results and discussion 35

6.1. Growth of yeast protoplasts 35

6.2. Internalization of FM4-64 41

6.3. Internalization of fluorescent beads 45

6.4. Spontaneous changes in membrane capacitance 46

6.4.1. Modes of exo- and endocytosis in yeast 46

6.4.2. Frequencies of exo- and endocytotic events 51

6.4.3. Energy requirement of exo- and endocytosis in yeast protoplasts 53

6.4.4. Vesicle size distribution 55

6.5. Fusion pores in yeast cells 57

6.6. Modulation of exo- & endocytotic frequencies via the SY1 *sec6-4* mutant 61

7.....Conclusions 69

8.....References 70
9.....List of Equations 80
10. ..List of Figures 81
11. ..Abbreviations 84
12. ..Acknowledgements 88
13. ..Ehrenwörtliche Erklärung 89
14. ..Own Work 90
15. ..Curriculum Vitae 91

2. Abstract

High resolution cell-attached patch-clamp recordings are used to analyze the kinetics of exo- and endocytosis in yeast. This technique is based on the fact that physical properties of cell membranes are comparable to the properties of a RC-circuit, consisting of a resistor and a capacitor in parallel. This means that changes in the plasma membrane surface, resulting from fusion and fission of vesicles, can be measured as changes in the membrane capacitance. Application of cell-attached patch-clamp recordings to *Saccharomyces cerevisiae* facilitates detection of exo- and endocytotic events, as discrete changes in the membrane capacitance at high temporal and spatial resolution. The results show four different kinetic modes of exo- and endocytosis in yeast, which were already reported from other eukaryotes. These modes include transient and permanent fusion and fission of vesicles. The measured capacitance changes were predominantly in the range of 0.2 - 1 fF, which corresponds to vesicle diameters of 90 - 200 nm. The vesicle size distribution showed a median of about 132 nm for endocytotic and 155 nm for exocytotic vesicles. Under well-defined nutrient conditions endocytotic and exocytotic events occurred at frequencies of 8.1 and 12.3 events per hour, respectively. In comparison, protoplasts deprived of glucose showed lower frequencies with nearly four events/h for exocytotic, and two events/h for endocytotic events. This result indicates energy requirement for exo- and endocytosis in yeast. Via capacitance measurements it was feasible to examine exo- and endocytosis frequencies, to determine vesicle sizes and to detect fusion pores in yeast cells. Because of the latter it was also possible to establish a rough classification of fusion pores conductance and diameters.

A temperature sensitive SEC mutant *sec6-4* inhibited in the secretory pathway revealed a direct relationship between recorded capacitance changes in the plasma membrane and exocytotic events. In this context cells of the aforementioned mutant were incubated at the restrictive temperature of 37 °C resulting in an accumulation of vesicles in the cytosol. After incubation 71.6 exocytotic and 16 endocytotic events/h were measured. As a control sample, cells were incubated at the permissive temperature of 25 °C. The measured frequencies were comparable to the reference strain BY4741, which results in 15.1 events/h for exocytotic and 9.2 events/h for endocytotic events. This demonstrates that event frequencies can be modulated.

Through this study it was possible to demonstrate that capacity measurements can be applied to yeast cells for the detection of single fission and fusion events. Analyses on yeast protoplasts suggest that this system can be used for the investigation of exo- and endocytosis via capacity measurements. This provides a new tool for analyzing both processes in yeast.

3. Zusammenfassung

Hochauflösende cell-attached Patch-Clamp Kapazitätsmessungen werden zum ersten Mal verwendet, um Exo- und Endozytose in Hefe zu untersuchen. Biologische Plasmamembranen haben ähnliche Eigenschaften wie Kondensatoren, deshalb weisen diese eine bestimmte Kapazität auf, die anhand der Patch-Clamp Technik bestimmt werden kann. Da die Kapazität eines Kondensators/biologischen Membran von der Oberfläche abhängt, kann man Veränderungen an der Plasmamembranoberfläche, die bespielweise durch Fusion oder Abschnürung von Vesiklen verursacht werden, als Änderungen in der Kapazität messen. Bei Anwendung von cell-attached Patch-Clamp Messungen an *Saccharomyces cerevisae* war es möglich einzelne exo- und endozytotische Ereignisse als Änderungen in der Plasmamembrankapazität, mit hoher zeitlicher und räumlicher Auflösung, zu detektieren. Die Ergebnisse zeigen vier unterschiedliche kinetische Typen von exo- und endozytotischen Ereignissen auf, welche ebenfalls in Eukaryoten beobachtet werden können. Sie können in transiente und permanente endo- und exozytotischen Ereignissen eingeteilt werden. Die gemessenen Kapazitätsänderungen liegen im Bereich von 0.2 - 1 fF, welche umgerechnet Vesikeldurchmesser im Größenbereich von ca. 90 - 200 nm entsprechen. Der Median der Vesikelverteilungen liegt bei ca. 132 nm für endozytotische und bei 155 nm für exozytotische Vesikel. Bei guten Nährstoffbedingungen beträgt die Frequenz 8.1 Ereignisse pro Stunde für Endozytose und 12.3 Ereignissen pro Stunde für Exozytose. Auch wenn diese Frequenzen etwas niedrig erscheinen, stimmen sie gut mit den gemessenen Daten in Hefezellen und -protoplasten überein. Protoplasten, die ohne Glukose inkubiert wurden, weisen niedrigere Frequenzen auf mit 3.8 exozytotische und zwei endozytotische Ereignisse pro Stunde. Das zeigt, dass die Protoplasten Energie für die Prozesse von Exo- und Endozytose benötigen. Darüber hinaus können neben der Bestimmung von Vesikelgrößen und der Ereignisfrequenzen, auch Fusionsporen in Hefen gemessen werden und eine grobe Einteilung der Leitfähigkeiten und der Porengrößen vorgenommen werden.
Weitere Untersuchungen werden anhand einer Temperatursensitiven Mutante *sec6-4* des Hefestamms SY1 durchgeführt. Durch die Mutation wird der sekretorische Weg, bei einer Inkubationstemperatur von 37 °C, inhibiert. Ziel war es, einen direkten Zusammenhang zwischen exozytotischen Ereignissen und gemessene Kapazitätsänderungen herzustellen. In diesem Zusammenhang werden die Zellen dieser Mutante bei einer einschränkenden Temperatur von 37 °C für drei Stunden inkubiert, um Vesikel im Zytosol akkumulieren zu können. Danach wurden die Zellen bei Zimmertemperatur gemessen. Pro Stunde konnten 71.6 exozytotische Ereignisse und 16 endozytotische Ereignisse gemessen werden. Als Kontrolle wurden die Zellen ebenfalls für drei Stunden bei einer nicht-einschränkenden Temperatur von 25 °C, bei der der sekretorische Weg nicht inhibiert ist, inkubiert und gemessen. Bei dieser Temperatur wurden pro Stunde 15.1 exozytotische und 9.2 endozytotische Ereignisse, ähnlich zum Referenzstamm BY4741, gemessen. Diese

Ergebnisse demonstrieren, dass die Frequenzen anhand von Mutationen im sekretorischen oder endozytotischen Weg moduliert werden können.

In dieser Arbeit konnte die Methode der Kapazitätsmessungen für die Untersuchung von Exo- und Endozytose an Hefe etabliert werden. Es war zum ersten Mal möglich einzelne Vesikel in Echtzeit in Hefe aufzulösen und deren Durchmesser zu bestimmen. Außerdem konnte man auch zum ersten Mal Fusionsporen von Vesikeln in Hefe untersuchen und den Fusionsporendurchmesser bestimmen. Mit den Untersuchungen konnte gezeigt werden, dass Hefe Protoplasten ein geeignetes System für die Untersuchung von Exo- und Endozytose durch Kapazitätsmessungen sind. Dies stellt eine weitere Untersuchungsmöglichkeit für beide Prozesse in Hefe dar.

4. Introduction

In eukaryotic cells exo- and endocytosis are crucial processes participating in numerous physiological functions like polar growth, cell division, signaling and motility (Grote *et al*., 2000; Sedwick, 2009; Delic *et al*., 2013). The major tasks of exo- and endocytosis include secretory vesicle cargo release, delivery of membrane resident proteins to the plasma membrane, uptake of external solutes and membrane recycling (Wu *et al*., 2014). In addition, the ratio of exo- and endocytosis determines the size of the membrane surface area. Both processes are highly regulated and can be divided in different sub-steps. Yeast cells have proved a useful model for the study of endo- and exocytosis. A key step in advancing the understanding of both phenomena was the utilization of yeast mutants for molecular analysis of proteins involved in the fusion/fission processes (Novick & Scheckman, 1979). Major advantages of yeast cells are straightforward cultivation, short generation times, easy genetic manipulation and their close similarities to other eukaryotic cells regarding comparable sets of proteins (Zanetti *et al*., 2012), analogous cell processes and gene homology (Finger & Novick, 1998b). Yeast, therefore provide a useful tool for the advancement of insight into diseases based on the dysfunction of exo- or endocytosis, e.g., Alzheimer's, Parkinson's, diabetes mellitus, atherosclerosis and ischemia, as well as liver and heart diseases (Yoshida, 2007). Delineating the parallels in the endo- and exocytotic pathways between yeast and mammalian cells would allow application of new discoveries from one system to the other and, thus, filling the persisting knowledge gaps.

4.1. Secretory pathway in yeast

The initial step of the secretory pathway is the transfer of a protein through the membrane of the endoplasmatic reticulum (ER) or the incorporation of proteins into the ER membrane, in the case of membrane proteins (Delic *et al.*, 2013). Translocation of proteins can occur co-translationally (ribosome-coupled) or post-translationally (ribosome-uncoupled) depending on the signal peptide of the protein (Zimmermann *et al.*, 2011). This step is followed by protein folding, glycosylation and maturation in the ER (Delic *et al*., 2013). Correctly folded proteins bud from the ER as vesicles coated by cytoplasmic coat protein complex II (COPII) and are transported to the cis-Golgi (Dancourt & Barlowe, 2010; Zanetti *et al*., 2012). Some proteins are further glycosylated in the Golgi and remain in the cisterna during maturation, to be finally transported to the target compartment (Malhotra & Mayor, 2006; Dancourt & Barlowe, 2010). From the trans-Golgi network (TGN) vesicles are carried along actin cables to the plasma membrane or to the vacuole. The process finishes with vesicle docking and fusion with the target membrane (Hou *et al*., 2012; Fig. 1). During the fusing process soluble *N* -ethylmaleimide–sensitive fusion protein attachment protein receptors (SNARE proteins) are involved in the merging of the membranes (Ferro-Novick & Jahn, 1994; Rothman & Warren, 1994). SNAREs

are proteins located at target membranes (t-SNAREs) and at vesicle membranes (v-SNARES). When vesicles dock at a target membrane, v-SNAREs interact with t-SNAREs, facilitating fusion of the vesicle with the target membrane (Finger & Novick, 1998b).

The process of exocytosis can occur in a constitutive or non-constitutive manner (Kelly, 1985). The latter is observed when large amounts of proteins are released in a short period of time and at a high rate. This kind of secretion is triggered by a cytoplasmic messenger, and termed regulated exocytosis (Kelly, 1985). The change of the intracellular calcium concentration has become generally accepted as a crucial parameter in regulated exocytosis (Katz 1969; Llinás & Heuser 1977; Kelly, 1985). In course of the process in question, vesicles accumulate near the plasma membrane and fuse with it in response to a triggering stimulus. In contrast, during constitutive exocytosis, vesicles do not accumulate in the cytosol in large numbers and fuse with the plasma membrane soon after being formed at the Golgi-apparatus. Constitutive exocytosis is insensitive to changes in the cytosolic calcium concentration (Lew & Simon, 1991).

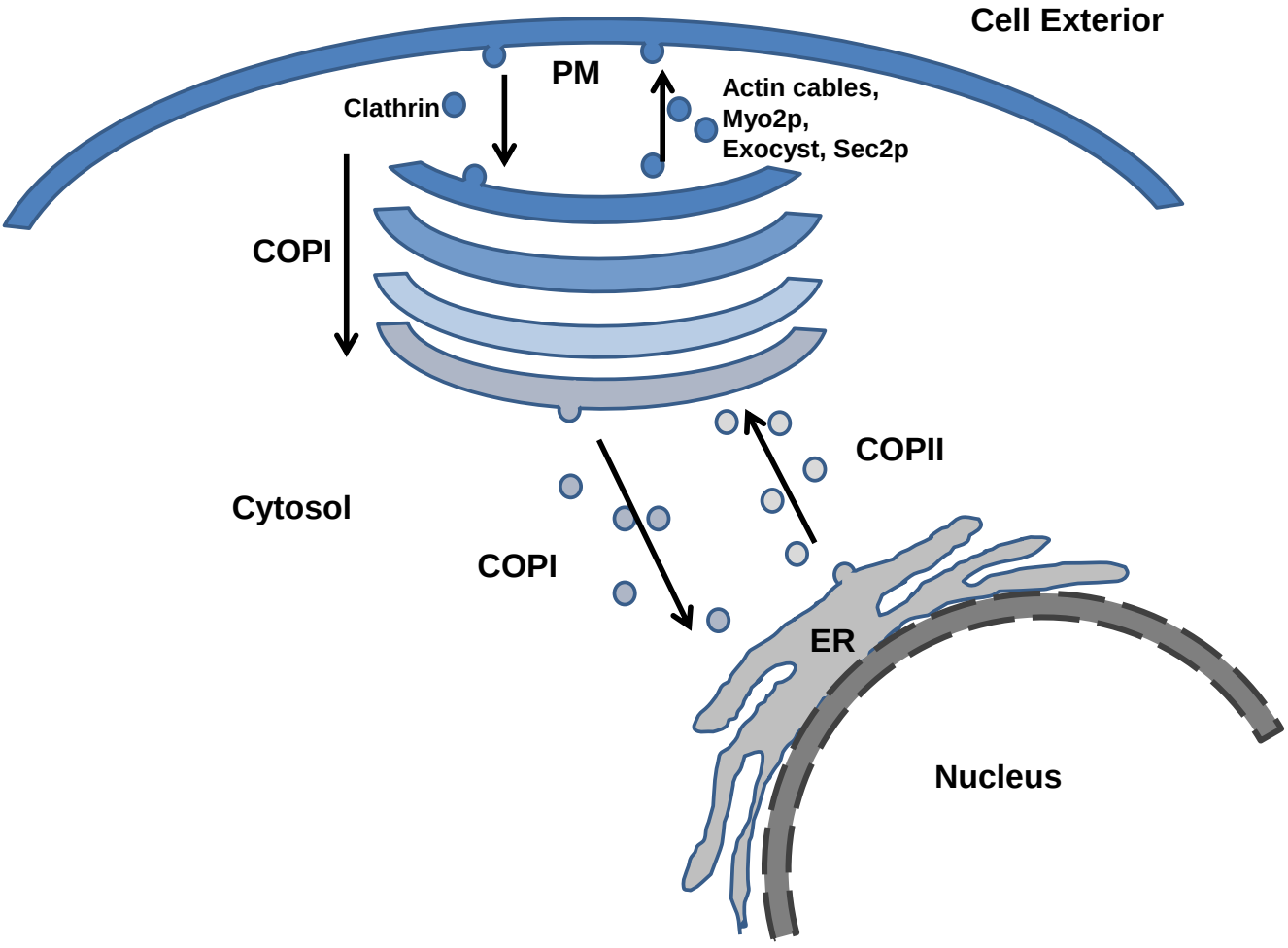

Figure 1: An overview of the secretory and retrograde pathway in yeast cells.

Newly synthesized and folded proteins are transported from the ER to the *cis*-Golgi through COPII vesicles via the secretory pathway. Membrane proteins are incorporated into the vesicle membrane and transported by vesicles to their target membrane. COPI vesicles are responsible for the retrograde transport to the *cis*-Golgi and the ER. In the ER and in the Golgi proteins are marked by glycosylation for the target membrane. Most of the synthesized proteins remain in the cell interior. Those which are destined for secretion are packed into secretory vesicles and transported from the TGN to the plasma membrane via actin cytoskeleton and actin associated proteins (Adapted from Delic *et al*., 2013).

4.2. Mechanism of vesicle targeting and fusion: the final steps of exocytosis

The secretory pathway delivers newly synthesized proteins and lipids to the plasma membrane. This involves several vesicle fusion and fission events to transport cargo within the cell. Each fission and fusion are comprised of several steps and different sets of proteins depending on the cell compartment (e.g. from ER to Golgi or from TGN to plasma membrane; Delic *et al*., 2013). Finally, the

vesicle is transported and tethered to the target membrane, which results in fusion of these membranes.

In recent decades, identification of specific temperature-sensitive *sec* mutants has provided a tool for the detection of molecular components involved in membrane trafficking in yeast (Novick *et al*., 1980). These mutants offered the possibility to study constitutive exocytosis in an alternative manner, facilitating determination of the final sub-steps of vesicle transport and docking, prior to the fusing process (Novick & Scheckman, 1979; Novick *et al*., 1980). It was observed that some of the *sec* mutants, e.g. *sec6-4* mutant, accumulate secretory vesicles in the cytosol at restrictive temperature. It was, therefore, deduced that the mutated Sec proteins are late-acting factors in the secretory pathway during the fusion of post-Golgi vesicles with the plasma membrane (Finger & Novick, 1998b; Grote *et al.*, 2000; Brennwald & Rossi, 2007). In the following passage, the function of the mentioned Sec proteins is explained. Yeast secretory vesicles coming from the trans-Golgi network are transported along actin cables to the plasma membrane e.g. to a nascent bud tip of a daughter cell. For vesicle transport Sec2p is required as the nucleotide exchanging factor for Sec4p, a rab family GTPase (Walch-Solimena *et al.*, 1997). Activation of Sec4p promotes myosin (Myo2)-dependent transport of vesicles to the secretory sites (Govindan *et al*., 1995; Finger & Novick, 1998b; Schott *et al*., 1999). Vesicle docking at the specific sites is performed by a large protein complex termed exocyst, consisting of eight proteins, six late-acting proteins (Sec3p, Sec5p, Sec6p, Sec8p, Sec10p and Sec15p) and two additional proteins, Exo70p and Exo84p, which are essential for the fusion process (TerBush & Novick, 1995; TerBush *et al*., 1996; Fig. 2). Tethering of a vesicle is mediated by the assembly of the exocyst initiated by Sec15 protein binding to Sec4 protein on the secretory vesicle (Guo *et al.*, 1999). After docking, the remaining components of the protein complex are recruited. Sec3 protein, another component of the exocyst, is a spatial landmark for exocytosis that defines the sites for polarized secretion. This component is localized in the plasma membrane, even in the absence of exocytosis (Finger & Novick, 1998a). The assembly of the exocyst may be essential for vesicle tethering at the plasma membrane (Grote *et al*., 2000).

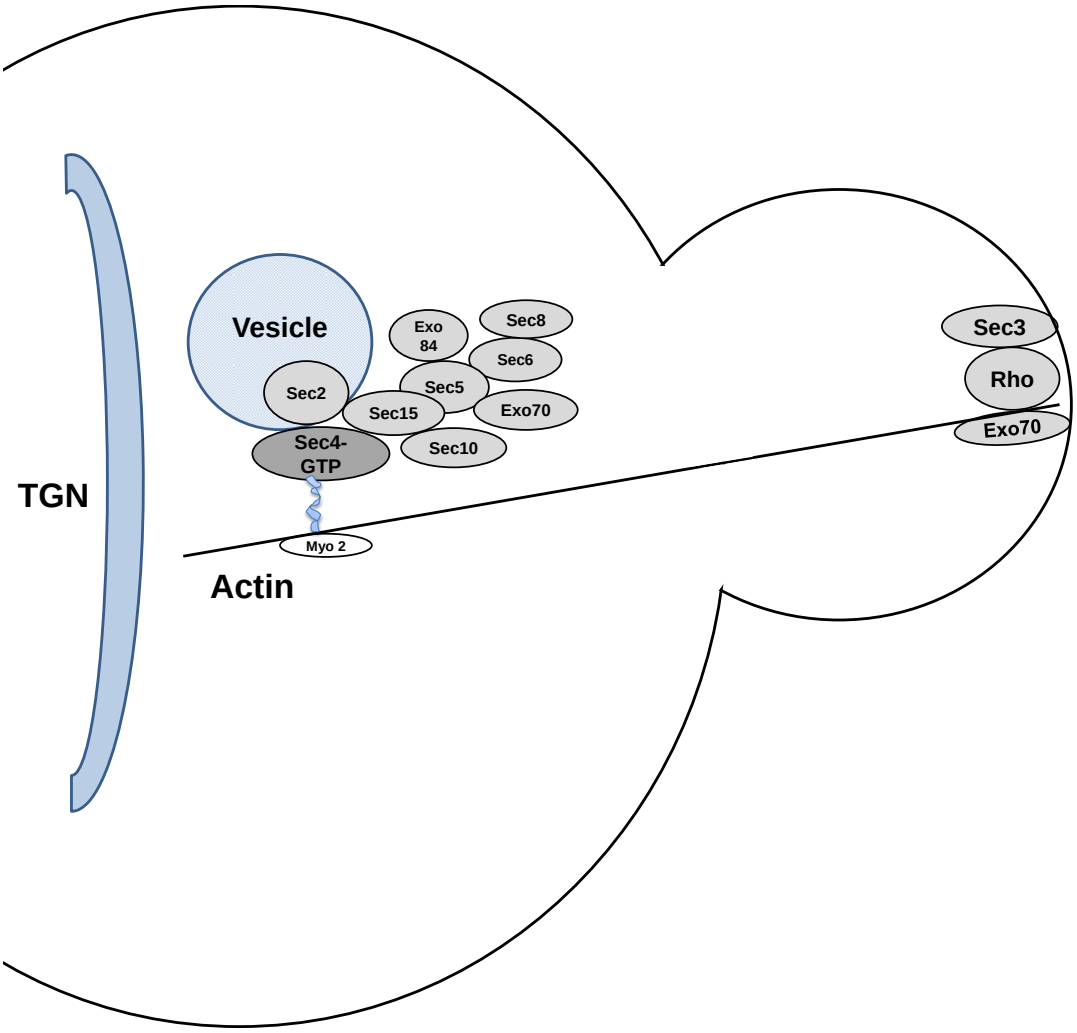

Figure 2: An overview of the transport components of secretory vesicles that are carried from the TGN to the plasma membrane.

The most important proteins that interact in this final pathway are the actin cytoskeleton, actin associated proteins (like Myo2) and the protein complex called the exocyst consisting of eight subunits (Sec3p, Sec5p, Sec6p, Sec8p, Sec10p, Sec15p, Exo70p and Exo84p). These proteins are also involved in the docking and tethering process (adapted from Guo *et al*.,1999).

After vesicle docking, vesicle fusion finishes the process of exocytosis. For the fusion step SNAREs, Sec1 and Sec18 proteins are necessary to merge the membranes. The SNARE proteins are required in all fusion steps of intracellular transport (Ferro-Novick and Jahn, 1994). In yeast the SNARE proteins are termed as Snc proteins incorporated in secretory vesicles (v-SNAREs) and Sso/Sec9 proteins, which are located in the plasma membrane (t-SNAREs; Aalto *et al*., 1993; Protopopov *et al*., 1993; Brennwald *et al*., 1994). In each membrane SNARE proteins are integrated for the fusion process. In yeast the Snc proteins are encoded by the *SNC1* and *SNC2* genes and the Sso proteins by the *SSO1* and *SSO2* genes. Structural and biochemical data propose that the SNARE complex functions as a passive catalyst to merge the vesicle membrane with the target membrane during the

fusion process. V-SNAREs and t-SNAREs act as anchoring proteins, helping to bring both membranes together. During this process a fusion pore is formed (Delic *et al*., 2013). Another important protein is Sec1, which binds to the assembled SNARE complexes but not to free SNARE proteins (Carr *et al*., 1999). Sec1 protein probably plays a role in SNARE protein assembly, while Sec18 protein appears to be responsible for the disassembly of the SNARE complexes. The latter was demonstrated in a *sec18-1* mutant that accumulates Snc protein complexes in the plasma membrane (Grote *et al*., 2000).

4.3. **Fusion pores**

During the final step of exocytosis an aqueous channel, the fusion pore, is formed and the vesicle content is released to the extracellular space. Fusion pores provide a link between the vesicular lumen and the extracellular compartment. In higher eukaryotes, they may play a key role in neurotransmitter and hormone release and therefore in cell communication (Lindau & Alvarez de Toledo, 2003; Jorgacevski *et al*., 2011). In yeasts, cell communication is observed in the context of the mating process, with cells of opposite mating types responding to pheromones secreted by their counterparts (α - or a- factor; Manfredi *et al.*, 1996). In general, the releasing process can be extremely rapid, reaching times of less than 100 µs (Lindau & Alvarez de Toledo, 2003). Depending on the fate of the fusion pore two types of exocytosis can be distinguished (Jorgacevski *et al.*, 2012). Full-fusion exocytosis is characterized by the complete incorporation of a vesicle into the plasma membrane (Heuser & Reese, 1973). This kind of exocytosis has short-lived fusion pores, which are difficult to detect or measure because of their negligible resistance. The other type of exocytosis is termed transient exocytosis (Ceccarelli *at al*., 1973; Neher & Marty, 1982) or “kiss-and-run” exocytosis (Henkel and Betz, 1995). This type is characterized by reversible vesicle fusion, which means that a vesicle docks with the membrane for a short time and removes again. The physiological relevance of transient exocytosis is still under discussion (LoGiudice & Matthews, 2006). The process of vesicle fusion namely the transition of none-fused vesicles to fused vesicles is associated with a loss of energy (Liu & Parpura, 2010). On the other side the process of vesicle fission is also coupled with energy consumption (Schmid & Carter, 1990; Heidelberger, 2001, Liu *et al.*, 2009). From an energetic point of view it is unlikely that transient events represent a full vesicle cycle (exocytosis followed by endocytosis). It is more likely, that transient events represent one vesicle docking to the membrane and leaving again. Thus, repetitive transient events are probably the flickering of one and the same vesicle and at the same time repetitive fusion pore openings can be measured (Debus & Lindau, 2000; Jorgacevski *et al.*, 2012). This observation modified the first assumption that fusion pores are short-lived intermediates during full-fusion (permanent fusion) exocytosis and that the release of vesicle cargo follows an all-or-nothing event (Kabaso *et al*., 2013). These so-called “pulsing pores” with repetitive opened and closed states (Stenovec *et al*., 2004; Fernandez *et al.*, 1984) suggest that

fusion pores are structures that have to be stabilized (Jorgacevski *et al*., 2012). The fact that different fusion pore diameters can be measured indicates that fusion pores are probably structures which have to be stabilized (Heuser & Reese, 1973; Jorgacevski *et al*., 2012). This raises the question how fusion pores are stabilized. The stability is probably obtained by different properties of the membrane that include e.g. the shape of lipids, proteins of membrane area and/or the interaction between both. This question is discussed in more detail by Jorgacevski J. *et al*., 2012. However, established narrow fusion pores seem to be energetically favorable for the fusion process (Jorgacevski *et al*., 2010). The release of vesicle cargo through the fusion pores can be controlled by two parameters, the dwell-time (the time during fusion pore is formed) and the diameter of the fusion pore (Vardjan *et al*., 2007). These two parameters are different in stimulated cells or in resting cells (Vardjan *et al*., 2007). For example 53 % of the fusing events in resting anterior pituitary lactotroph cells, which secret the hormone prolactin form very small fusion pores (< 0.5 nm), which results in unproductive exocytosis (no cargo release). In contrast, stimulating the cells prolongs the opening of fusion pores and expands 70 % of the initial narrow fusion pore diameter to > 1 nm in lactotrophs (Vardjan *et al*., 2007), resulting in productive exocytosis (cargo release) and fast cargo release. It is possible that a stimulus activates already fused vesicles, which have narrow fusion pore diameters to dilate and release vesicle cargo (Vardjan *et al*., 2007).

Fusion pore properties and dynamics have been the topic of numerous studies with electrochemical, fluorescence or electrophysiological methods (Lindau & Alvarez de Toledo, 2003). The patch-clamp membrane capacitance (C_m) technique allows measurements of sub-nanometer fusion pores with temporal resolution of milliseconds in living cells (Vardjan *et al*., 2007; Rituper *et al*., 2013; Chapter 5.10.3). To date, fusion pores were already analyzed in mammalian (Vardjan *et al*., 2007; Rituper *et al*., 2013) and plant cells (Bandmann *et al*., 2011) with this technique. In yeast cells fusion pores were already detected but not analyzed in detail (Carrillo *et al*., 2015).

4.4. **Endocytosis in yeast**

Endocytosis is the process of plasma membrane invagination whereby substances from the extracellular space are first absorbed into the vesicle lumen and then inside the cell. Eukaryotes need this process for nutrient uptake, regulation of cell size and membrane composition or recycling of membrane components (Liu *et al*., 2009; Wu et al., 2014; Goode *et al*., 2015). The endocytotic vesicles carry lipids, proteins, extracellular molecules and fluids into the cells interior. The internalized proteins are transported to and sorted in the early endosome, the first compartment for endocytotic vesicles. Lipids and proteins for recycling are further transported to the TGN. The degradation of lipids and proteins takes place in the late endosome (LE) or pre-vacuolar compartment (PVC). This compartment serves as a second sorting and labeling station for endocytosed material. During the sorting process the multivesicular body (MVB) is formed, which contains vacuolar proteins and also

proteins for degradation (Fig. 3). Finally the mature MVB fuses with the vacuole and releases both, proteins for degradation and proteins targeted for the vacuole into the vacuolar lumen (Shaw *et al*., 2011).

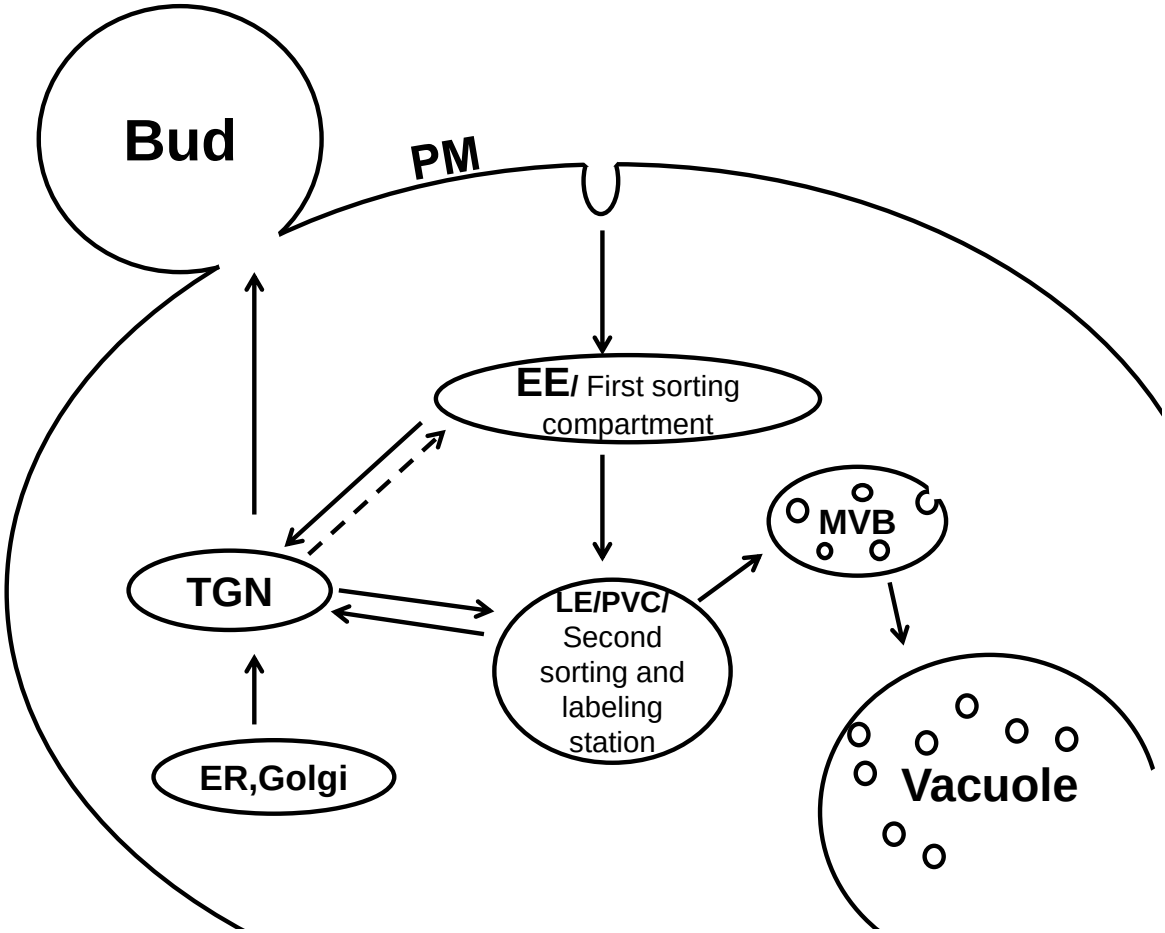

Figure 3: Overview of the endocytotic pathway in yeast.

The different protein-sorting compartments are represented by the early endosome (EE) and the late endosome (LE), which is also called pre-vacuolar compartment (PVC). The multivesicular body (MVB) consists of vesicles and proteins that are transported to the vacuole in order to be degraded. In the trans-Golgi network (TGN) proteins from the plasma membrane are recycled and transported back to the target membrane (adapted from Shaw *et al.* 2001).

The vesicle invagination is an energetically unfavorable process that lasts typically ~ 1-2 minutes in yeast. Unlike in mammalian cells, actin and actin polymerization are essential for endocytosis in yeast to overcome the high turgor pressure and membrane tension (Kaksonen *et al*., 2005). So far two types of endocytotic pathways have been described for yeast. The first discovered pathway was the clathrin-mediated endocytosis (CME; Pearse, 1976). This pathway is characterized by a clathrin-coat assembly that stabilizes the membrane curvature of the vesicle membrane and turns this energetic unfavorable process into an energetic favorable one (Liu *et al*., 2010; Weinberg and Drubin, 2012).

The coat proteins anchor and regulate actin filaments while bending the membrane (Heuser & Evans, 1980). This type of endocytosis has been extensively studied in the past in yeast and mammalian cells (Liu *et al*., 2006; Liu *et al*., 2009). Until recently yeast cells have been thought to rely solely on the CME pathway (Weinberg & Drubin, 2012). Prosser and Wendland (2012) suggested that yeast also has a clathrin-independent endocytotic pathway (CIE) as found in mammalian and plant cells. They discovered an endocytotic pathway that relies on the GTPase Rho1, suggesting that CIE does exist in yeast. Furthermore, it could be demonstrated that the Rho1-dependent endocytosis in yeast shows some similarities to the RhoA-dependent endocytosis in mammalian cells (Prosser & Wendland, 2012).

4.5. **Fission mechanism of endocytotic vesicles**

The process of vesicle fission during endocytosis is divided in several stages. A rough division of the process would be in two steps: the invagination of the cell membrane and pinching off of the endocytotic vesicle. To change the shape of the membrane, cells need strong mechanical forces that lead to a high energy loss. To resolve this problem and make the bending of the membrane possible, biochemical reactions that provide the energy are necessary. These reactions involve several protein and lipid interactions. In yeast cells, the deformation of the membrane starts with recruiting phosphoinositides ($PI(4,5)P_2$ (PiP_2)), which cover the membrane at the endocytotic site. In the second stage PIP_2 causes the recruiting of coat proteins, filamentous actin (F-actin) and myosin (Fig. 4). Actin polymerization, myosin motor activity and actin associated proteins provide the pulling force exerted on the bud for membrane invagination (Kaksonen *et al*., 2003; Jonsdottir & Li, 2004; Kaksonen *et al*., 2005; Sun *et al*., 2006). During the fission process the PIP_2 -level along the membrane invagination vary. The high levels of PIP_2 at the beginning of endocytosis help to recruit clathrin and other coat proteins at the endocytotic site where the membrane will start to bend (Sun *et al*., 2006; Sedwick *et al*., 2009). Membrane levels of PIP_2 are increased by enzymes that phosphorylate lipid precursors to generate PIP_2. Later, PIP_2 levels in the membrane must be reduced to allow coating proteins (clathrin and SlaI) to drop-off and be replaced by another set of proteins responsible for vesicle trafficking within the cell (Liu *et al*., 2009; Liu *et al*., 2010). To reduce high levels of PIP_2 membrane lipids are dephosphorylated by enzymes called phosphatases. The initial membrane curvature promotes the recruitment of BAR (Bin/Amphiphysin/Rvs) proteins domains (BDP) in yeast; that assemble in the tubule region (Liu *et al*., 2009; Liu *et al*., 2010). These proteins bind better to curved membranes and reinforce the curving process (Liu *et al*., 2010). Furthermore Liu J. and co-workers proposed that BDPs at the tubule protect the subjacent PIP_2 from hydrolysis by the phosphatase (Fig. 4). At the neck of the collar the membrane swells to form a bulb. The PIP_2 in this bulb and at the interface between the collars of the pocket is quickly dephosphorylated when the neck is strongly curved (Liu *et al*., 2009). Dephosphorylated PIP_2 takes up less space in a membrane, so that different PIP_2 levels at

collar and bulb junction create a force that acts like a noose (Liu *et al*., 2009; Liu *et al*., 2010). This noose would lead to a breakdown of the membrane at the collar/bulb interface and further to the pinching off of the bulb/vesicle (Liu *et al*., 2009; Liu *et al*., 2010). The model of Liu J. *et al.*, 2009 fits with the temporal and spatial data measured in budding yeast.

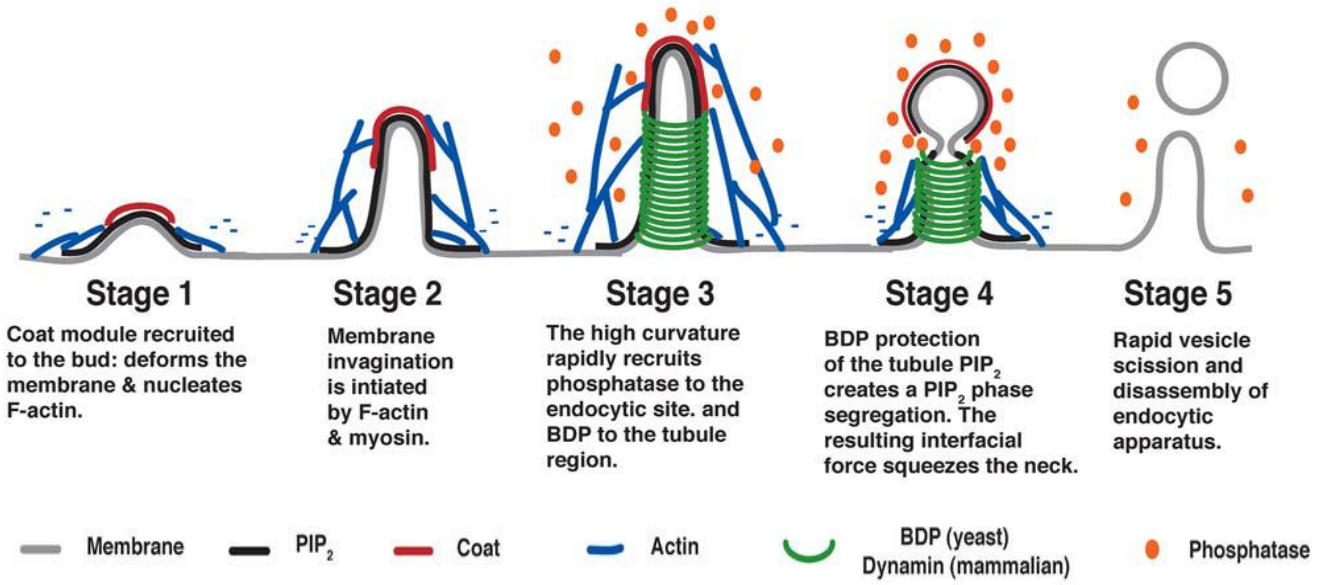

Figure 4: A model to describe the first steps of clathrin-medited endocytosis and vesicle fission (Liu *et al*., 2009).

4.6. **Plasma membrane of yeast cells**

The budding yeast *Saccharomyces cerevisiae* coordinates and regulates cell surface growth and secretion to different membrane areas at different cell cycle stages. To manage this, membranes are divided in different specialized compartments where different subsets of vesicles are delivered. A cellular membrane consists of several different lipid types. The lipid composition found in yeast membranes consists of phosphatidylcholine, phosphatidylethanolamine, phosphatidylinositol, phosphatidylserine, sphingomyelin, diacylglycerol, ergosterol, etc. (van Meer *et al*., 2008). This variety makes the plasma membrane heterogenic and thus the existence of micro domains/ lipid rafts within the membrane possible. This new form of cell membrane structure was studied in mammalian cells (Brown & London, 1998a; Brown & London, 1998b), further in fungi (Young *et al*., 2002, Malínská *et al*., 2003) and plant cells (Sutter *et al*., 2006; Homann *et al*., 2007). These micro domains or “lipid rafts” are membrane areas rich in sterols and sphingolipids that function as platforms for the attachment of proteins (Simons & Ikonen, 1997). Plasma membrane areas rich in sphingolipids and sterols are more stable than areas with less sterols and sphingolipids where phospholipids prevail. Studies in model membranes showed that sterols and sphingolipids can cluster into liquid ordered domains (Mouritsen & Jorgensen, 1997). Sphingolipid acyl chains have the ability to form tightly

packed platforms together with sterols. This compact zone of condensed bilayers has been termed the liquid-ordered state (Brown and London, 1998; Munro, 2003) and represents lipid rafts. These special membrane areas are segregation and sorting areas where proteins are incorporated specifically (Bagnat *et al*., 2001). In yeast, lipid rafts have been implicated in protein/lipid sorting and cell polarity (Bagnat & Simons, 2002). The segregation capacity of rafts also provides the basis for the polar organisation of proteins at the cell surface during the mating process (Bagnat *et al*., 2001; Bagnat & Simons, 2002).

4.7. **Capacitance measurements in the study exo- and endocytotic events**

The understanding of the dynamics of exo- and endocytosis has advanced in the past three decades thanks to the development and application of various analytical approaches. A particularly impact was made by the patch-clamp technique, modified to measure cell capacitance (Neher and Marty 1982). The method uses the fact that physical properties of cell membranes resemble *inter alia* the electrical properties of a capacitor and a resistor (Fig. 5). A capacitor is an electrostatic energy-storing device with the charge storage capacity dependent on its surface area. Consequently, the membrane capacitance depends on the cell surface area. The process of endo- and exocytosis is associated with changes in the surface area of the membrane and, thus, with changes in membrane capacitance. In other words, the membrane capacitance is proportional to the membrane surface size. Small changes in the membrane capacitance resulting from fusion or fission of vesicles are in the range of picofarad and can be measured by the membrane capacitance recording technique (Neher and Marty, 1982; Hamill *et al*., 1981; Rituper *et al*., 2013a). In the 70s Neher and Sakmann developed the patch-clamp method to demonstrate the flow of current across the plasma membrane, more specific through ion channels (Neher & Sakmann, 1976). After a successful application on cells to investigate the function of ion channels the patch-clamp technique was adapted for the recording of unitary exocytotic and endocytotic events, which were detected as discrete changes in the membrane capacitance (Hamill *et al*., 1981; Neher and Marty, 1982). Since then this technique has been further developed and became an important tool for the investigation of exo- and endocytosis in eukaryotes e.g. in mammalian cells and in plant cells (Vardjan *et al*., 2007; Bandmann *et al*., 2011; Rituper *et al*., 2013a). Capacitance measurements provide the possibility to detect events in real time, *in vivo* with a high temporal and spatial resolution. Furthermore, this technique provides detailed information on the kinetic and size of vesicles. It provides a useful tool to understand the complex kinetics of exo- and endocytosis. This made it possible for the first time, to distinguish between permanent and transient fission/fusion events and to detect fusion pores (Ceccarelli *et al*., 1972; Debus & Lindau, 2000) via changes in the membrane conductance. Capacitance measurements have also been applied to study the regulatory role of, for example, cytosolic Ca^{2+} in exocytosis (Kreft *et al*., 2004; Borisovska *et al*.,

2005; Vardjan *et al*., 2013) or to examine the function of sphingolipids (Flasker *et al*., 2013) and cholesterol during exocytosis (Rituper *et al*., 2012).

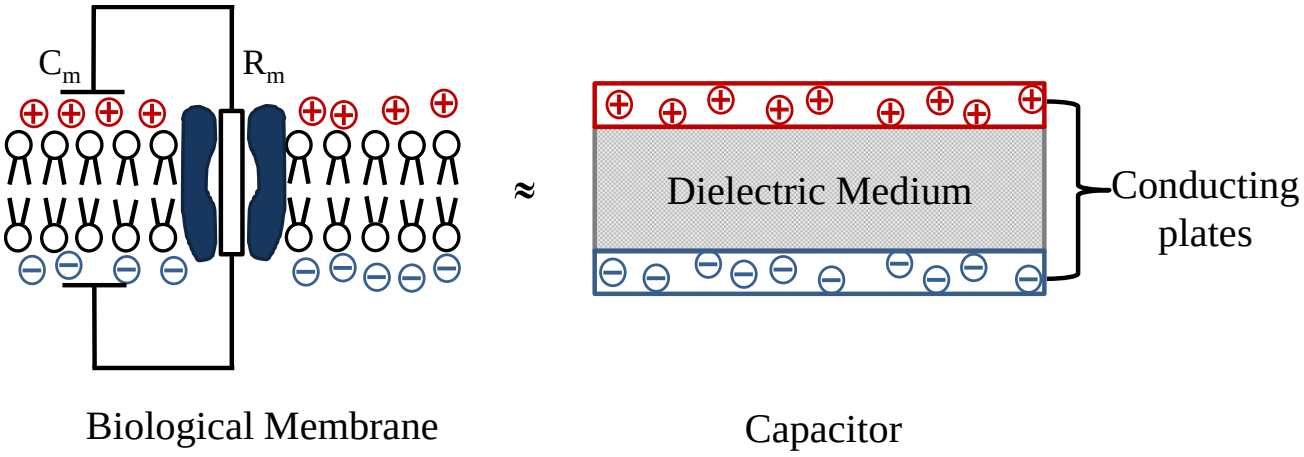

Figure 5: The equivalent circuit of a plasma membrane with a resistance (ion channel (blue)/ R_m) and a capacitance (lipid-bilayer/ C_m) compared with a plate capacitor.

Yeast has been widely used as a eukaryotic model organism to study exo- and endocytosis, but so far capacitance measurements have not been applied. The patch-clamp technique was already established 30 years ago in yeast protoplasts for the recording of ion channel activity in vacuoles and in the plasma membrane (Gustin *et al.*, 1986; Bertl & Slayman 1990; Bertl & Slayman 1992). Capacitance recordings are similar to recordings of currents through ion channels. For both methods the patch-clamp technique is applied, which can be used in different recording modes. In this work differences between the cell-attached and the whole-cell configuration are explained. With the cell-attached configuration changes in capacitance or the ohmic current of the patch underneath the pipette can be measured (Fig. 11A in chapter 5.10.2). This configuration enables the resolution of single exo- or endocytotic events in real-time. The whole-cell configuration is used to detect macroscopic changes in the membrane capacitance of the cell or to measure the ohmic current of the entire membrane (Fig. 11B in chapter 5.10.2). This is described in more detail in chapter 5.10.2. To date capacitance measurements have not been applied to yeast cells.

4.8. Aim of the research: application of capacitance measurements in the study of vesicle fission and fusion in yeast cells

Yeast has become a pioneer organism to study the function of individual genes and proteins, as well as their interactions in order to understand cell processes and properties of eukaryotes (Botstein & Fink, 2011). Especially in context with the physiological processes of exo-/endocytosis and vesicle trafficking, yeast cells have provided a model organism for study. One of the most prominent finding

of the last four decades was the identification of the protein-complex exocyst in yeast (Novick *et al*., 1980; Nakamoto *et al*., 1991).

To support and supplement this research field with an additional investigation tool, this work was concerned with the establishment of high-resolution capacitance measurements in yeast cells to study exo- and endocytosis. This method has successfully been applied in mammalian and plant cells, but so far not in yeast cells. One of the most important advantages is that exo- and endocytotic events can be measured *in vivo* with a high temporal and spatial resolution. This provides the possibility to directly investigate the effects of different parameters, e.g. temperature or osmolarity and to study blockers or mutants. Furthermore, through electrophysiological techniques it was possible to determine vesicle sizes, different types of exo- and endocytosis as well as fusion pore conductance and diameter. These parameters have so far not been investigated in yeast.

For the performance of capacity measurements a direct access to the plasma membrane is required. Hence, protoplasts have to be isolated by digesting the cell wall before measuring. Therefore the first and very important aim of this study was to demonstrate that protoplasts are physiologically intact and able to grow or internalize membrane, thus to perform exo- and endocytosis. The next part of the study deals with a broad analysis of exo- and endocytotic events measured in cell-attached capacity measurements. Furthermore, a *sec*-mutant (*sec6-4*) was used to demonstrate how exocytosis is impaired by a restrictive temperature. Experiments with this mutant confirmed that the detected events are the product of changes in the plasma membrane surface and thus of exo- and endocytosis. Altogether, this project will provide a new tool for investigation of exo- and endocytosis in yeast and therefore a further step in understanding these complex processes.

5. Material and methods

5.1. Yeast strain and culture conditions

The experiments were performed on the yeast reference strain BY4741 (*MATa; his3Δ1; leu2Δ0; met15Δ0; ura3Δ0*; Euroscarf, Frankfurt) and the temperature sensitive strain SY1 (*MATα, ura3-52, leu2-3,112, his4-619, ts sec6-4*) for capacity measurements and for the observation of protoplast growth. This temperature sensitive mutant is not able to perform exocytosis at the restrictive temperature of 37 °C. At 25 °C the process is not inhibited and cells can grow in a normal way (Guo *et al*., 1999; Lamping *et al*., 2005; Sivaram *et al*., 2006). Unless otherwise indicated, BY4741 cells were grown overnight at 30 °C and SY1 at 25 °C in liquid YPD (Yeast Peptone Dextrose) on a rotary shaker at 200 – 250 rpm.

5.2. Protoplast preparation

Protoplasts from yeast were prepared as described in detail (Bertl and Slayman, 1990; Bertl *et al*., 1998). A 10 mL aliquot of the overnight grown cell suspension was centrifuged at 500 g for 5 min. The pellet was resuspended in 3 mL of incubation buffer (50 mM KH_2PO_4 adjusted to pH 7.2 with KOH, 40 mM ß-mercaptoethanol) and incubated on a rotary shaker for 15 min at room temperature. Three millilitres (mL) of protoplasting buffer (50 mM KH_2PO_4, 2.4 M sorbitol, adjusted to pH7.2 with KOH, 40 mM ß-mercaptoethanol, 150 mg bovine serum albumin (BSA) and 0.5 – 1 mg Zymolyase 20-T) was added to the suspension, vortexed and incubated at room temperature for 45 min. Protoplasts were harvested by centrifugation for 3 – 5 min at 500 g, resuspended in 10 mL of stabilizing buffer (230 mM KCl, 10 mM $CaCl_2$, 5 mM $MgCl_2$, 5 mM Tris/MES at pH 7.2) and supplemented with 1 % glucose.
Protoplasts of the strain SY1 were isolated at 37 °C/ 25 ° for capacity measurements. For protoplast growth SY1 were harvested like described above and shifted after isolation to the both temperatures.

5.3. Growth of isolated protoplasts

Freshly isolated protoplasts were incubated in stabilizing buffer with or without addition of 1 % glucose (or 1 % sorbitol) and incubated at 30 °C for five days. SY1 (*sec6-4*) protoplast were incubated at the restrictive temperature of 37 °C (block of exocytosis) and at the permissive temperature of 25 °C (exocytosis takes place). Pictures were taken every 48 hours using a Canon EOS450D digital camera (Canon Inc., Tokyo, Japan) connected to a Zeiss IM-100 inverted microscope (Carl Zeiss Microscopy, Göttingen, Germany).

5.4. **Uptake of fluorescent beads**

The uptake of fluorescent nano beads (FluoSpheres, Life Technologies Corp., Darmstadt, Germany) of different sizes (0.02 µm; 0.04 µm and 0.1 µm) was monitored in intact cells and in isolated protoplasts. Nano beads were diluted 1:10 with double distilled water. A 20 µL aliquot of the diluted nano beads was sonicated directly before use for 5-10 min and mixed with 180 µL of the cell or protoplast suspension. The mixtures were incubated for 20 min at 25 °C and 10 µL aliquots were used for microscopic documentation on a Leica TCS SP5 II spectral confocal microscope (Leica Microsystems). Fluorescence was observed using excitation at 488 nm from an argon laser and emission was detected between 505 - 575 nm.

5.5. **Uptake of FM4-64**

Protoplasts were isolated from the yeast strain BY4741 and incubated overnight in a stabilizing buffer supplemented with 1 % glucose. Before recordings, protoplasts and intact cells were incubated with 20 µM of the fluorescent endocytosis marker FM4-64 (Invitrogen, Life Technologies Corp., Darmstadt, Germany) for 30 min at 30 °C and washed with a fresh stabilizing buffer supplemented with 1 % glucose. Internalization was observed at different times (0, 60, 90, 120 and 150 min) on a Leica TCS SP5 II spectral confocal microscope (Leica Microsystems) with excitation at 488 nm and emission between 600 - 700 nm. For experiments with ikarugamycin (IKA), cells and protoplasts were incubated with 20 µM FM4-64 and 30 µM IKA for 30 min and washed. After washing the cells/protoplasts the same concentration of IKA was added again. The internalization was observed after 0, 60 and 120 min on the microscope.

5.6. **Growth assay**

The growth assay was made for the phenotypical characterization of the SY1 strain at 37 °C and 25 °C. Cells of the temperature sensitive SY1 strain and the wild type strain BY4741 (as control strain) were incubated over night at 30 °C in YPD on a rotary shaker at 200 - 250 rpm. 1 mL of each overnight culture was centrifuged at 6000 x g and the pellet was resuspended in 1 mL of double distilled water (ddH_2O). The OD = 1 at a wave length of 600 nm was adjusted for each preparation (stock solution). Out of this stock solution further dilutions were prepared (1:10, 1:100, 1:1000) for both strains with ddH_2O. 7 µL from each dilution and each strain were dropped on a YPD plate. In total two plates were prepared with both strains. On each plate drops (7 µL) of the four different concentrations of each strain were applied in a row keeping ca. two cm distance between both strains/rows. One plate was incubated at 25 °C and the other one at 37 °C for three days.

5.7. **Localization of Tok1-GFP**

For expression of an N-terminal GFP-fusion construct of the yeast plasma membrane potassium channel *Tok1,* the SY1 strain was transformed with a centromeric plasmid pGreg576 (Jansen *et al.*, 2005). In this plasmid *TOK1-GFP* expression is under control of the *GAL1* promoter. SY1 cells containing the plasmid were grown overnight in SD (-ura) on a rotary shaker at 250 rpm and at 25 °C. The next day the cells were shifted to SGal (-ura) media and incubated at 37 °C for 3 h. A control preparation was incubated at 25 °C for the same time period. After incubation, half of each preparation was used for protoplast isolation. The buffers were maintained in the respective temperature during protoplast preparation. Protoplasts were harvested by low speed centrifugation (500 x g) and resuspended in standard stabilizing buffer containing 1 % glucose, which stops expression of TOK1-GFP. The exocytosis block was relieved by shifting the protoplasts to the permissive temperature (25 °C). Incorporation of Tok1-Gfp into the plasma membrane by fusion of the accumulated vesicles was monitored over a period of 180 min using a 100-x oil objective (HCX PL APO CS 100x/1.44) on a Leica TCS SP5 II spectral confocal laser scanning microscope (Leica Microsystems, CLSM) with excitation at 488 nm and emission between 505 - 580 nm.

5.8. **Evaluation of CLSM data**

The images were converted with the “LAS AF Lite”- Suite software to .jpeg data. The recordings were evaluated with the WCIF_ImageJ collection of PlugIns, designed for scientific multidimensional images (written by Wayne Rasband of the National Institute of Health, Maryland). For analysis the integrated density, mean gray value and area were chosen from the menu item “set measurements”. In order to obtain the relative fluorescence from the recordings at each particular time it was necessary to measure all values inside the cell and for the complete cell. To obtain the total fluorescence of cells/ protoplasts the membrane was traced (Fig. 6A).The values for the inside of the cell were acquired by tracing an area underneath the plasma membrane which was on average nearly 30 % smaller than the total area (Fig. 6B). For each particular time six cells were evaluated. The background noise of the recordings was determined in order to correct the values (corrected value = integrated density - area x background). The corrected values were used to calculate the relative fluorescence:

$$relative\ fluorescence = \frac{corrected\ integrated\ density(inside)}{corrected\ integrated\ density\ (total)} \qquad \text{(eq. 1)}$$

The standard error of the mean (SEM) was calculated as followed:

$$SEM = \frac{standard\ deviation}{\sqrt{number\ of\ values}} \qquad \text{(eq. 2)}$$

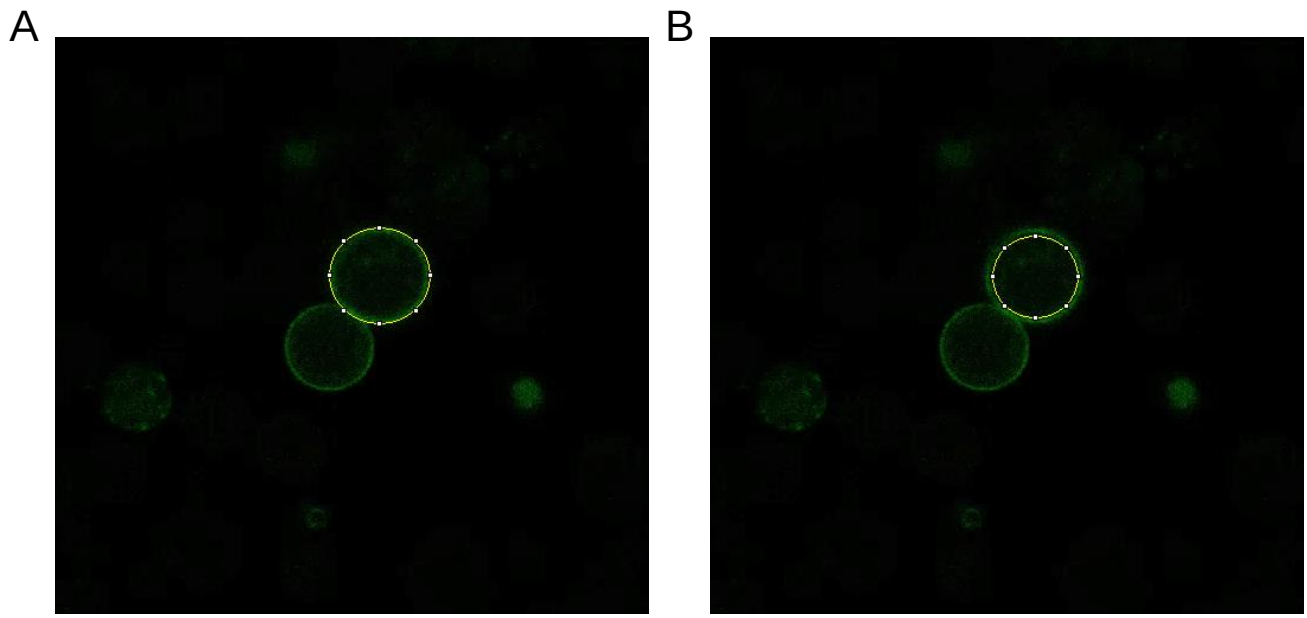

Figure 6: Image of a protoplast expressing Tok1-Gfp, recorded with the confocal laser scanning microscope.

This image was evaluated with image J. The yellow circle represents the area of the cell which was analyzed. **(A):** The total fluorescence of the cell was calculated by tracing the plasma membrane. **(B):** The fluorescence in the cytosol and in cell compartments inside the cell was calculated by marking the area with a circle underneath the membrane. The area was in average nearly 30 % smaller than the total area. Measured values were used to calculate the relative fluorescence for each time point of the experiment. The same procedure was done for intact cells.

5.9. **Electron microscopy**

Cells of the temperature sensitive *sec6-4* mutant (SY1) were grown overnight in YPD (with 1 % glucose) at the permissive temperature of 25 °C or at the restrictive temperature of 37 °C for 3 h on a rotary shaker at 200 rpm. From these cultures the cells were diluted 1:100 and grown at the 25/37 °C temperature to an OD_{600} of 1. Immediately before freezing, the cells of these OD_{600} = 1 preparations were harvested by centrifugation. Aliquots from the pellet were transferred into 100 µm deep specimen carriers (Carrier No. 241 and No. 242, Wohlwend GMBH, Sennwald, Switzerland) and frozen through high pressure in a Bal-Tec HPM 010 (Bal-Tec, Liechtenstein). Freeze substitution was carried out with a setup similar to the one described (McDonald & Webb, 2011), using a copper bloc

inside a styrofoam box on a shaker. Freeze substitution was done overnight in dry acetone containing 1 % OsO_4 and 1 % glutaraldehyde. After the vials reached 10 °C (in our setup this occurs after about 16 h) the material was released with a needle from the specimen carriers and washed twice with dry acetone for 10 min. Afterwards the cells were en bloc stained for 60 min with 0.5 % uranyl acetate in acetone. Subsequently samples were infiltrated stepwise with Spurrs resin (25 %, 50 %, 75 %, 100 % one hour each step), put into fresh 100 % Spurrs and kept overnight on a rotating wheel for better infiltration. After another change of resin (3 h), samples were embedded in Beem capsules and polymerized for 24 h at 60 °C.

Ultrathin sections (70 nm) were cut on a Leica Ultracut S ultramicrotome (Leica, Wetzlar, Germany). Images were taken with a FastScan F214 digital camera (TVIPS, Gauting, Germany) on a JEM1400 (JEOL; Tokyo, Japan) transmission electron microscope operated at 80 kV.

5.10. **Electrophysiology**

5.10.1. The fundamental principles of capacity measurements

Biological membranes have electrical characteristics that are similar to the characteristics of an electrical circuit with a capacitance (membrane) and a conductance (ion channels) in parallel (Fig. 5). This minimal equivalent circuit can be transferred to small spherical cells like yeast protoplasts. A specific voltage (V) is applied across the membrane of a small cell and the resulting membrane current (I_m) is the sum of two electrical components. These components are the resistive component of the ionic current (I_R) and the capacitive component (I_C) of the current resulting from the change in the amount of charge per time unit at the membrane (Lindau, 2012; Rituper *et al*., 2013a).

$$I_m = I_R + I_C \qquad \text{(eq. 3)}$$

The central part for electrophysiological capacity measurements is a two-phase lock-in amplifier. This amplifier consists mainly of a multiplier, a low-pass filter and a phase adjuster (Fig. 7).

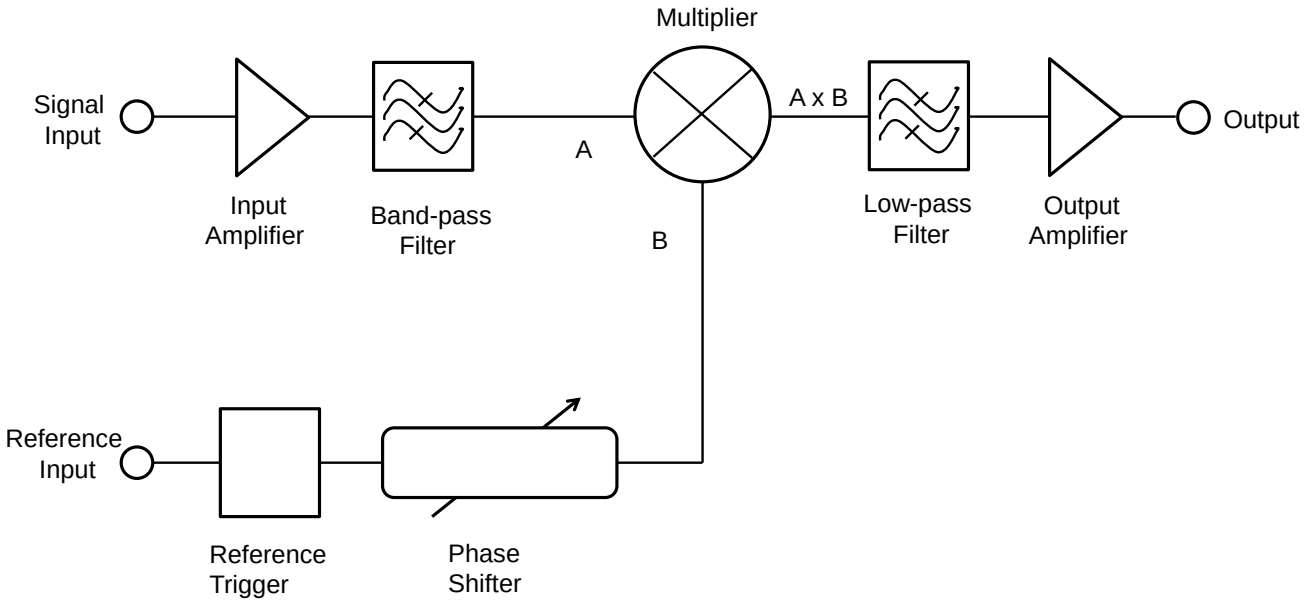

Figure 7: Overview of a Lock-In amplifier. Adapted from (http://www.physik.uni-regensburg.de/studium/praktika/a2/download/versuch5a.pdf)

Through this phase-sensitive device it is possible to separate the total membrane current into its resistive and capacitive component (Fig. 8B). To measure capacitive currents an alternate (ac) voltage, like a sinus command voltage of the form $V(t) = V_0 \sin(\omega t)$ (eq. 4) is applied to the cell, whereby ω represents the angular frequency and V_0 the amplitude (Fig 8A). This results in capacitive and ohmic currents caused by a change in the amount of charge per time unit separated by the membrane. The resulting current can be expressed in the following form

$$I(t) = \frac{V_0 \sin(\omega t)}{R_m} + C_m V_0 \omega \cos(\omega t) \qquad \text{(eq. 5)}$$

whereby R_m is the membrane resistance and C_m the membrane capacitance. The resulting signal is the sum of two sinusoidal currents, where the resistive current is in phase (I_R) with the command voltage and the capacitive current is phase shifted by 90° with respect to the driving voltage (I_m) (Fig. 8B). Thus, to calculate changes in the C_m and R_m, the complex admittance (Y) of the minimal equivalent circuit is measured and divided into the imaginary (*Im*) and real (*Re*) components by the lock-in-amplifier (Rituper *et al*., 2013a). For measurements the phase angle has to be adjusted correctly. To verify this, a 100 fF calibration pulse was applied as described in chapter 5.10.5 (Fig. 16).

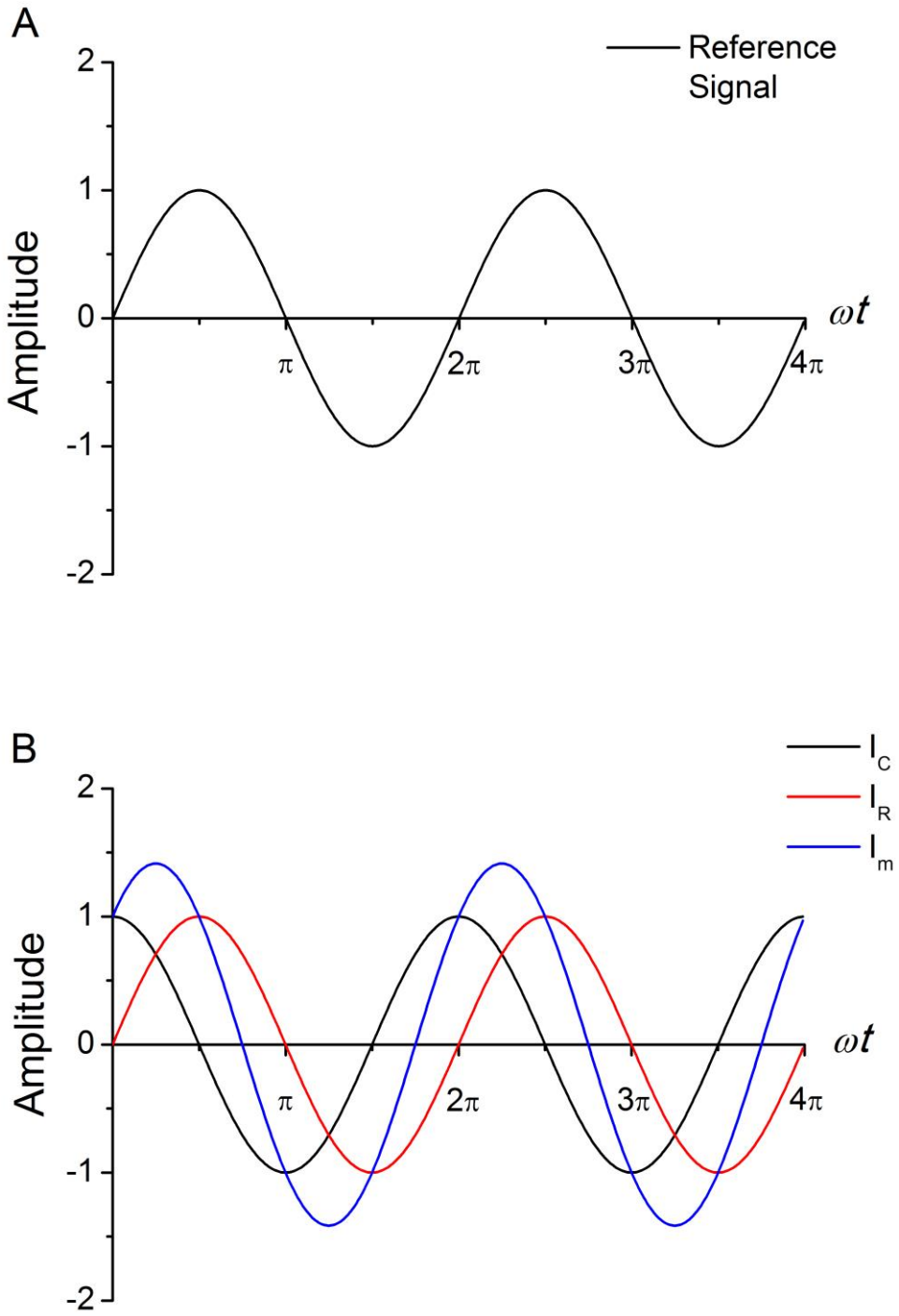

Figure 8: (A) The reference voltage. In B the output signal represents the resulting current (blue, I_m) which can be separated in the capacitive component (black line/I_C) and the resistive component (red line/I_R) of the output signal.

To separate the signals, the multiplier of a lock-in-amplifier basically makes a multiplication between the reference signal and the output signal at a specific phase. In figure 9 the resulting signals after passing the multiplier are depicted. A multiplication between the reference signal and the signal in phase results in a positive sinusoidal signal (Fig. 9, black line). In contrast, a multiplication between the reference signal and the signal out of phase (90° shifted), results in a sinusoidal signal with negative and positive values (Fig. 9, red line).

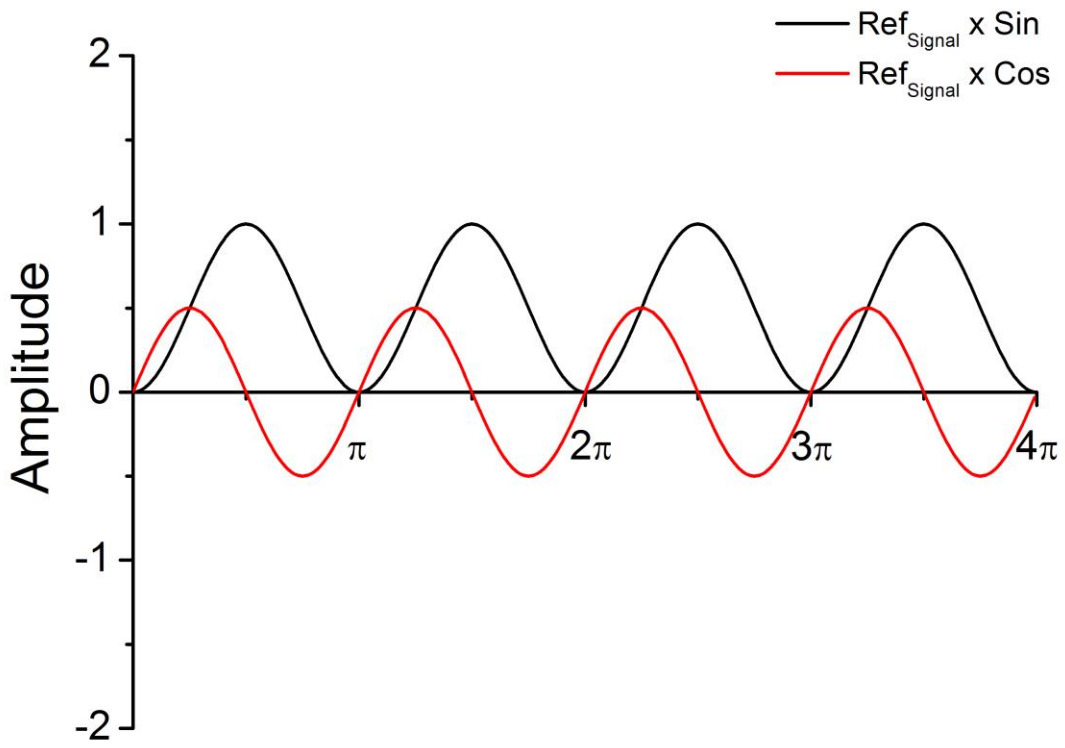

Figure 9: The resulting signals after passing the multiplier.
The black line represents a cross-correlation between the reference signal and the signal in phase. The red line is the result of a cross-correlation between the reference signal and the signal 90° phase shifted (cosine).

The resulting output signals are finally low-pass filtered, resulting in direct-current (dc) signals (Fig. 10).

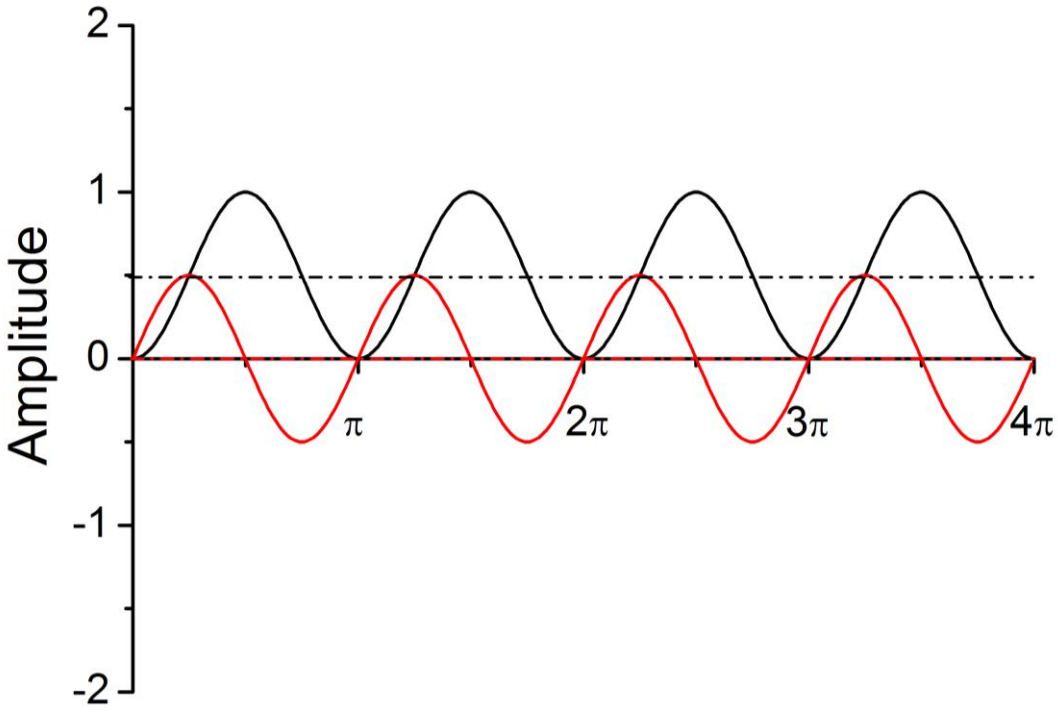

Figure 10: An illustration of the ac signals after being low-pass filtered and converted into dc signals.

The resolution of the signal depends on the frequency and the amplitude of the driving voltage. To obtain satisfactory results the driving sine wave frequency and amplitude must be chosen correctly. An increase of the frequency decreases the noise as a square root function. A linear decrease of the noise can be achieved by an increasing of the sine wave amplitude. Thus there are two possibilities to improve the signal to noise ratio (SNR). Both ways have disadvantages, e.g. large amplitudes can cause measurement errors due to changes in the G_m generated by activation of voltage-dependent channels. Depending on the amplifier and on the size of cells, frequencies as high as 40 kHz and amplitudes up to 200 mV (root mean square (r.m.s.)) can be applied without problems (Rituper *et al.*, 2013a).

5.10.2. Whole-cell vs. cell-attached configuration:

There are two configurations to examine exo- and endocytosis via capacitance measurements in cells. For whole-cell measurements a connection between the cytosol and the pipette solution is required. The application of a negative pressure (suction) breaks the membrane under the pipette (Fig. 11A). In the whole-cell configuration, changes in capacitance (ΔC_m) over the whole membrane

can be recorded. The resolution obtained by this configuration is limited and single events cannot be resolved. Thus, in this configuration it is not possible to distinguish between the different event types.
To improve SNR the cell-attached configuration is preferred. In this mode the membrane is still intact and only changes in the membrane area (patch) underneath the pipette are recorded (C_{pa}; Fig. 11B). For this purpose the C_s has to be compensated and the phase has to be adjusted to measure correctly the changes in the out-of-phase lock-in signal which is proportional to the changes in the capacitance of the patch (C_{pa}). This patch-clamp configuration allows monitoring changes in membrane capacitance in the range of unitary events with a high temporal resolution. It also enables the detection of the different event types. Depending on the quality of the seal between the pipette and the membrane, the amplitude, the frequency of the driving voltage signal and the properties of the setup, different resolution limits can be achieved. In this work, the resolution limit was approximately at ~ 0.26 fF or 100 nm (Chapter 6.4). When unitary events are transient/permanent the measurement of the conductivity of the fusion pores is feasible.

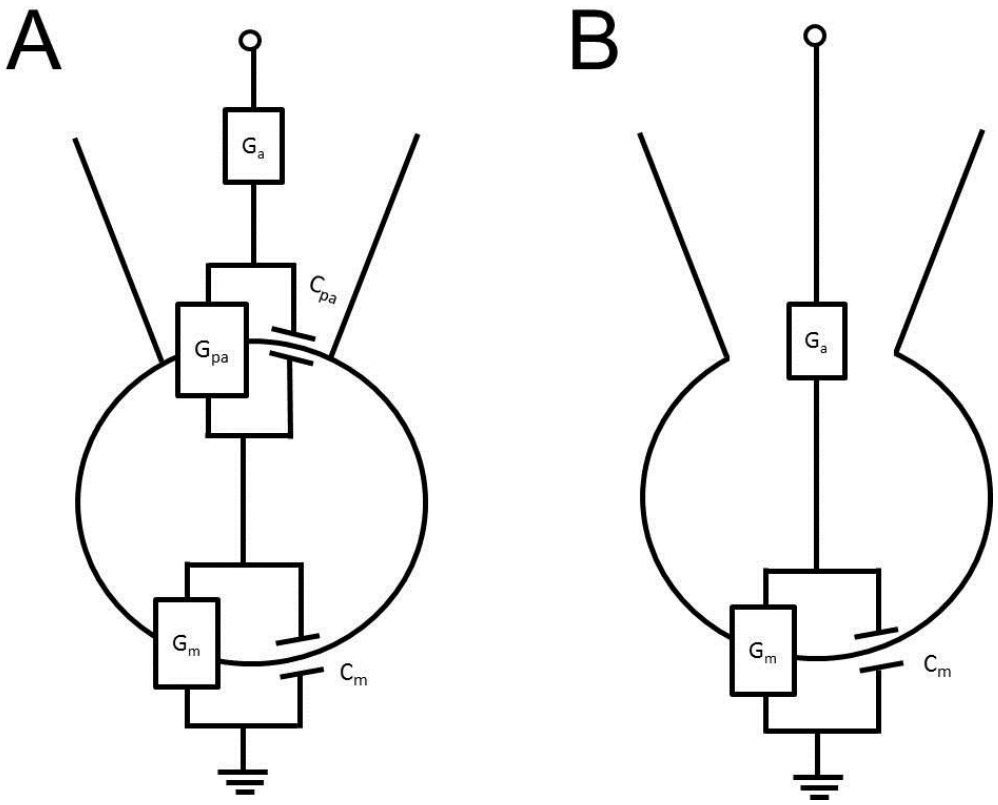

Figure 11: The minimal electrical circuit of whole-cell and cell-attached configuration.
(A) The minimal electrical circuit of the whole-cell mode consists of the access conductance (G_a) and the membrane conductance (G_m) connected in series and parallel with the membrane capacitance (C_m). **(B)** In the minimal circuit of the cell-attached mode two parameters have to be added. The conductance (G_{pa}) and the capacity (C_{pa}) of the membrane patch underneath the pipette which are connected parallel. Both are in series with the other three parameters (Rituper *et al*., 2013a).

Calculation of parameters in the cell-attached configuration

The data of this work was recorded in the cell-attached configuration. When the phase angle is correctly adjusted, the out-of-phase signal is proportional to changes in the C_{pa}. Recorded changes in the membrane capacitance and changes in the membrane conductance can be calculated as follows:

$$C_V = \frac{1}{\omega}\frac{Re^2+Im^2}{Im} \qquad \text{(eq. 6)}$$

$$G_P = \frac{Re^2+Im^2}{Re} \qquad \text{(eq. 7)}$$

Where *Re* represents the amplitude of the real part of the admittance signal (in pS) and *Im* represents the amplitude of the imaginary part of the signal (in pS; Rituper *et al*., 2013a). The calibration pulse of 100 fF is applied to verify correct phase-angle settings and to convert calculated C_V (pS) into fF (Fig. 16).

Since the membrane capacitance is proportional to the membrane surface area, the diameter of the endo- or exocytotic vesicle can be determined from the recorded changes in membrane capacitance. These changes in membrane capacitance C_m are used to calculate the surface area (A) and thus the diameter (d) of endo-/exocytotic vesicles from $C_m = C_{spec} \bullet A$ (eq. 8), where $A = \pi \bullet d^2$ (eq. 9) and C_{spec} is the specific membrane capacitance, being about 8 mF/m^2, as determined from conventional whole cell patch-clamp recordings (Homann & Tester, 1998).

5.10.3. Fusion pores analysis: the equivalent circuit of fusion pores

In cell-attached experiments, changes in the *Im* are sometimes accompanied with changes in the *Re* trace. These changes are caused by a transient change in the membrane conduction G_m of the patch (Fig. 12). These changes are provoked through fusion pores, formed during fusion and fission processes (Kabaso *et al*., 2013). In figure 12 the equivalent circuit of a fusion pore is depicted. The capacity of the vesicle is termed C_V and the conductance of the fusion pore is termed G_P, both are connected in series.

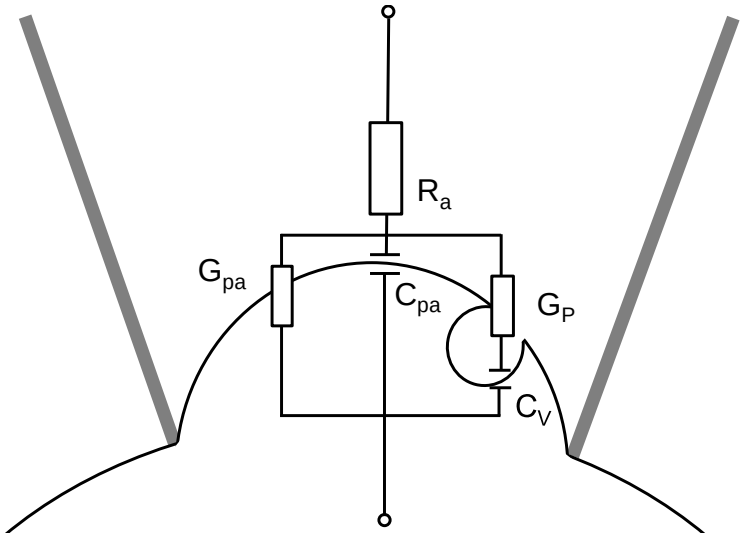

Figure 12: The equivalent circuits of a membrane patch including the conductance of a fusion pore in the cell-attached configuration.

The fusion pore conductance (G_P), the capacitance of the vesicle (C_V), the patch conductance (G_{pa}), the patch capacitance (C_{pa}) and the access resistance (R_a) are depicted.

The simultaneous changes should not be a result of incorrect phase-angle settings of the lock-in amplifier. The phase of the lock-in amplifier should be adjusted to nullify the changes in the *Re* signal trace. To verify this, a manual calibration pulse was applied to ensure no projection in the *Re* trace and correct phase angle settings (Fig. 16; Chapter 5.10.5). Theoretically, an increase in the *Re* trace is due to an additional conductance current through the fusion pore (Fig. 13). Δ*Re* and Δ*Im* have finite values, which can be used for the calculation of the unknown G_P. C_V and G_P can be obtained from the *Re* and the *Im* parts of the admittance signal as shown above.

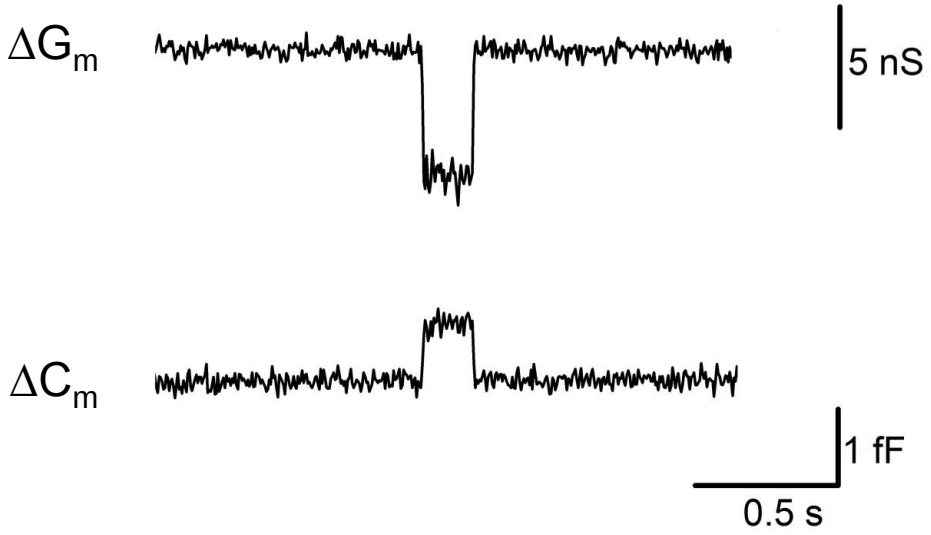

Figure 13: Example for the simultaneous change of the membrane capacitance and the membrane conductance.

Currents were measured in the cell-attached configuration. The reflection in the ΔG_m trace represents the conductance of a fusion pore.

The radius r_{FP} of the fusion pore can be calculated with the following equation (Rituper *et al*., 2013a):

$$r_{FP} = \sqrt{\frac{G_P \rho \lambda}{\pi}} \qquad \text{(eq. 10)}$$

Whereas G_P is the pore conductance, ρ is the resistivity of the saline solution (100 mΩ) and λ is the estimated length of two membrane thicknesses (15 nm). In the case of mammalian cells the length of a gap junction is estimated (Rituper *et al*., 2013)

Reflections in the *Re* traces are marked and evaluated in the same way and with the same programs as changes in the *Im* trace.

5.10.4. Experimental conditions

Capacitance measurements on yeast protoplasts were performed with external recording solution containing: 165 mM KCl, 10 mM $CaCl_2$, 5 mM $MgCl_2$, 1 mM MES, 1 % Glucose titrated with Tris to pH 7.5. The pipette solution consisted of 50 mM KCl, 250 mM Sorbit, and 0.1 mM $CaCl_2$ (Bertl *et al*., 1998). With these solutions, tip resistances of the patch pipettes were 10 – 15 MΩ. In order to minimize pipette capacitance, the shank of the pipette tips was coated with paraffin. Recordings were made using a dual-phase lock-in patch-clamp amplifier (SWAM-2C; Celica d.o.o., Ljubljana, Slovenia). Membrane patches were clamped at -40 mV (voltage-dependent ion channels of yeast cells are closed at this voltage; Bertl *et al*., 1998) and a sine wave of 111 mV r.m.s. and 1.6 kHz was applied. Data were low-pass filtered at 100 Hz and sampled at 200 Hz using the CellAn software (Celica d.o.o, Ljubljana, Slovenia). The measuring time for one file was maximal 1200 seconds. As reference a test pulse of 100 fF was applied after sinus compensation during the measurements.

5.10.5. Data analysis

For analysis the .rec data were loaded into MATLAB (MathWorks Inc., Natick, USA). Events were determined and categorized in the different types via the following terms. A change in capacitance (C_m) was categorized as a vesicle fusion/fission event when its amplitude was at least twice as large as the noise width (Chapter 6.4.1, Fig. 14A) and the rise time of the change in membrane capacitance less than 0.2 seconds (Fig. 14B).

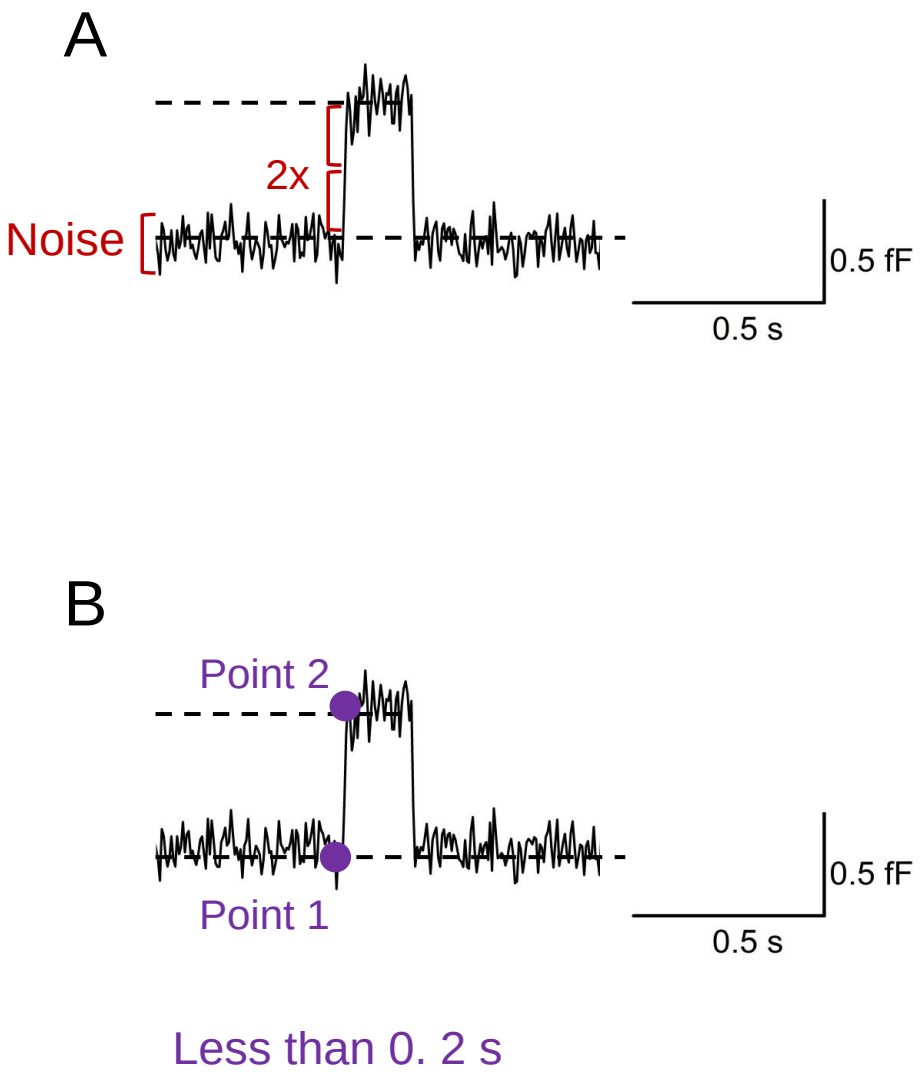

Figure 14: Characterization of events.

Changes in the membrane capacitance, which were at least twice as large as the noise could be considered as events **(A)**. In all measurements the duration between the capacitance change from one stable level to another (purple dots, point 1 and 2) was less than 0.2 seconds **(B)**.

Transient changes were distinguished from permanent changes when the upward step of a capacitance change had the same amplitude as the downward step (Fig. 15; Fig. 29). The time between both changes (dwell-time) was not less than 30 ms.

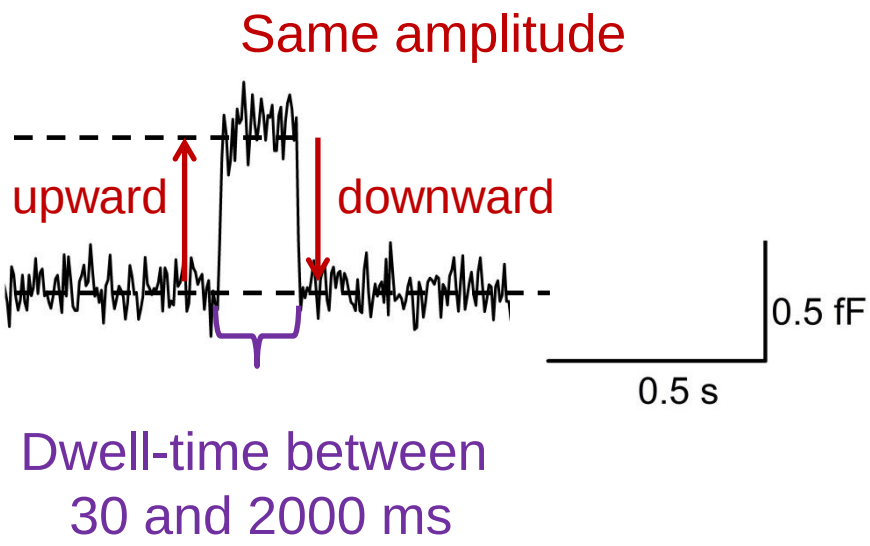

Figure 15: Characterization of transient events.

The capacitance trace of a transient exocytotic event is represented. To categorize an event as transient event the upward and the downward change in the capacitance trace has to have nearly the same amplitude. The time between upward and downward step was less than 2 seconds and not less than 30 ms.

***Analysis with MATLAB*:**

MATLAB was primarily used to identify and define events manually. First, the reference test pulse in the capacitance trace (*Im*) was marked for the analysis with four points (Fig 16B purple dots). Then each fusion or fission event was marked with four points and categorized in the four different kinetic modes (transient up/transient down (Fig. 17A purple dots), permanent up/permanent down (Fig. 17B purple dots). Changes in the *Re* trace were marked the same way. The whole trace of one measurement period (1200 s) was analyzed and the detected events were marked and stored as .txt data.

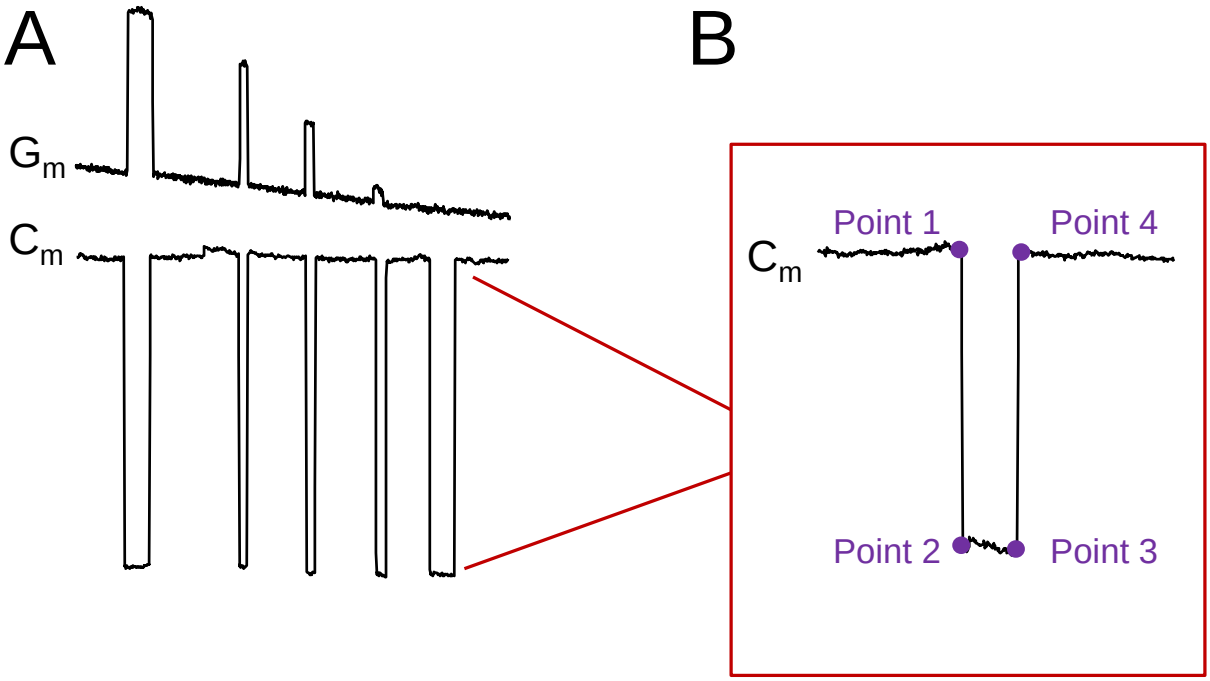

Figure 16: Representative responses of membrane conductance and capacitance during calibration with a reference pulse (test pulse).

The test pulse is a useful tool to adjust the phase angle **(A)** but it is also used as reference pulse for the evaluation of the detected changes in the membrane capacitance (events). **(B)** The test pulse was marked at the data extracted with MATLAB with four points. These points are used to determine the amplitude of the test pulse, which was used as reference for further analysis.

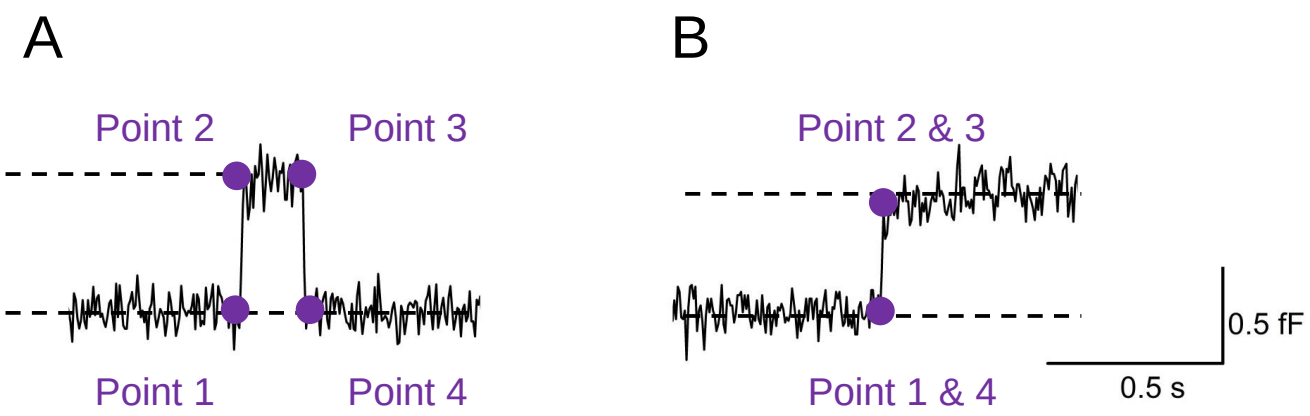

Figure 17: The capacitance trace of a transient (A) and a permanent (B) exocytotic event are represented.

Defined events were marked with four points (purple dots) in the data extracted with MATLAB for further analysis.

The defined events (.txt data) were stored on a MySQL Community Server 5.1.49 database (Oracle Inc., Redwood Shores, USA). Quantitative analyses were done with the CAMMC web application (yQ-it GmbH, Seligenstadt, Germany (http://130.83.95.142/TUD-Cammc/index.php#r=Home/&_r_left_grpmenuframe_grpmenu_menuitem2=pressed&load=Home)). The CAMMC is a database created to facilitate the evaluation of the data. This database makes it is possible to calculate vesicle sizes, dwell-times, fusion pore diameters etc.

6. Results and discussion

6.1. Growth of yeast protoplasts

Membrane capacity measurements used for the analysis of exo- and endocytosis are based on the patch-clamp technique, which requires direct access to the plasma membrane of the cell. Yeast cells are surrounded by a layer of polysaccharides and glycoproteins, which form the cell wall (Kollár *et al*., 1997). To obtain free access to the cell membrane, the cell wall has to be digested enzymatically (Bertl *et al*., 1998). Through this the shape of a cell changes from egg-shaped in intact cells to perfectly spherical shaped in cell protoplasts (Fig. 18A). The cell wall not only forms the shape of a cell, but also serves as a protection barrier, e.g., in the case of osmotic stress. Therefore the question emerges, whether the removing of the cell wall and thus the turgor pressure influences the processes of exo- and endocytosis. To investigate this, protoplasts were isolated from the wild type strain BY4741 as described in chapter 5.2. After isolation protoplasts were incubated at room temperature for five days in an isotonic stabilizing buffer supplemented with 1 % glucose. Protoplasts can easily be differentiated from intact cells based on their shape and optical refraction specially observed in phase contrast. Protoplasts appear spherical and dark and intact cells are bright and egg-shaped (Fig. 18A). During this incubation period pictures were taken every 48 h and the diameter of the protoplasts was determined. After isolation of protoplasts there are some intact cells that can remain in the preparation (Fig. 18A, 48 h). This can be the case if cells are too old and their cell wall is hard, tight and difficult to digest. Directly after isolation, the average protoplast diameter (n= 20) was 4.5 µm ± 0.1. Using the equation $A = \pi d^2$ (Chapter 5.10.2), a diameter of 4.5 µm corresponds to a membrane surface area of 63.6 µm² ± 4. 48 h after isolation, the diameter increased (nearly tripled) to 11.7 µm ± 0.3, corresponding to a membrane surface area of 430 µm² ± 25. Protoplasts remained growing for more than five days after isolation. 96 hours after incubation the diameter was on average, 16.7 µm ± 0.6, which can be translated to a membrane surface area of 895 µm² ± 66. It is interesting to note that, during five days of incubation, the protoplasts increased nearly 14- to 25- fold in the membrane surface area. This enlargement cannot be explained by mechanical membrane tension only. Detailed investigation on mechanical properties of the plasma membrane of plant protoplasts showed that membrane enlargement through mechanical tension was limited to an area increase of only 2-3 % (Wolfe & Steponkus, 1983). Thus, any larger increase in membrane surface area, as in the case of protoplasts 96 hours after incubation, must involve insertion of new material, which is caused by fusion of vesicles with the plasma membrane. It is theoretically possible that a process which does not involve vesicle fusion, e.g. lipid transfer by carrier proteins followed by flippase-mediated equilibration across the bilayer, could also be responsible for the increase in membrane area (Funato & Riezman, 2001; Lev, 2010).

Growth of a yeast protoplast from 4 µm to 15 µm in diameter within 96 h (Fig. 18A &B) means an increase in the membrane surface area of 660 μm^2. Accordingly the fusion of 21 000 secretory vesicles with a diameter of 100 nm was expected. This number showed the minimum number of events. This means only exocytotic minus endocytotic events. The fusion of these estimated 21 000 vesicles in 96 h yields a frequency of 216 fusion events per hour (3.6 per minute) and cell. With an average diameter of 10 µm for the protoplasts and a membrane area of the patch in cell-attached recordings of about 5 μm^2, 216 fusion events per hour and cell are equivalent to 3.6 events per hour and patch (or 0.06 per minute and patch). These numbers represent one exocytotic event every 17.5 minutes. The frequency of events seems to be low, requiring rather long recording times for reliable monitoring of single endo-/exocytotic events in yeast using the patch-clamp technique. However, it was demonstrated that in other systems the frequency of events can be increased by different factors like osmolarity (Jorgacevski *et al*., 2008), calcium level within the cell (Alés *et al*., 1999; Elhamdani *et al*., 2006) and lipids or cholesterol composition (Rituper *et al*., 2012; Rituper *et al*., 2013b).

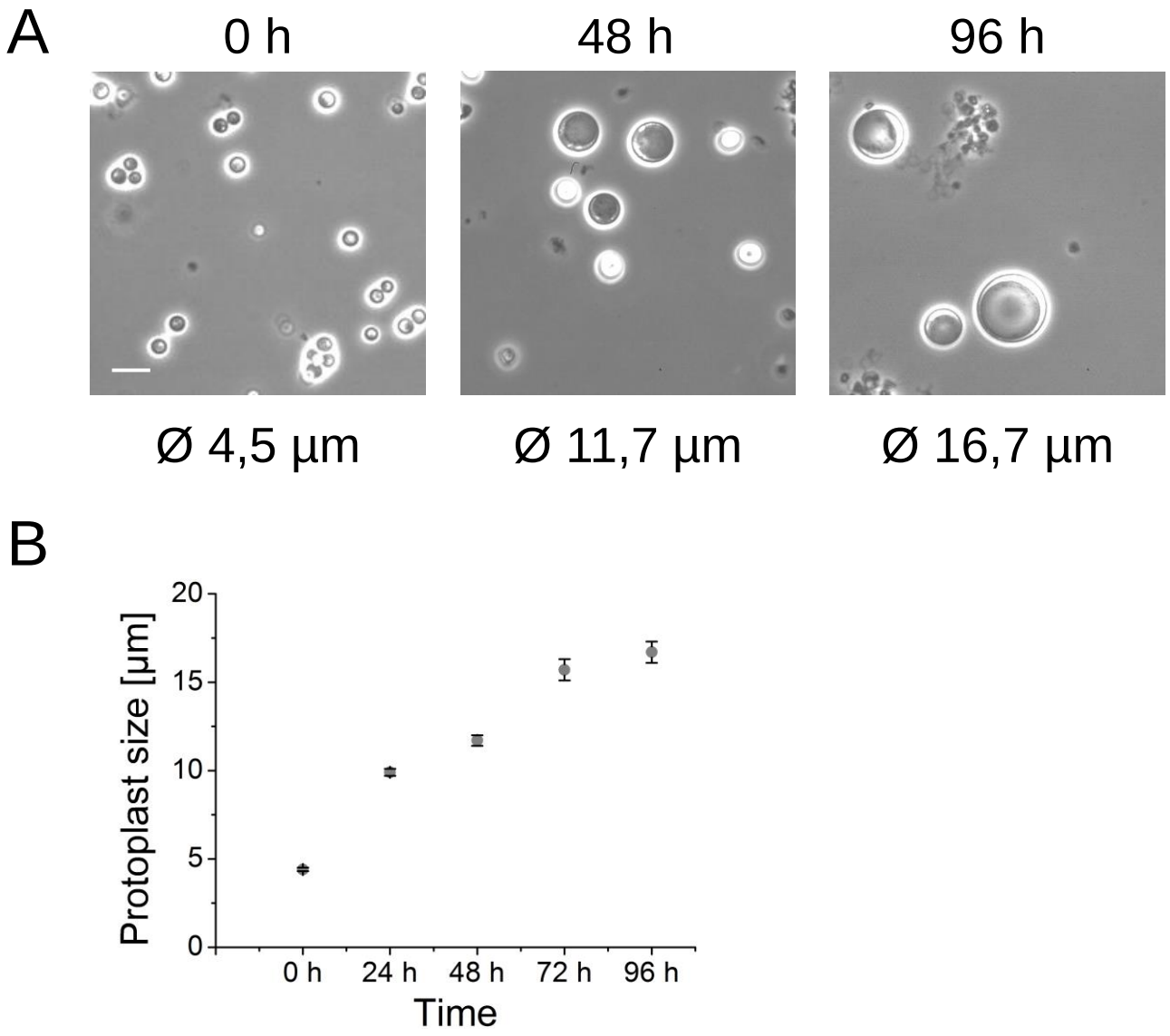

Figure 18: A: Growth of yeast protoplasts observed during an incubation period of 96 h.
Protoplasts from the haploid strain BY4741 were incubated at 25 °C in standard incubation buffer (see chapter 5.2) in the presence of 1 % glucose. Pictures were taken every 48 h during four days. Intact cells (in the 48 h preparations) are easily identified by their shape and by their bright appearance. The scale bar is 10 µm. **B:** The average diameter of 20 protoplasts, measured at each time point. Error bars represent standard error of the mean (SEM).

Exocytosis is a requisite for the increase in protoplast size. This can be demonstrated by the use of a temperature sensitive secretory mutant. The strain SY1 is a *sec6-4* mutant that carries a point mutation in the *SEC6* gene encoding for one of the components of the exocyst protein complex mentioned in chapter 4.2. The point mutation leads to an exchange of leucine at position 633 into proline, at the C-terminus within hydrophobic core of the subdomain B. This mutation probably destabilizes the α-helix of the protein (Sivaram *et al*., 2006). The exocyst is a protein complex that

participates in the tethering process at the plasma membrane. It has been demonstrated that defects on particular proteins of this complex lead to accumulation of secretory vesicles in the cytosol at 37 °C (Fig. 19; Guo *et al*., 1999). The *sec6-4* mutation has no effect on the secretory pathway at the permissive temperature of 25 °C, and the cells perform exocytosis (Fig. 19, 25 °C; Fig. 20, left panel). The restrictive temperature of 37 °C destabilizes the protein, and vesicles are not able to dock at the membrane (Sivaram *et al*., 2006).

To observe the effect of the *sec6-4* mutation, electron microscopic (EM) recordings were performed (Fig. 19). For this prupose, cells from a fresh overnight culture were divided in two aliquotes and incubated at both temperatures for 3 h. For imaging, the cells were frozen and subsequently, freeze substitution, staining and infiltration were carried out as described in chapter 5.9. At 37 °C, the accumulation of secretory vesicles in the cytosol could be observed clearly (Fig. 19, 37 °C), whereas at 25 °C, the vesicles were rarely visible (Fig. 19, 25 °C). Interestingly, membrane invaginations were detected in cells that grew at 25 °C, but not in those maintained at 37 °C (Fig. 19, middle panel). The EM analysis demonstrates that secretory vesicles cannot fuse with the plasma membrane.

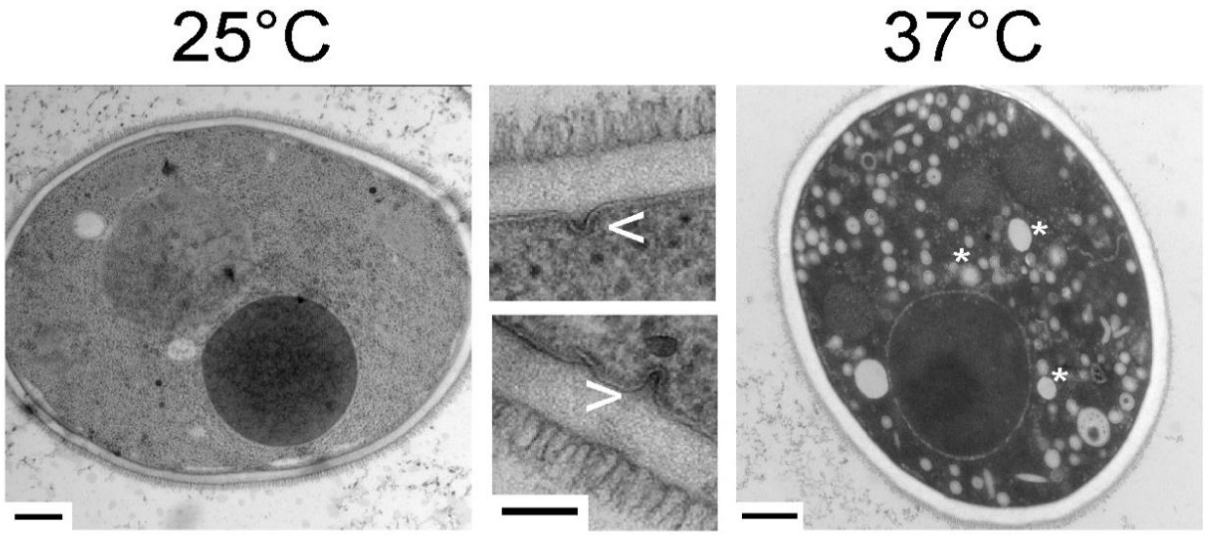

Figure 19: Transmission electron microscopic image of the temperature sensitive sec6-4 mutant (strain SY1).

At the restrictive temperature of 37 °C cells showed accumulation of secretory vesicles (right panel), but not at the permissive temperature (25 °C, left panel). Scale bars for outer pictures, 400 nm. Membrane invaginations (marked by arrows), indicating exocytotic activity at different stages can be identified in magnifications from the left picture (center panel), but were not seen in the cells incubated at 37 °C, where exocytosis is blocked. Scale bar for center pictures, 100 nm.

When protoplasts of the SY1 strain (*sec6-4* mutant) were incubated in stabilizing buffer (+1 % glucose) at 25 °C and at 37 °C over a period of 72 h (Fig. 20), two different results are obtained. At the permissive temperature of 25 °C protoplasts grew to giant protoplasts as observed in reference

strain BY4741 (Fig. 18). At 37 °C, the size of protoplasts increased only minimally, consistent with the temperature dependent block of exocytosis in this mutant. To exclude high temperature as a reason for growth inhibition, control protoplasts of the reference strain BY4741 were also incubated at 37 °C. In contrast to the SY1 cells they grew in a normal way, despite the high temperature. This confirms that the enlargement of the protoplast membrane surface area is an effect caused by exocytosis, which can be blocked by a temperature shift in this mutant.

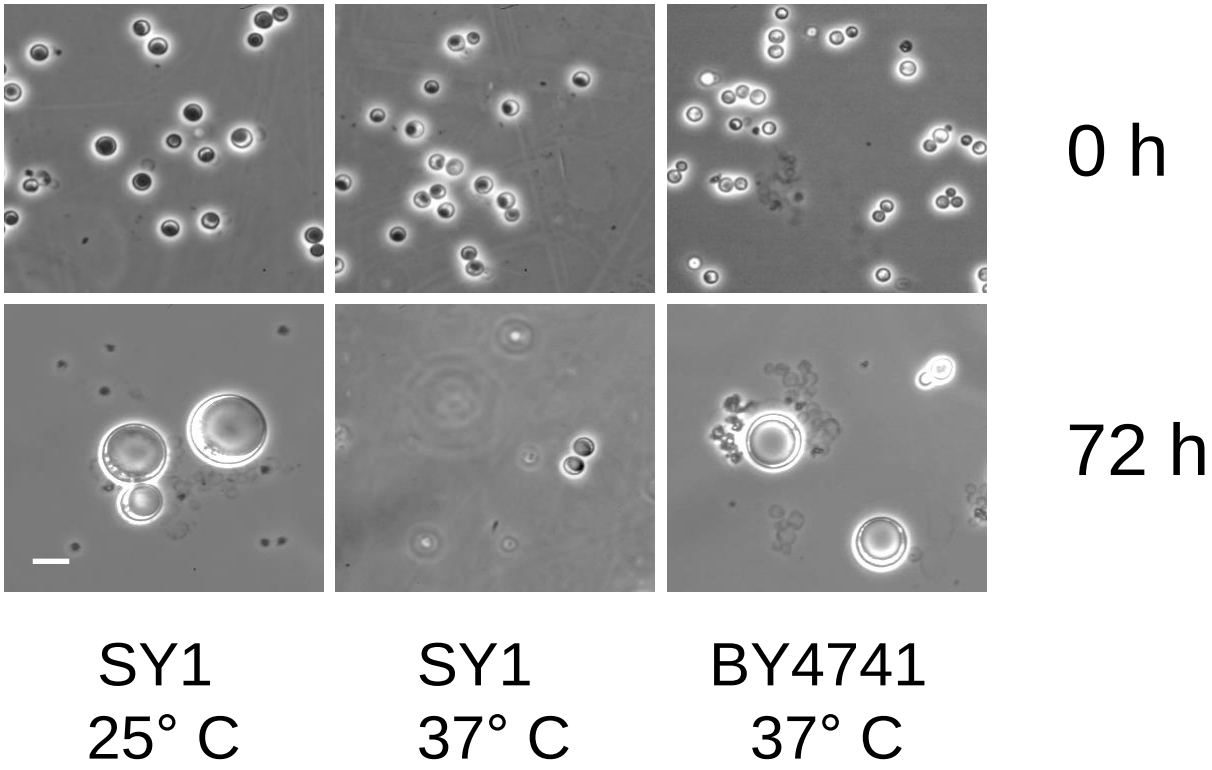

Figure 20: Protoplast growth of the strain SY1 during an incubation period of 72 h.
SY1 protoplasts grew normally at 25 °C, but did not expand over 72 h at 37 °C, where exocytosis is blocked (center panel). It should be mentioned that after 72 h at 37 °C, most of the SY1 protoplasts were broken, but the few surviving protoplasts remained small. Protoplasts of the reference strain BY4741 showed a strong growth also at the elevated temperature (right panel). Scale bar, 10 µm.

Altogether these results demonstrate that protoplasts are able to enlarge their membrane surface continuously, which means that protoplasts are able to perform exocytosis and to grow even without a cell wall and turgor pressure. This growth of yeast protoplasts is apparently energy dependent, as it does occur in the presence (Fig. 21, left panel), but not in the absence of glucose (Fig. 21, middle panel). Similar protoplast growth was also observed with galactose and other carbon sources which can be used for energy production (data not shown). Thus this process is not specific to glucose. To exclude that the presence of glucose has an effect on bath tonicity and thus on exo- and endocytosis, we performed experiments with sorbitol (Fig. 21, left panel) instead of glucose. The result shows that

in the presence of sorbitol protoplasts are not able to enlarge their diameter. Only a small change in the size can be observed during an incubation period of 72 h.

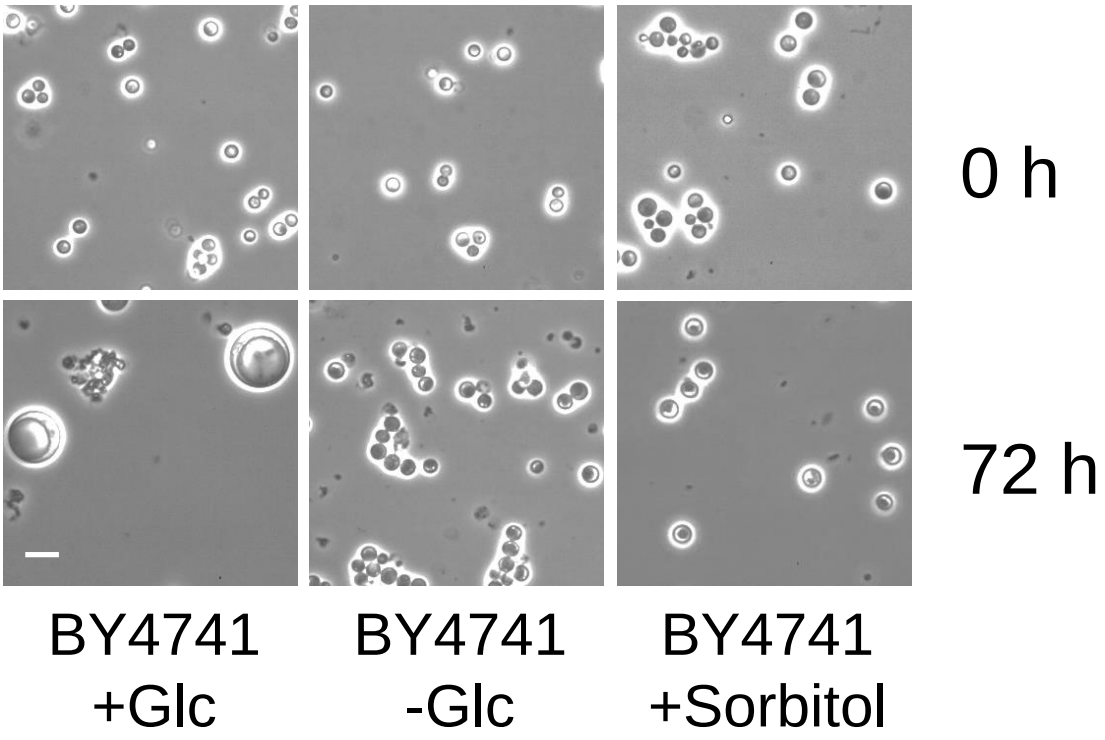

Figure 21: Growth of yeast protoplasts with and without glucose.

Comparison of protoplasts from the haploid reference strain BY4741 incubated at room temperature in standard stabilizing buffer (see material and methods) in the absence (center panel) and in the presence of 1 % glucose (left panel). Pictures were taken from freshly prepared protoplasts (0 h) and after 72 h. Note especially the increased fractional volume occupied by vacuoles and the appearance of giant protoplasts in the presence of glucose (left bottom panel). In the absence of glucose (center panel) protoplasts enlarged their size little. Moreover, in the presence of sorbitol (right panel) protoplasts enlarged their size only slightly. Scale bar, 10 µm.

Under normal culture conditions with an appropriate carbon/nitrogen supply (rich medium like yeast extract-pentose-dextrose (YPD) medium) and temperature (20 – 30 °C), yeast cells display a doubling time of about 90 min, which means the individual cell is doubling its size nearly every 90 min. Therefore, a haploid cell of approximately 4 µm in diameter doubles the membrane surface area of 50 μm^2 every 90 min or provides 50 μm^2 of fresh membrane material through exocytosis. Assuming an average diameter for exocytotic vesicles of 100 nm, this requires about 1600 vesicles/cell cycle (90 min with appropriate nutrient supply), 1070 vesicles/h or 18 vesicles/min. The growth rate and the exocytotic activity of protoplasts as described above, is therefore roughly in the same range as of a normal growing cell (216 *vs.* 1070 vesicles/h). Insofar, yeast protoplasts are physiologically intact. Therefore yeast cells are an appropriate system for studying physiological processes such as endo- and exocytosis.

6.2. **Internalization of FM4-64**

Previous experiments confirmed that yeast protoplasts are alive and apparently taking up and metabolizing glucose for growth. This process requires incorporation of new membrane material into the plasma membrane by exocytosis. In order to test whether yeast protoplasts are also able to internalize membrane material from the cell surface via endocytosis, the membrane marker FM4-64 was used in isolated yeast protoplasts. FM4-64 is a membrane selective fluorescent marker and belongs to the group of amphiphilic styryl dyes (Betz *et al.,*1996). In polar solutions these dyes are almost non fluorescent. After contact with membranes (e.g., the plasma membrane or the tonoplast), the hydrophobic tail of the dye compound intercalates with the bilayer, abundantly increasing the fluorescence, while its electrically charged head group prevents the dye from crossing the membrane. This means that the dye can only be transported into the cell via fission of vesicles, thus endocytosis. Therefore FM dyes are commonly used for tracking and examining endocytosis in eukaryotic organisms (Emans, 2002; Gaffield & Betz, 2006).

Overnight grown protoplasts from the haploid yeast strain BY4741 were incubated for 30 min with 20 µM of the endocytosis marker FM4-64. The fluorescence within the protoplasts and cells was followed by using a confocal laser scanning microscope (CLSM). Membrane staining was observed just before washing (0 min) and up to 150 min after removal of the fluorescent marker from the external medium in 30 min intervals. After the removal of the marker protoplasts/cells were resuspended in stabilizing buffer with glucose. Figure 22 shows the staining of the plasma membrane of yeast protoplasts at the beginning of the experiment with some scattered fluorescent spots inside the protoplasts. After 60 min the plasma membrane shows almost no fluorescence anymore, but clear staining of inner membrane compartments. Especially the tonoplast becomes visible through some fluorescence, but also do other not well defined intracellular locations (Fig. 22, center left panel). After 90 min, FM4-64 fluorescence was associated almost only with the tonoplast (Fig. 22, center right panel). After another 30 min the fluorescence distribution was almost the same. This indicates the removal of membrane material from the plasma membrane with a subsequent translocation towards the cell and incorporation into the vacuolar membrane.

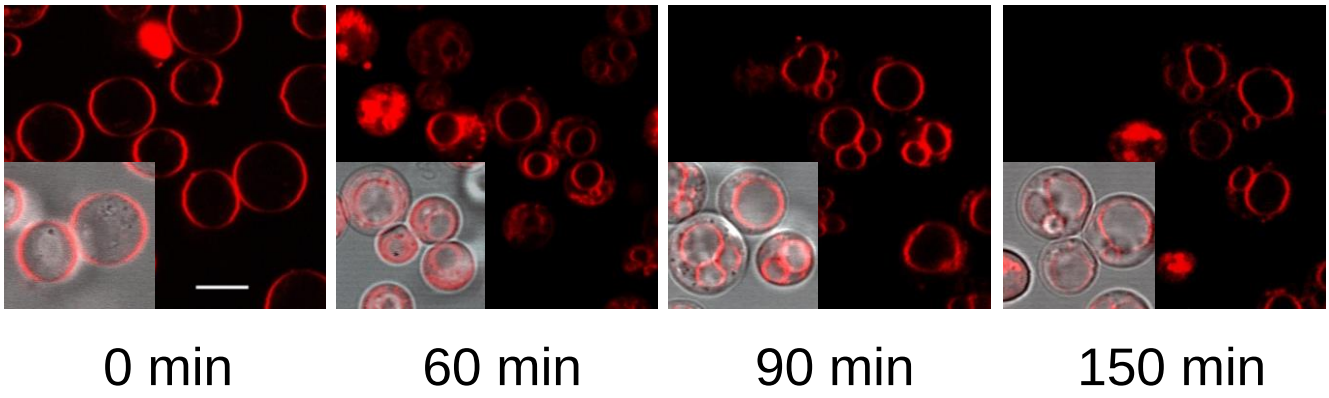

Figure 22: Internalization of the fluorescent endocytosis marker FM4-64 in yeast protoplasts.
Protoplasts from the yeast strain BY4741 were incubated in 20 µM FM4-64 for 30 min and washed in stabilizing buffer containing 1 % glucose. Pictures were taken on a Leica CLSM immediately before washing (0 min), 60 min, 90 min and 120 min after removal of FM4-64 from the external medium. Note the relocation of the fluorescence from the plasma membrane and the appearance of a fluorescent inner ring (right panel), representing the vacuolar membrane. The corresponding overlays are inserted to guide the eye. Bar, 5 µm.

Translocation of the fluorescence marker can also be represented by relative fluorescence: the ratio of fluorescence from the inside of the cell to that of the whole cell (Fig. 23). At 0 min the relative fluorescence was low at approximately 20 %. After 60 min the value increased to nearly 85 %, indicating redistribution of the fluorescence signal towards the inside of the cell. At the following points of time the value remained almost constant. This result illustrates again that protoplasts are able to internalize FM4-64 and, consequently lipids, via endocytosis.

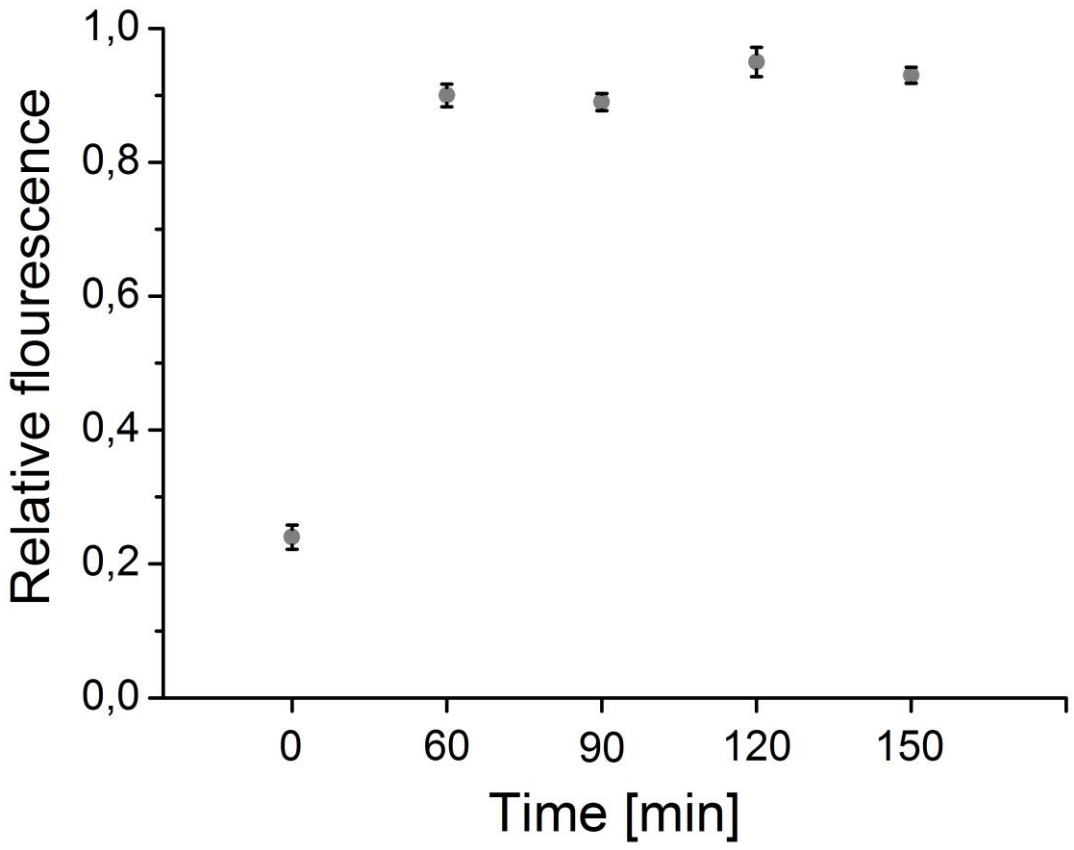

Figure 23: Relative Fluorescence of FM4-64 in yeast protoplasts.

The internal fluorescence was set in relation to the total fluorescence of the protoplast. For each point of time the average of 10 cells was taken. At 30 min the cells were washed and a recording was not possible. Error bars represent SEM.

In this context, inhibition of endocytosis was subsequently investigated in intact cells and protoplasts through application of ikarugamycin (IKA), a general inhibitor of clathrin-mediated endocytosis, with FM4-64 used as marker (Bandmann *et al*., 2012; Luo *et al*. 2001). Intact cells were incubated with 20 µM of FM4-64 and 30 µM IKA. As a control a sample without IKA was prepared. Initially (Fig. 24, left panel), the FM dye was located at the plasmalemma in both preparations. After 60 min, no redistribution of the marker was observed in the IKA-treated sample. The staining remained limited to the plasma membrane, while small fluorescence spots could be detected directly underneath or next to it (Fig. 24, middle panel). In absence of the inhibitor, the FM signal relocated, in small fluorescent rings, into the interior of the cells, representing the staining of the tonoplast. After 120 min, cells prepared with IKA still exhibited only membrane-associated fluorescence, while in the control cells the staining was mainly observed in the cell interior, at the tonoplast (Fig. 24, right panel).

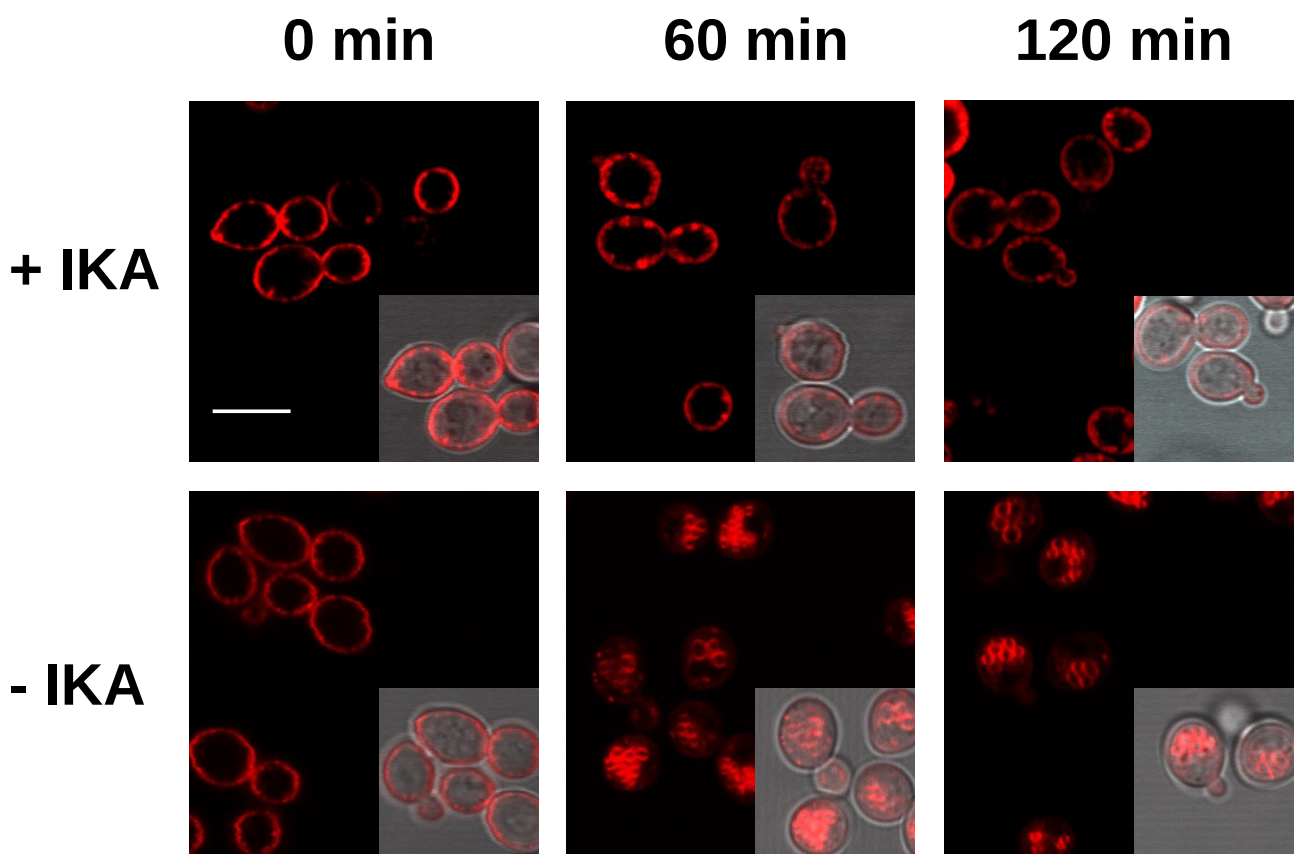

Figure 24: Inhibition of the internalization of the fluorescent endocytosis marker FM4-64 by IKA in intact yeast cells (BY4741).

Cells were incubated in 20 µM FM4-64 and 30 µM IKA for 30 min in stabilization buffer with 1 % glucose. Protoplasts were washed with the same buffer. The pictures were taken on a Leica CLSM at 0, 60 and 120 min. Cells in the preparation with IKA were not able to internalize FM4-64 even after 120 min. Small spots near the plasma membrane are visible. Cells without IKA showed at 60 and 120 min small fluorescent rings within the cells (middle and right panel), representing the vacuolar membrane. The small grey insets show the corresponding bright field images and overlays to guide the eye. Bar, 5 µm.

Figure 25 depicts the results of analogous IKA-mediated inhibition performed upon yeast protoplasts. After 60 min of incubation, no internalization of FM4-64 in the IKA-treated sample was observed, suggesting inhibition of endocytosis (Fig. 25, bottom-middle panel), at 120 min, internal membrane compartments exhibited slight fluorescence (Fig. 25, bottom-right panel). This could indicate that FM4-64 was internalized in a slower manner, suggesting clathrin-independent endocytosis (CIE) taking place in the protoplasts. Prosser and co-workers (2011) discovered a novel endocytotic pathway - the “Rho1 mediated endocytosis” in yeast. Before this discovery the existence of CIE in yeast was not unequivocally verified.

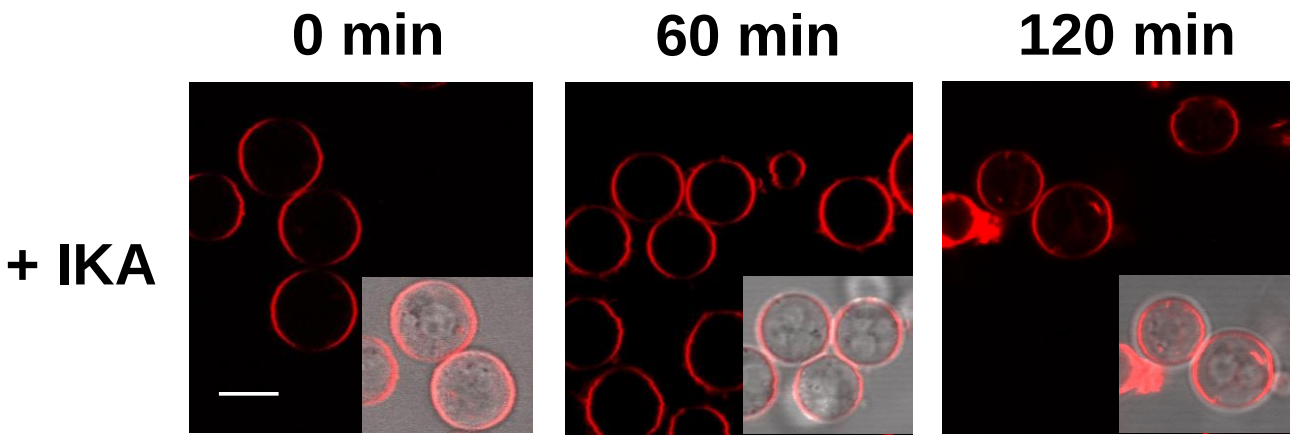

Figure 25: Inhibition of the internalization of the fluorescent endocytosis marker FM4-64 in yeast protoplasts by IKA.

Protoplasts from the yeast strain BY4741 were incubated in 20 µM FM4-64 and 30 µM IKA for 30 min. Protoplasts without IKA are shown in figure 22. Pictures were taken on a Leica CLSM at 0, 60 and 120 min. Protoplasts treated with IKA were not able to internalize FM4-64. The small grey insets show the corresponding bright field images and overlays to guide the eye. Bar, 5 µm.

6.3. **Internalization of fluorescent beads**

To observe endocytosis of particles of a certain size from the cell exterior into the cytosol, small spherical nano beads or microspheres were used (Bandmann *et al.*, 2012). To investigate this yeast cells and protoplasts were incubated with fluorescent nano beads of 20, 40 or 100 nm diameter. The appearance of fluorescence within the protoplasts/cells was followed by using a CLSM. Figure 26 compares internalization of fluorescent nano beads in intact yeast cells with isolated protoplasts. After 20 minutes the cells/protoplasts incubated with 20 nm or 40 nm beads showed internal fluorescence, whereas no fluorescence could be observed with 100 nm beads (data not shown). This is consistent with the work of Bandmann *et al*. 2012, who observed exclusion of particles in the same size range in intact BY-2 cells, even though BY-2 protoplasts could internalize particles of up to 1000 nm. In yeast, internalization and size exclusion in freshly prepared protoplasts and intact cells were the same, indicating that the yeast-specific mechanism of bead internalization was different from that characteristic for plant cells. It is also interesting to observe that the cell wall is not a limiting factor for the internalization of particles. Another parameter for size exclusion seems to play a key role. It can be assumed that size selection is due to the small collars formed during the invagination process of an endocytic vesicle (Liu *et al*., 2006; Liu *et al*., 2009; Liu *et al*., 2010). In average, the invagination collar has a diameter of 35 - 45 nm and is 150 - 250 nm long (Mullholland *et al*., 1994; Liu *et al*., 2006). This would be in agreement with the particle size exclusion observed in this experiment and would represent the limiting factor for the internalization of nano beads.

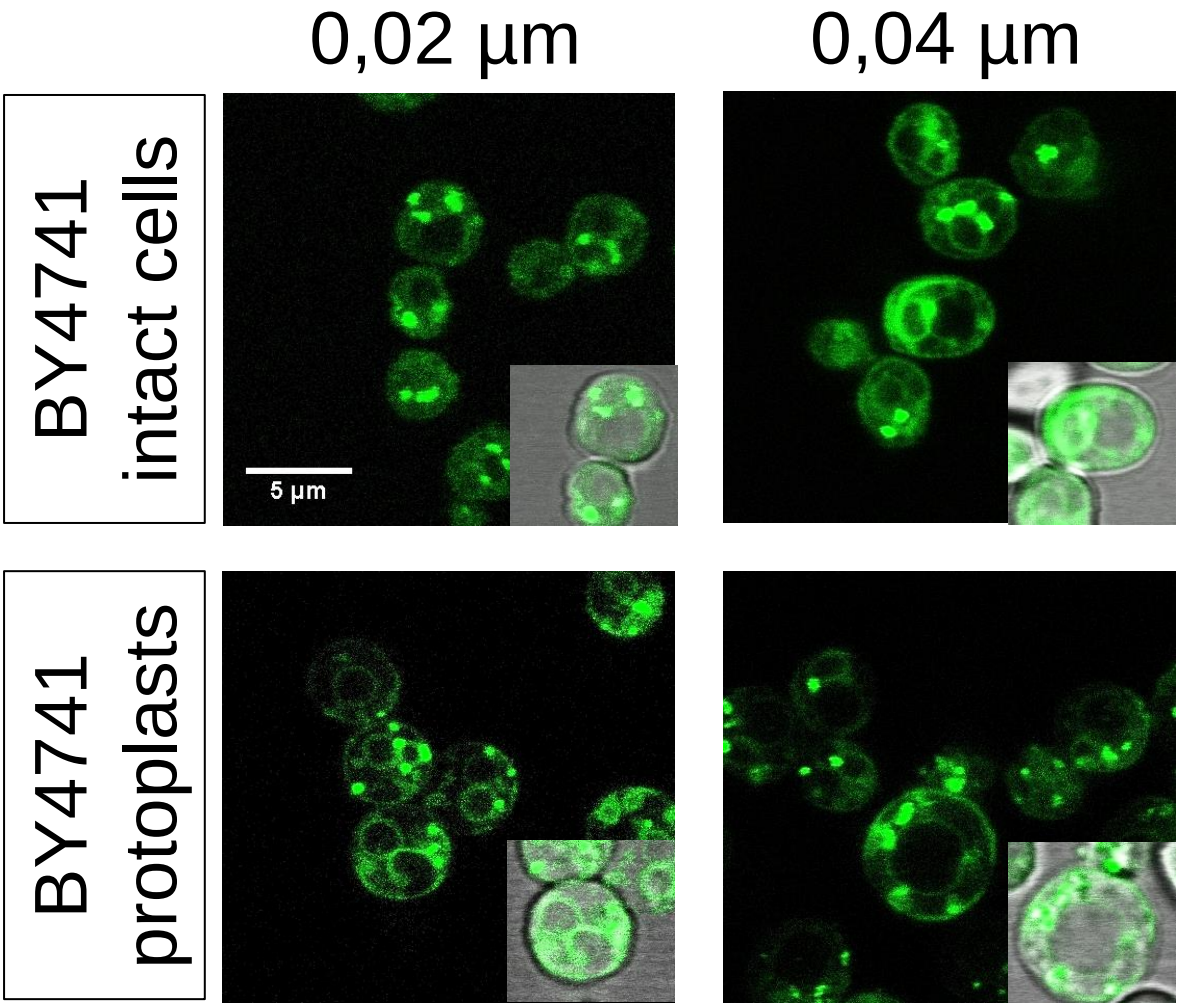

Figure 26: Internalization of fluorescent beads.

Yeast cells and protoplasts were incubated 20 min with fluorescent nano beads in the sizes of 20, 40 and 100 nm before CLSM recordings. Intact cells as well as protoplasts were able to internalize 20 and 40 nm particles but not beads with a size of 100 nm (data not shown).

6.4. Spontaneous changes in membrane capacitance

6.4.1. Modes of exo- and endocytosis in yeast

The previous experiments confirmed that yeast protoplasts are still able to increase their membrane surface and to internalize membrane and particles, thus protoplasts are able to perform endo- and exocytosis. In order to directly detect individual endocytotic and exocytotic events in real time, capacitance measurements in the cell-attached configuration were performed on isolated yeast protoplasts. In figure 27 typical membrane capacitance (C_m) recordings with sudden changes in membrane capacitance are depicted. These C_m steps were either positive (upward steps), indicating an increase in membrane surface area through an exocytotic event, or negative (downward steps),

indicating a decrease in membrane surface area through an endocytotic event. A closer examination of the dynamics of vesicle fusion and fission shows that the C_m changes could be grouped in four different categories according to the different kinetic modes which were observed. This includes transient fusion/fission events as well as permanent fusion/fission of vesicles. These different fission and fusion modes were also observed in mammalian and plant cells, suggesting that these mechanisms are highly conserved among eukaryotes (Ceccarelli *et al*., 1973; Henkel *et al*., 2000; Weise *et al*., 2000; Thiel *et al*., 2009; Bandmann *et al*., 2011; Rituper *et al*., 2013a). Individual events are considered transient, if a change in membrane capacitance is followed rapidly, in less than two seconds, by another step of the same amplitude, but in the opposite direction (Fig. 27, right panel). Permanent events are characterized by rapid membrane capacitance changes into a new stable level (Fig. 27, left panel). These capacitance changes from one level to another have to take place in less than 0.2 s.

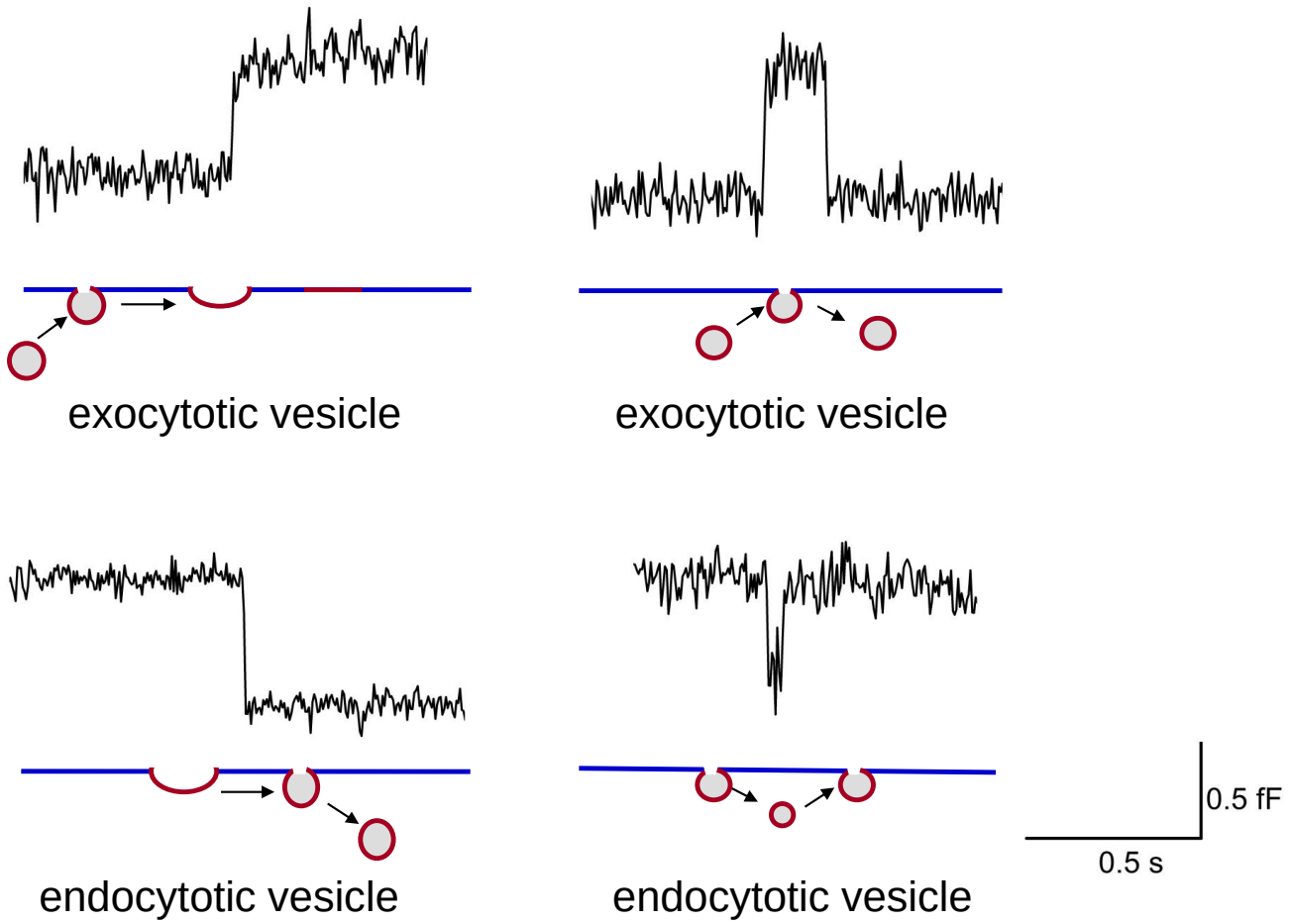

Figure 27: Examples of capacitance recordings from protoplasts of the yeast strain BY4741 in the cell-attached recording configuration.

Spontaneous changes in membrane capacitance can occur as transient events (right panel). These event types are characterized by a sudden change in membrane capacitance which is followed by a change in membrane capacitance of the same magnitude, but in the opposite direction. Permanent events as shown in the left panel, are characterized by a sudden change in the membrane capacitance to a new stable level. Upward deflections represent an increase in membrane capacitance resulting from an increased membrane area and indicating exocytotic events (upper left panel), whereas downward deflections represent a decrease in membrane capacitance resulting from a decreased membrane area and indicates endocytotic events (lower left panel). The depicted currents are from this work. The illustrations were adapted from Bandmann *et al*., 2011.

The background noise in of 9 current traces was calculated. The analysis was realized with amplitude histograms calculated from the current traces (Fig. 28). The range of the noise can be calculated by fitting the data of the amplitude histogram with a Gauss function of the form: $(y_0 + A\, e^{[-\left(\frac{x-x_0}{width}\right)^2]})$ (eq. 11). The width of the Gauss function represents the standard deviation, the width of the “bell”. In this case the width also describes the range of the noise. In this work the background noise ranged from 0.09 to 0.22 fF with an average value (n = 9) of 0.12 ± 0.01 fF. The detection of small vesicles in

the range of 100 nm in diameter with a change in capacitance 0.26 fF could be resolved (see chapter vesicle size distribution).

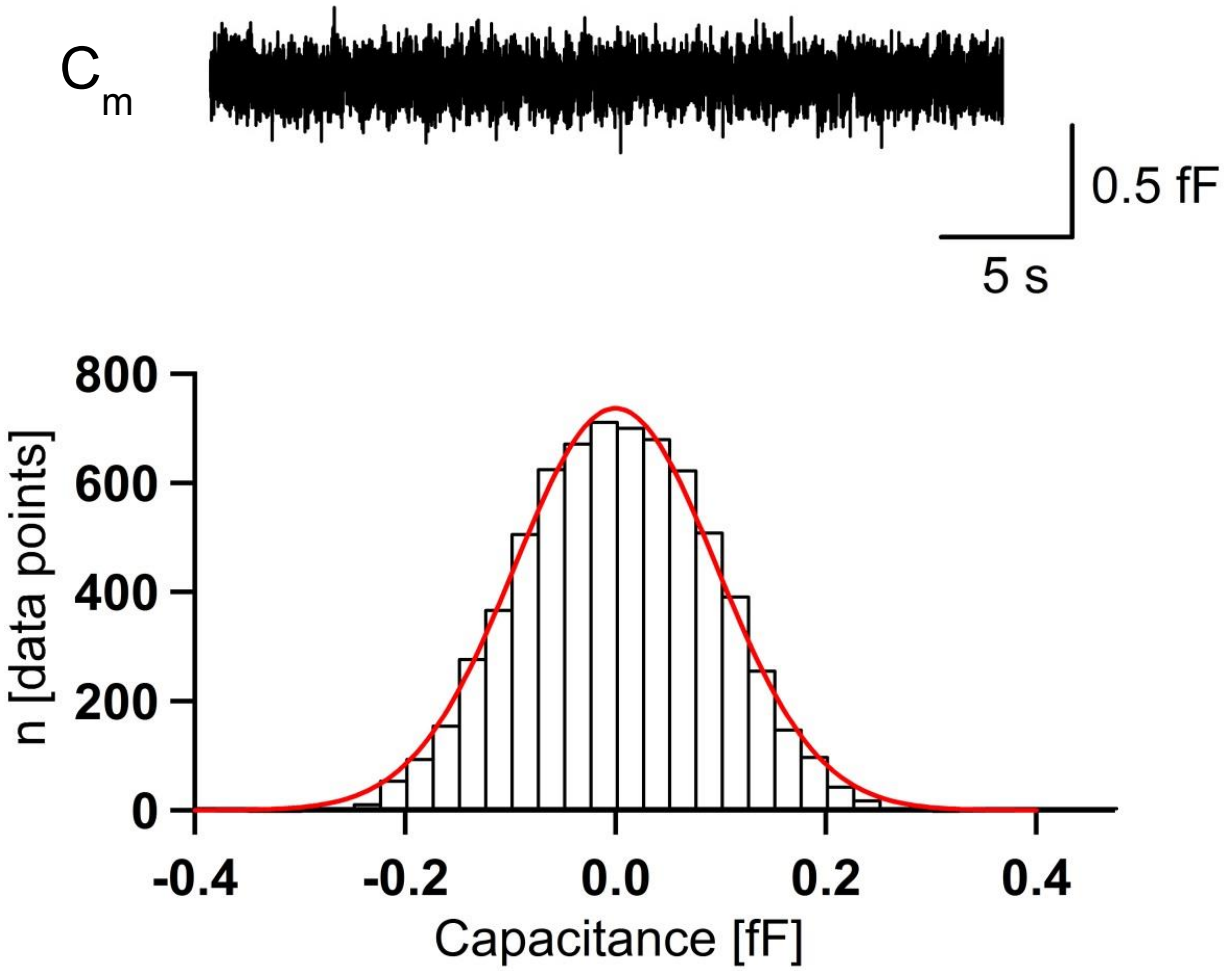

Figure 28: This represents the amplitude histogram of an *Im* current trace.
On the top an *Im* current trace is depicted, which can be represented as an amplitude histogram (bottom). The data of the histogram were described with a Gauss function in order to determine the width. This value can be used to estimate the background noise of the measurements. In this trace the width was 0.137 fF ± 0.001. The error is represented as standard deviation (SD).

To further analyze transient capacitance changes the amplitudes of the upward (on-step) steps were plotted against the amplitudes of the downward steps (off-step) of all transient events (Fig. 29). To bring the amplitudes of upward steps and downward steps of exocytotic and endocytotic events in relation, the values were described with a linear regression with a slope of 1.02 (correlation coefficient of 0.95), which show that on- and off-steps of transient events were of identical size. The correlation of the upward and downward steps shows that the capacity changes were throughout the same size (Fig. 29).

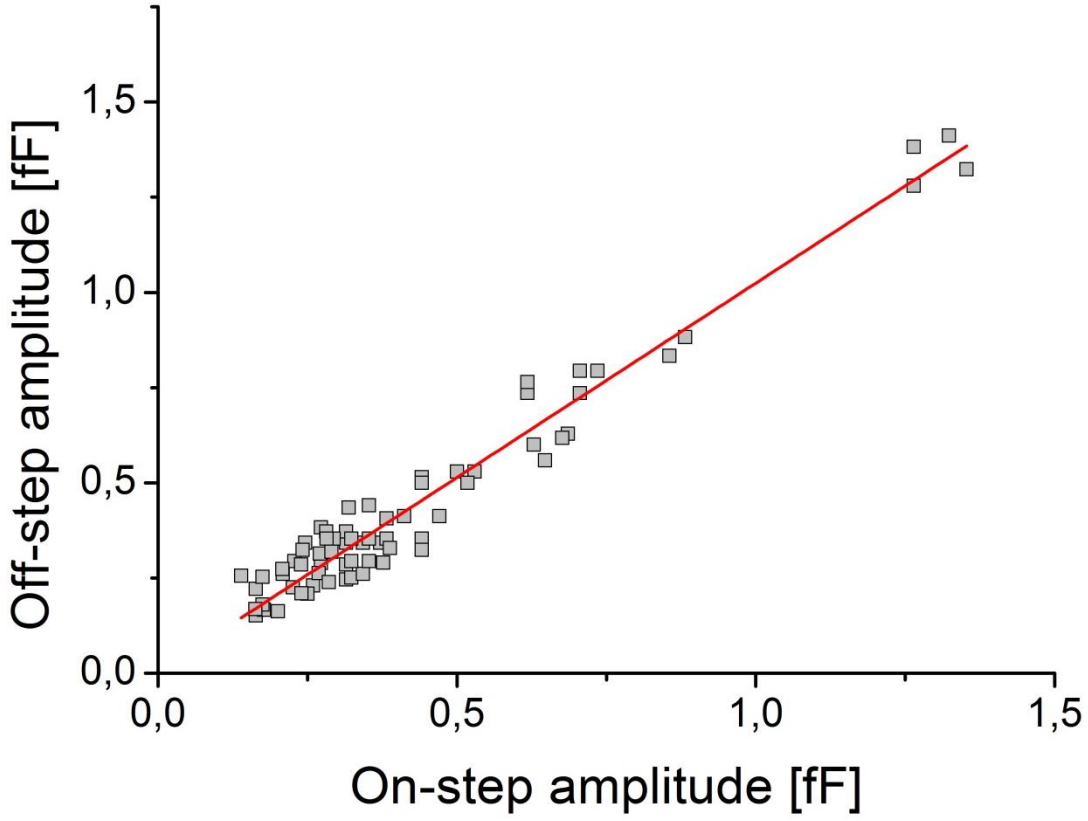

Figure 29: Correlation between amplitudes of the upward and the downward step of the transient membrane capacity changes.

The on-steps of transient exocytotic and transient endocytotic events were plotted against the corresponding off-steps. The line represents the linear regression with a slope of 1.02 (correlation coefficient of 0.95) for exo- and endocytotic events.

In addition to the simple transient or permanent events shown above, a variety of more complex events were observed (Fig. 30). These include transient exocytotic events and successive, staircase like permanent endocytotic and exocytotic events (Fig. 30C, D, E). Also, successive transient events as shown in figure 30B were observed. These compound events consisting of different amplitudes of on- and off-steps, indicate that vesicles of different sizes fuse successively with, or fission from the plasma membrane (Lollike *et al*., 2002; Toyooka *et al*., 2009; Wu *et al*., 2014). Similar complex events were also reported from BY-2 Protoplasts (Bandmann *et al*., 2011). Mainly staircase like, permanent compound events were detected.

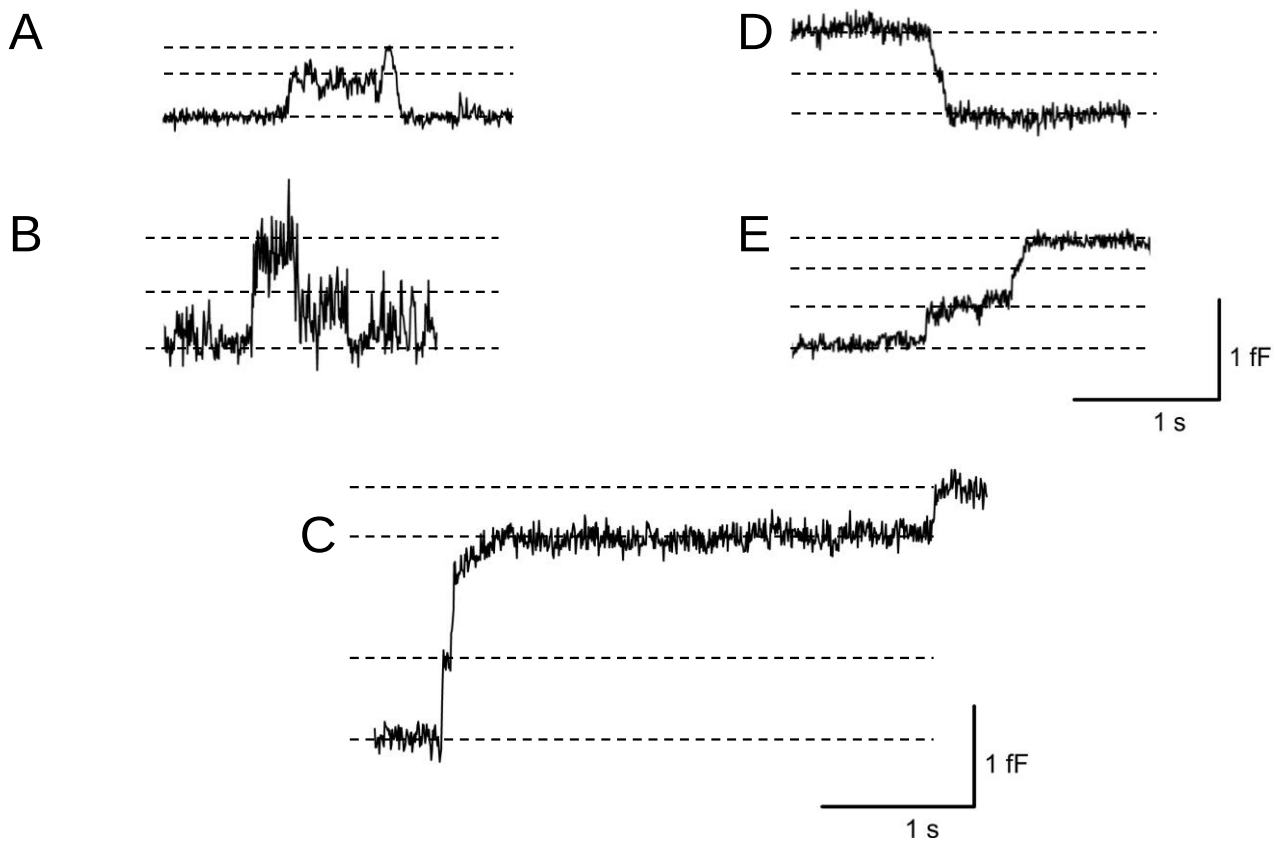

Figure 30: Examples of more complex capacitance changes in yeast protoplasts.
Cell-attached recordings reveal complex sequences of exo- and endocytotic events with various amplitudes of capacitance steps, as indicated by the dashed lines. Capacitance changes can occur in a staircase like with sequential downward steps (D), indicating sequential fission of vesicles of similar size. Sequential upward steps (E, C) indicate fusion of several vesicles with different sizes. Occasionally flickering occurs, indicating repeated transient, incomplete fusion of vesicles (A, B).

The observation of these different types of capacitance changes demonstrate that the yeast system represents the dominant kinetics of exo- and endocytosis well, which are found in various eukaryotes (Weise *et al*., 2000; Thiel *et al*., 2009; Toyooka *et al*., 2009; Rituper *et al*., 2013a).

6.4.2. Frequencies of exo- and endocytotic events

The capacitance measurements in the cell-attached mode as described above were performed on 10 protoplasts. 80 % of them showed sudden changes in membrane capacitance in the fF range, indicating endo-/exocytotic activity. This does not mean that 20 % of the protoplasts were not performing endo-/exocytosis. In cell-attached patch-clamp experiments only a fraction of the cell surface (ca. 5 µm² nearly 1 %) is examined for endo-/exocytotic activity by the open pipette tip. The probability of observing endo-/exocytotic activity is rather low and long recording times would be necessary. Especially, cell membranes are not homogeneous, but organized into various domains

(Chapter 4.6). Moreover, endo-/exocytotic events are not necessarily evenly distributed over the entire cell surface; while some domains might be highly active, others are completely devoid of any endo-/exocytotic activity. This may depend on the lipid and/or protein composition of the individual membrane domains (Grossmann *et al.*, 2008). It has been demonstrated that for example special exocytotic sites for polarized secretion are marked by proteins, like Sec3p, as spatial landmarks in budding yeast (Finger *et al*., 1998a).Thus, the probability of observing exocytosis at these bud sites should be higher. The experiments in cell-attached mode suggest a low frequency of events in yeast. Yeast cells are not excitable cells like neurons and exocytotic events are regulated in a constitutive way (Kelly 1985), so a low frequency was expected. This could be confirmed in ten different experiments of capacitance measurement recordings. A more detailed view in figure 31 represents the frequency of the different exo- and endocytotic modes observed at 25 °C. Overall, the observed frequencies were 8.2 fission and 12.3 fusion events per hour, with the highest frequency observed for transient exocytotic events (8.1 ± 0.4 events/h) and the lowest frequency for transient endocytotic events (2.5 ± 0.1 events/h). The frequency of permanent events was similar (5.7 ± 0.3 endocytotic events/h and 4.2 ± 0.2 exocytotic events/h). It has to be considered that the measured frequencies are only a portion of frequency events in the whole cell.

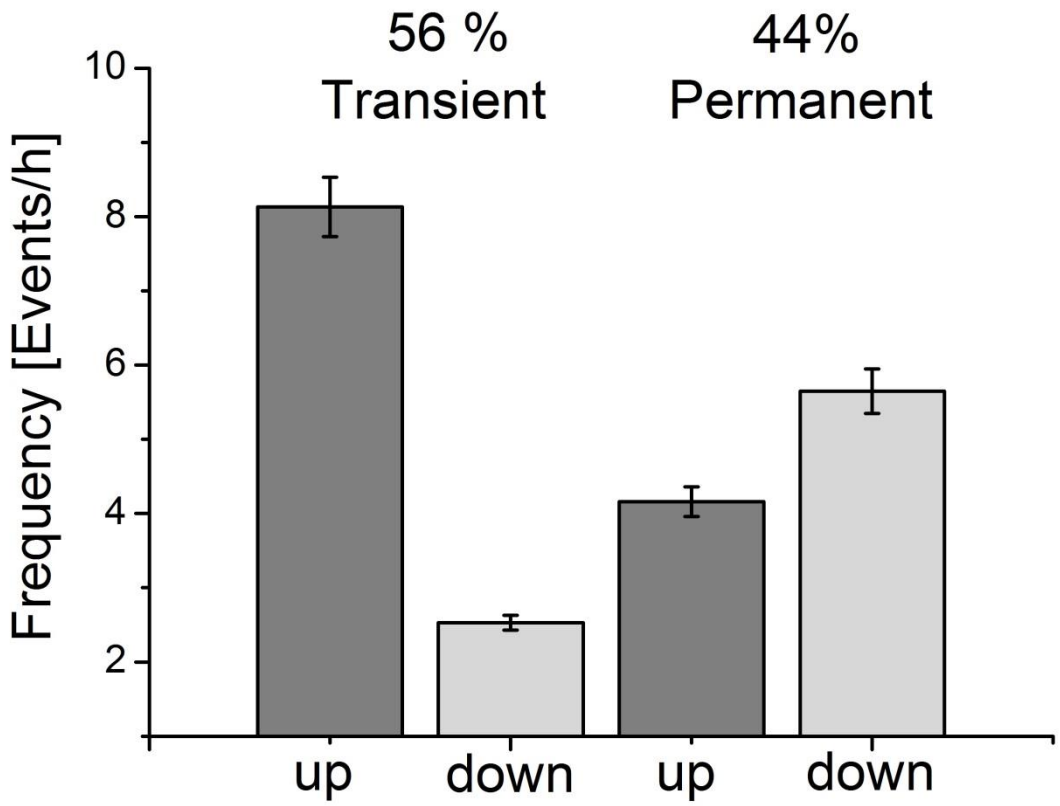

Figure 31: Frequency of the different modes of endo-/exocytotic events recorded from yeast protoplasts from the yeast strain BY4741 in the presence of glucose.

Data were collected from different protoplasts and represent the means of 10 independent experiments with a total of 133 events (61 transient up, 24 permanent up, 14 transient down and 34 permanent down) and a total recording time of 5.7 hours. Error bars represent SEM.

6.4.3. Energy requirement of exo- and endocytosis in yeast protoplasts

Exo- and endocytosis are ATP requiring processes (Holz *et al*., 1989; Robinson & Martin, 1998; Heidelberger, 2001; Theander *et al*., 2002). In exocytosis ATP is needed before and after docking of a vesicle (Burgoyne & Morgan, 1995; Robinson & Martin, 1998). The ATPase *N-ethylmaleimide-sensitive factor* (NSF; Söllner *et al*. 1993), which is an essential protein for exocytosis in mammalian cells requires ATP to function. This protein associates with membranes by binding *soluble NSF attachment Proteins* (SNAP) and *SNAP Receptors* (SNARE; Robinson & Martin, 1998). ATP hydrolysis caused by this protein provides energy, which is required for the termination of priming of vesicles (Scheller, 1995). It was suggested that NSF is responsible for the ATP dependent SNARE-complex disassembly (Söllner *et al*., 1993). In yeast Sec18p is the homologue of NSF which binds to yeast SNAREs Snc, Sso or Sec9 proteins (Grote *et al*., 2000). In response to insufficient nutrient supply, and thus low ATP concentration in the cell, the frequency of exocytotic events should

decrease. On the other hand, the process of endocytosis also requires energy, e.g., for depolymerization of clathrin from coated vesicles. ATP depletion of cells causes arrest of clathrin recycling (Clarke & Weigel, 1985; Brodsky, 1988). Since both processes involve ATP-depend reactions, the cells need energy-carrying molecules for correct activity.

In this context the energy-dependency of fission and fusion in protoplasts was investigated. In chapter 6.1 the growth of protoplasts, i.e. the increase of surface membrane area, was observed in the presence and absence of glucose. Cells depleted for glucose did not change their size. The initial observation that yeast protoplasts require an energy source for cell expansion is consistent with the observation that the internalization of gold particles occurs in an energy-dependent manner (Kim *et al*., 2006). This leads to the assumption that protoplasts depleted of glucose show lower event frequencies than protoplasts supplemented with glucose in the bath solution. Therefore, membrane capacitance measurements were performed in the presence and in the absence of glucose in the cell-attached mode on protoplasts of the strain BY4741. As shown in figure 32 endo-/exocytotic events occurred at a frequency of 5.9 ± 3.6/h (n = 7) in the absence of glucose and at 20.5 ± 7.0/h (n = 10) in the presence of glucose in the incubation medium. In the absence of glucose the frequencies of exo- and endocytotic events are reduced. The size membrane area underneath the pipette in the cell-attached mode is ca. 5 μm^2. Considering only this membrane area in a cell of 5 µm diameter, the total event frequencies are nearly 84 events per hour in the absence and 290 events per hour in the presence of glucose. The low frequencies for exo- and endocytosis in cells without glucose are explained by the assumption that both processes occur in a reduced way (Brodsky, 1988; Bittner *et al*., 1989; Holz *et al*., 1989; Eliasson *et al*., 1997; Heidelberger, 2001). These results are in accordance with the estimated frequencies calculated for protoplasts in chapter 6.1.

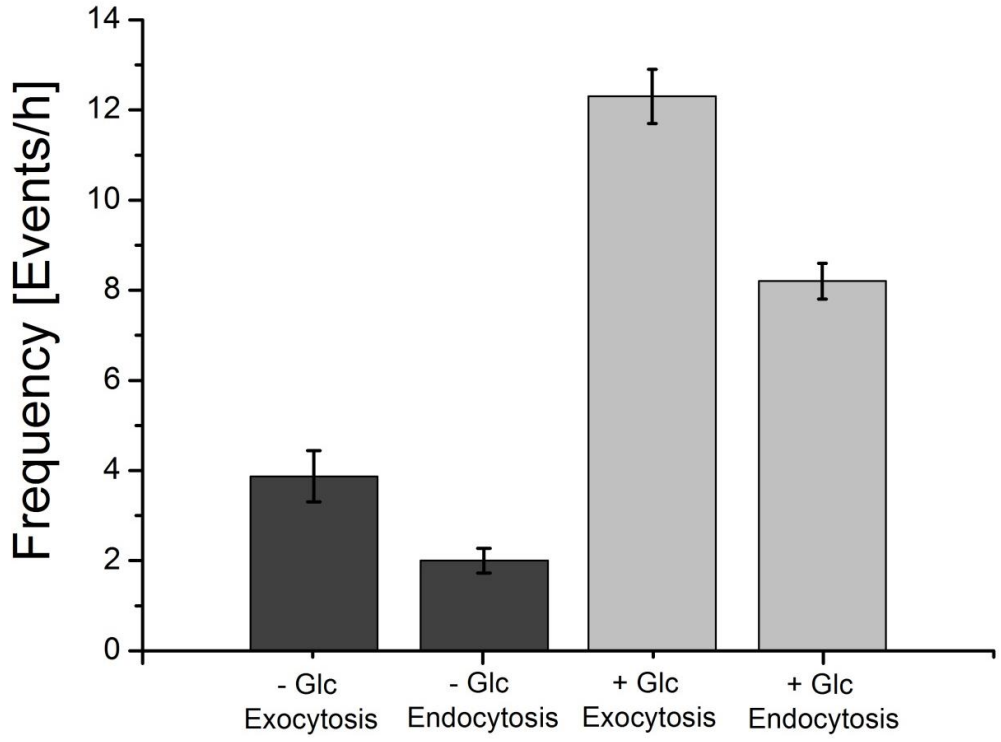

Figure 32: Frequencies of endo-/exocytotic events recorded from yeast protoplasts in the cell–attached patch-clamp configuration.

Data were collected from different protoplasts and contain all permanent and transient events. The data are the means of 10 independent experiments each, with error bars representing standard error of the mean (SEM).

6.4.4. Vesicle size distribution

Analysis of changes in capacitance resulting from endo-/exocytotic events in 8 independent experiments (total of 133 events) revealed, 60 % of the capacitance changes are in the range of 0.2 - 1 fF, corresponding to vesicle diameters ranging from 90 nm to 200 nm with a median value of 0.53 fF or 145 nm (Fig. 33). These numbers are based on the assumption that the specific membrane capacitance is about 8 mF/m^2 (Gentet *et al*., 2000; Homann & Tester 1998). In order to analyze the size distributions shown in figure 33, the measured capacitance changes are described by a lognormal distribution

$$N(C) = N_{max} exp^{[-(\frac{\ln(C/C_0)}{w})^2]} \qquad \text{(eq. 12)}$$

with N_{max} being the peak amplitude, C_0 the capacitance with the most frequent events (peak of the function), and w the width of the lognormal distribution defined as $ln(C/C_0)$ at $N(C) = 1/e$. Negative capacitance steps corresponding to endocytotic events and positive capacitance steps corresponding

to exocytotic events followed a lognormal distribution and showed a similar width of 0.83 and 0.81, respectively. However, the distributions has peaks at different capacitances with C_0 = 0.44 fF for the endocytotic events and C_0 = 0.6 fF for the exocytotic events, indicating that on average endocytotic vesicles (132 nm) are smaller than exocytotic vesicles (155 nm). The results show that vesicle sizes, determined by electrical measurements performed in this work, are similar to those established in the electron microscopic (EM) studies 60 and 300 nm, as described above. Hence, the electrophysiological method is very well suited for investigation of exo- and endocytosis of the prevailing vesicles in yeast.

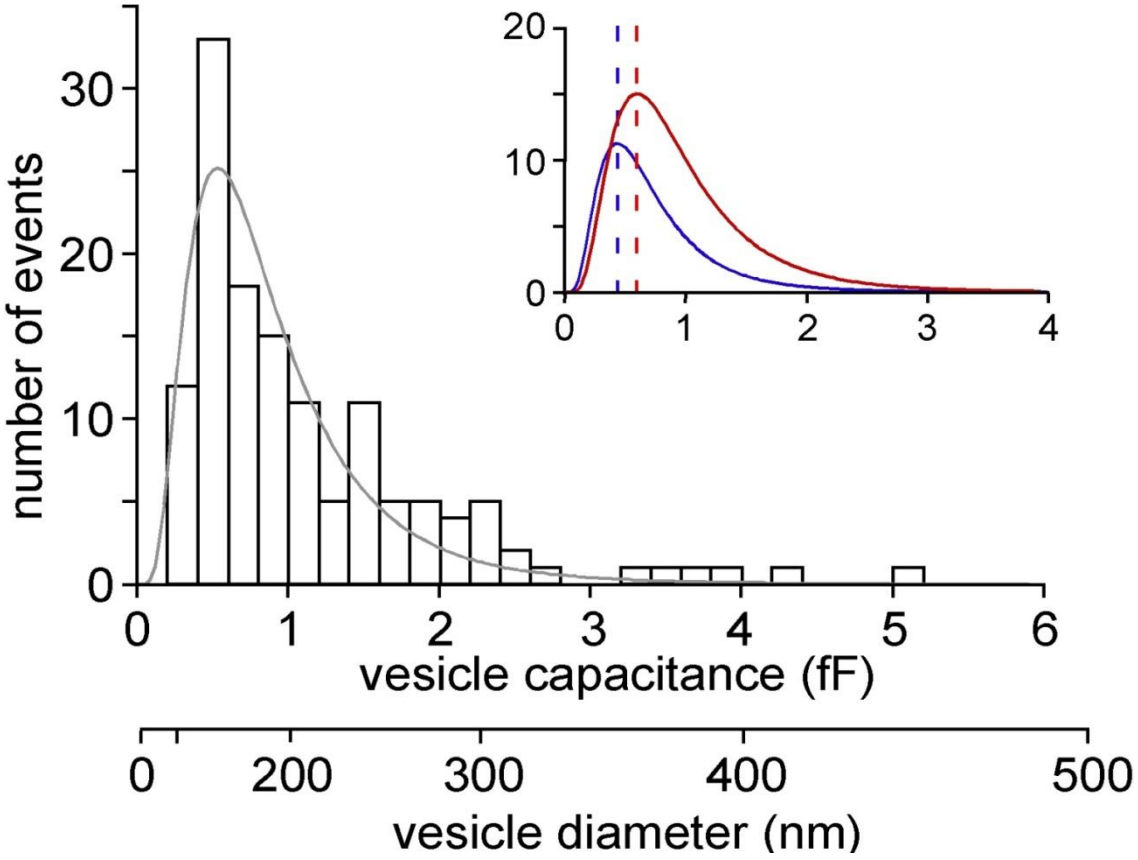

Figure 33: Vesicle size distribution of endo- and exocytotic events in BY4741.

Summary of all capacitance measurements collected from eight different protoplasts with a total number of events, n = 133 (endocytotic and exocytotic), recorded in the cell-attached configuration. The data follow a lognormal-distribution (solid grey curve) which centers at C_0 = 0.54 fF or 145 nm, with a width of w = 0.85. The width is defined as ln (C/C_0) at n = 1/e. Corresponding vesicle diameter values were calculated assuming a specific membrane capacitance of c = 8 mFm^{-2}, as determined by whole-cell patch-clamp recordings (Homann & Tester 1998). **Inset:** Distribution of capacitance steps related to endocytotic or exocytotic events. Data presented above, with a total of n = 48 endocytotic and n = 85 exocytotic events, recorded in the cell-attached configuration were analyzed separately. Both data sets follow a lognorm distribution centering at C_0 = 0.44 fF with a width of 0.83 for the endocytotic events (blue curve) and at C_0 = 0.6 fF with a width of 0.81 for the exocytotic events (red curve), respectively.

6.5. **Fusion pores in yeast cells**

In regulated exocytosis the merging between the vesicle and the plasma membrane leads to fusion pore formation. Fusion pores play an important role in secretion of signaling molecules such as transmitter, but also a key role in membrane recycling, translocation of receptors proteins and other membrane proteins (Kabaso *et al*., 2013; Chapter 4.3). In the non-fused state the fusion pore conductance (G_P) is equal to zero. During the fusion process the fusion pore dilates and the conductance of the patch changes to another level (Fig. 34). G_P is therefore a parameter to calculate the diameter of a fusion pore. In the cell-attached modus a change in the ΔG_P is reflected by an increase in the real part (*Re*) of the signal (Rituper *et al*., 2013a; material and methods chapter 5.10.3). This is the first time fusion pores are characterized by capacitance measurements in yeast. The experiments represent the first quantification of the size and frequency of fusion pores in yeast.

Figure 34 shows representative examples of simultaneous transient changes in the *Re* and *Im*, demonstrating reversible opening of the fusion pore during exo- and endocytosis. These simultaneous changes are not a result of incorrect phase-angle settings of the log-in amplifier. The phase of the lock-in amplifier was adjusted to set changes in the *Re* signal trace equal zero. To prove this, a manual calibration pulse was applied to ensure no projection in the *Re* trace and correct phase angle settings (Chapter 5.10; Fig. 16). Theoretically an increase in the *Re* traces and thus an increase in the conductance is expected. This is caused by the additional conductance current that flows through a narrow fusion pore of a non-completely fused vesicle (Fig. 12). In yeast incremental, decremental or no changes of the *Re* signal were detected as shown in figure 34 for transient or permanent events (Breckenridge & Almers, 1987; Lindau 1991; Henkel *et al*., 2000). The underlying mechanisms responsible for these changes are not fully understood yet. A possible explanation for this was suggested by Kabaso and co-workers 2013. They demonstrate that the decrease in the *Re* signal depends on the G_P as well as on the size of the fused vesicle.

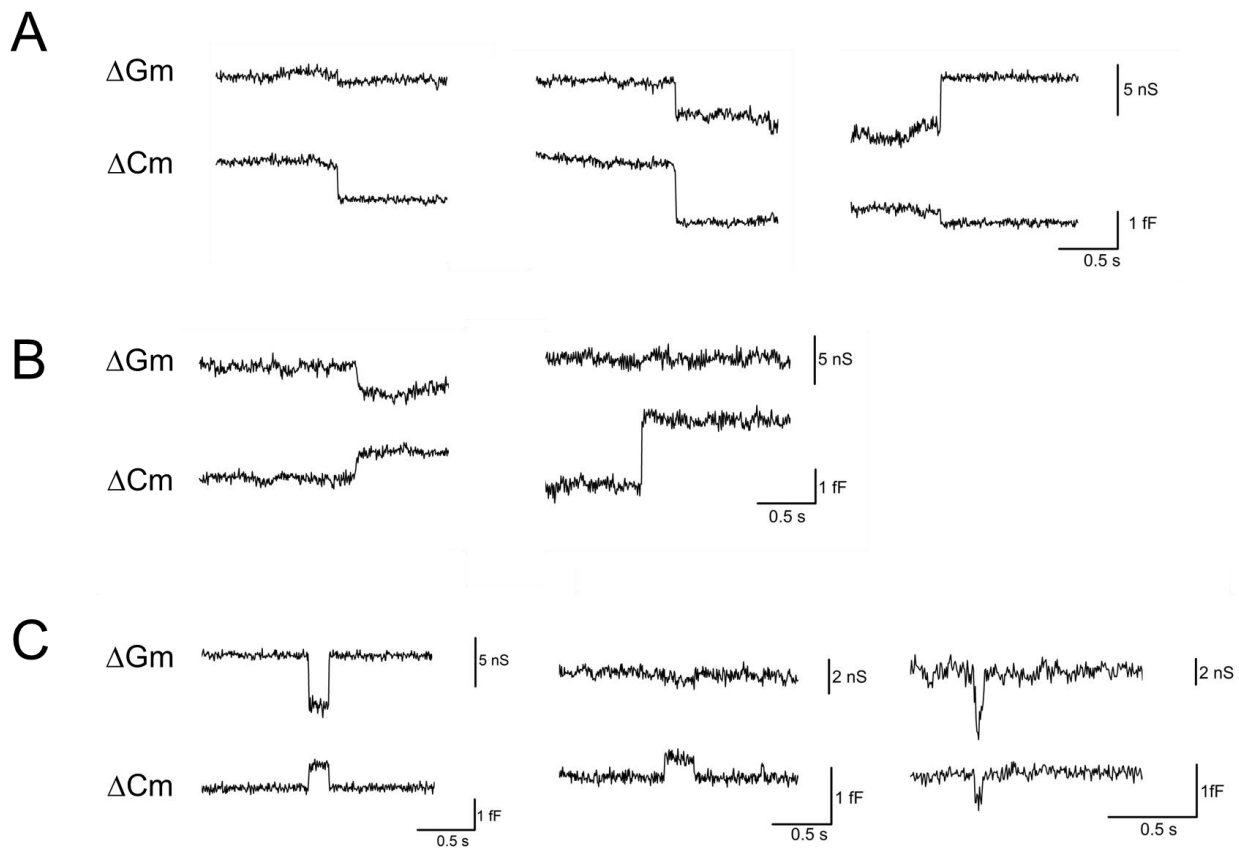

Figure 34: Examples for capacitance changes (ΔC_m) in the membrane with simultaneous changes in the conductivity of the membrane (ΔG_m).

This reflection represents the fusion pore conductivity. In **(A)** permanent endocytotic events are represented with an incremental, a decremental and a non-zero projection in the Re signal. **(B)** Shows permanent exocytotic events with decremental and non-zero projections. **(C)** Shows representative traces for transient events with decremental, incremental and non-zero projections.

From a total of 133 events recorded in 10 different experiments, 68 events showed changes in the Re signal and, thus, in the patch conductance. This represents 51 % of the events. From 75 recorded transient events, 42 were associated with a change in the patch conductance (56 %). 26 of the 58 recorded permanent events also showed a change in the patch conductance (45 %).

Figures 35 and 36 show the distribution of the calculated pore conductance for transient and permanent events. The median of transient exo- and endocytotic fusion pore conductance was 8.5 pS (range from 4 – 55 pS) and for permanent events 18.5 pS (range 4 – 65 pS).

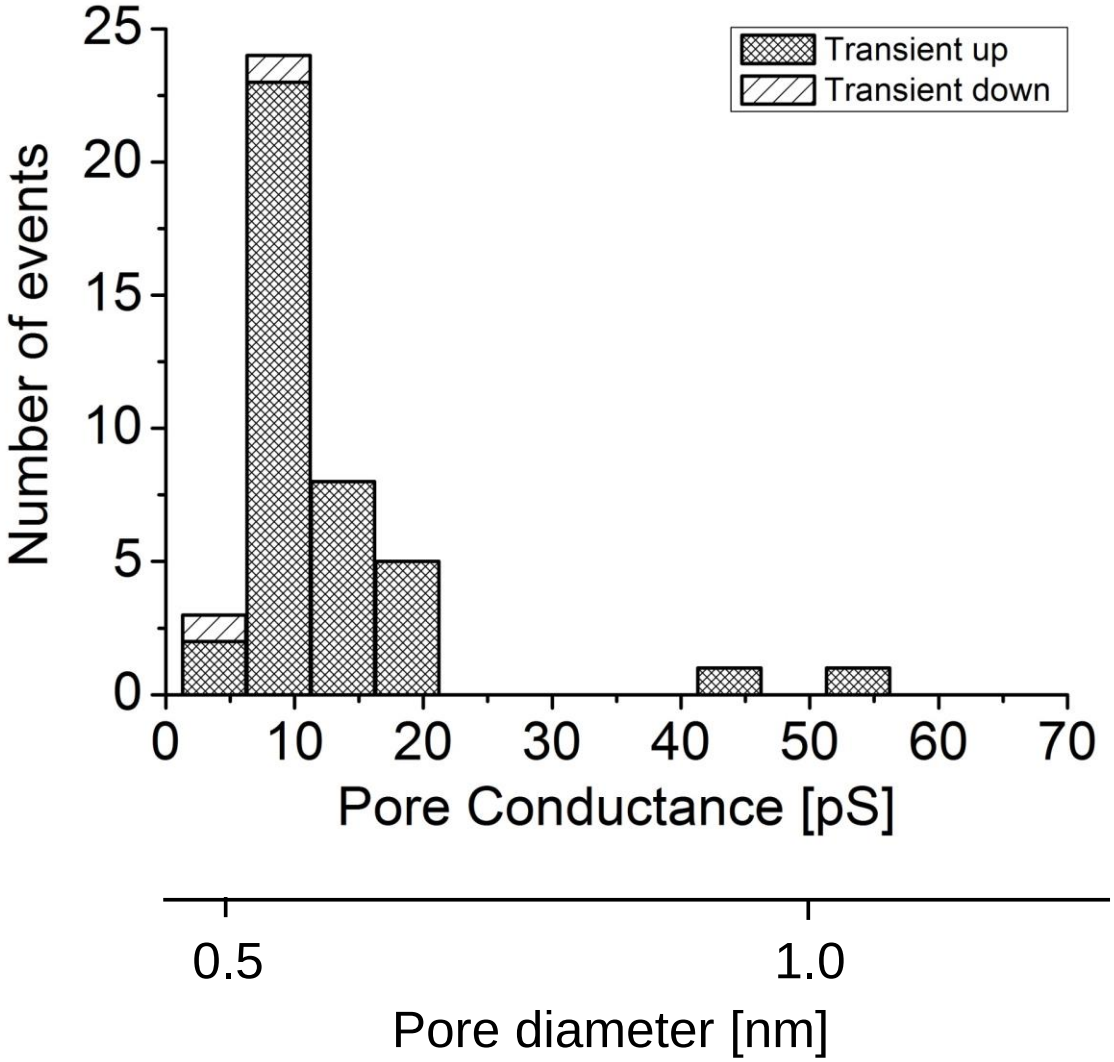

Figure 35: Distribution of fusion pore conductance calculated from transient changes in the patch conductance (transient changes in the *Re* signal trace) from 40 exocytotic and 2 endocytotic events.

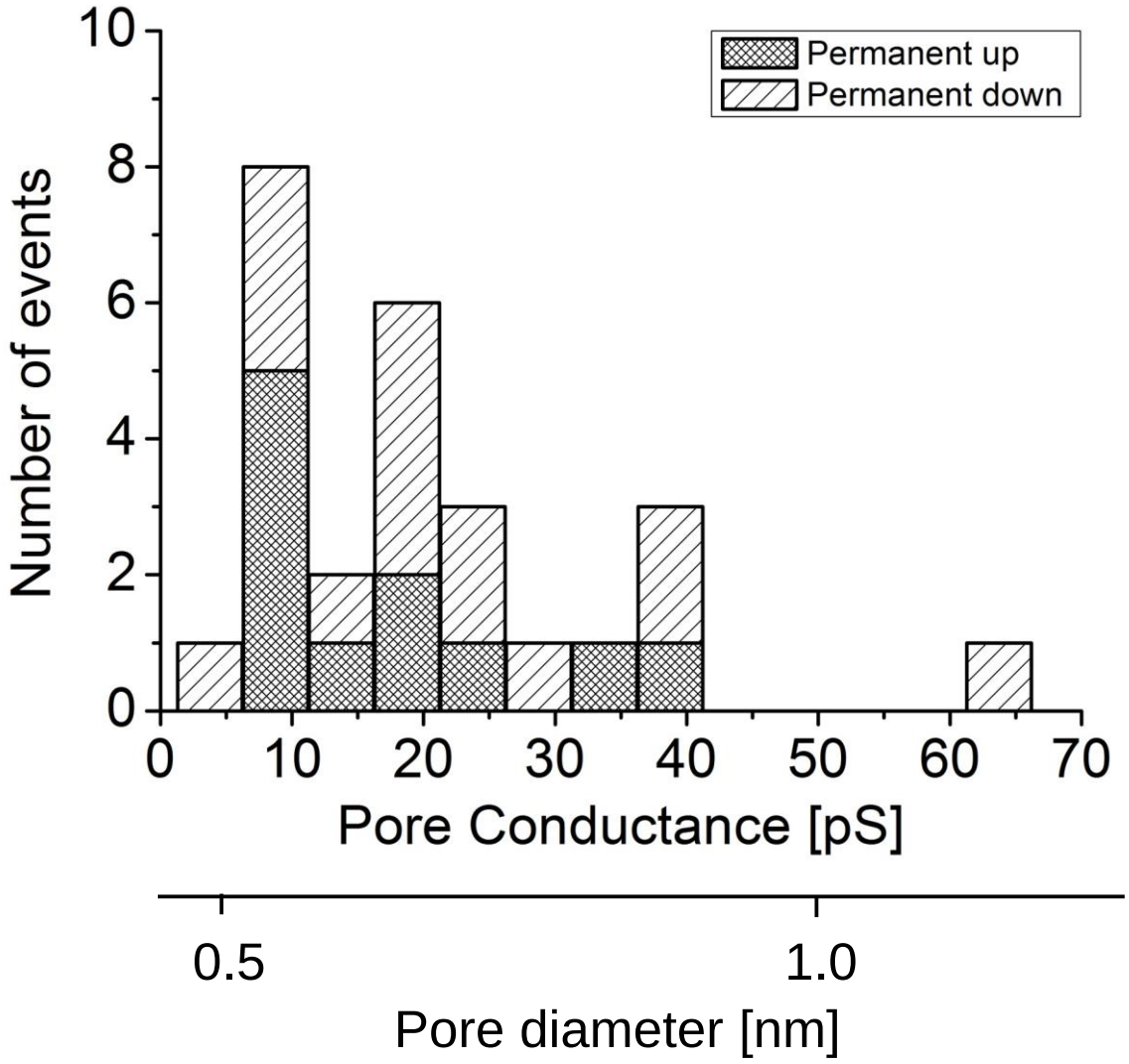

Figure 36: Distribution of fusion pore conductance calculated from permanent changes in the patch conductance (permanent changes in the *Re* signal trace) from 11 exocytotic and 15 endocytotic events.

In comparison to other eukaryotes, yeast cells show small conductances and hence small fusion pore diameters. The measurements show that in average fusion pores persist for 100 milliseconds (ms) at the plasma membrane. The time in which vesicle lumen is connected with the extracellular compartment (dwell-time) defines the time and the amount of cargo release. Studies in mammalian cells show that the dwell-time of fusion pores can be affected by different parameters, e.g. Ca^{2+} concentration (Alés *et al*., 1999; Elhamdani *et al*.,2006), hypotonicity (Jorgacevski *et al*., 2008) and phosphorylation (Henkel *et al*., 2001). In these studies the dwell-time of the fusion pores were longer, demonstrating that modulation of the fusion pore dwell-time could have an influence on vesicle cargo release.

6.6. **Modulation of exo- & endocytotic frequencies via the SY1 *sec6-4* mutant**

Previous results show that yeast is an adequate organism to study exo- and endocytosis by capacitance measurements. In chapter 6.1 we demonstrated that protoplast growth is inhibited in the strain SY1 at an incubation temperature of 37 °C (Fig. 20).The temperature sensitive secretory mutant (SY1) has a single point mutation in the Sec6-4 protein, which is part of the protein complex exocyst. The mutation L633P exchanges the lysin in the hydrophobic core of the subdomain B of the protein into a prolin. This probably destabilizes the α-helix and disrupts the hydrophobic packing contacts (Sivaram *et al*., 2006). The effect of this mutation is reversible at the nonpermissive temperature of 37 °C where secretion is inhibited and secretory vesicles are accumulated in the cytosol, as described before (Fig. 19; Chapter 6.1). At 25 °C the cells are able to grow in a normal way. In the growth-assay the effect of the mutation is also clear. Cells of the strain SY1 incubated at 37 °C are not able to grow due to the mutation. In comparison, cells of the strain BY4741 are able to grow well demonstrating that the temperature is not the limiting factor (Fig. 37).

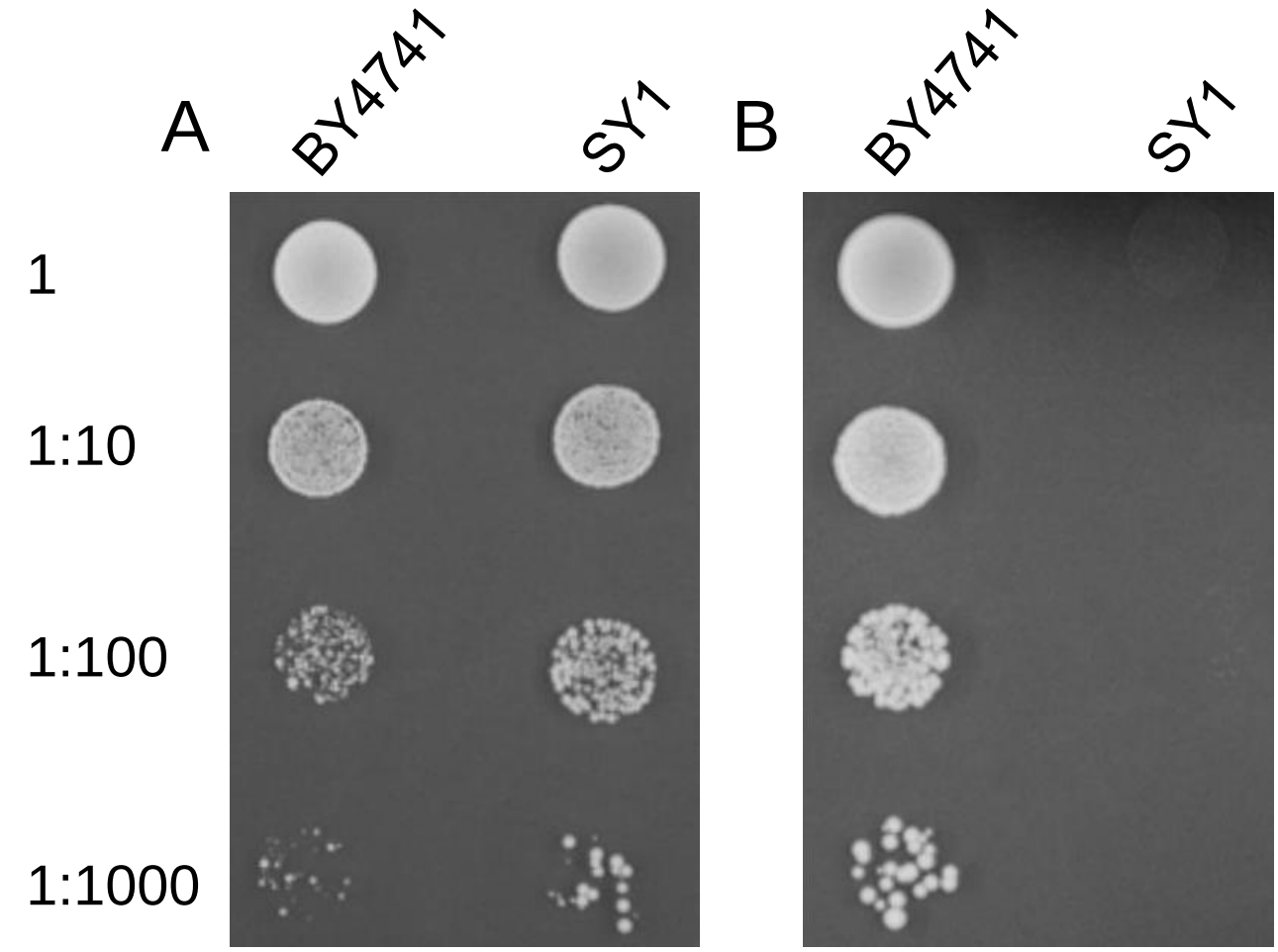

Figure 37: Growth-assay of yeast strains BY4741 and SY1 in complex media YPD

Cells were plated in different concentrations (1 - 1:1000). The concentration one refers to a cell density of OD =1 at λ=600 nm (approximately 10^7 cells). The other concentrations are diluted respectively. Cells were incubated for three days at 25 °C **(A)** and 37 °C **(B)**.

To calculate and visualize the time course for transporting the accumulated secretory vesicles to the plasma membrane, experiments using a GFP tagged membrane protein (Tok1) were performed. This protein is incorporated in the membrane and, thus, in the vesicles. The protein Tok1 is an outward rectifying potassium channel in yeast that is constitutively expressed. The potassium channel transports K^+ ions out of the cell at membrane potentials above the K^+ equilibrium (Ketchum *et al*., 1995; Bertl *et al*., 2003). To be able to localize the channel it was fused to the green fluorescence protein (Gfp). The expression of *tok1-gfp* could be controlled through a galactose promoter. The fusion protein was expressed in SY1 cells at the restrictive temperature (37 °C) in galactose containing media for 3 h. This resulted in an accumulation of fluorescent secretory vesicles in the cytoplasm (Fig. 38, 0 min). Afterwards, the cells were cultivated at the permissive temperature (25 °C) and, simultaneously, the expression of *tok1-gfp* was repressed by exchanging the medium to a

glucose-containing one. This procedure restarted exocytosis and Tok1-GFP was transported from the cytoplasm to the plasma membrane over a time period of about 180 min. The same procedure was applied for protoplasts with the difference that after 3 h of incubation at 37 °C the cells were digested and stored in stabilizing buffer with glucose (see material and methods 5.2). Recordings were made 0, 60, 120 and 180 min after the temperature shift for intact cells and protoplasts with the CLSM (Fig. 38). At the beginning (0 min) most of the GFP fluorescence was inside of the cell (secretory vesicles) in both preparations. After 120 min, cytoplasmic fluorescence was significantly reduced and the ring of the plasma membrane became visible. In intact cells the plasma membrane showed up already after 60 min. About 180 min after the temperature shift, most of the fluorescence was relocated from the cytoplasm into the plasma membrane.

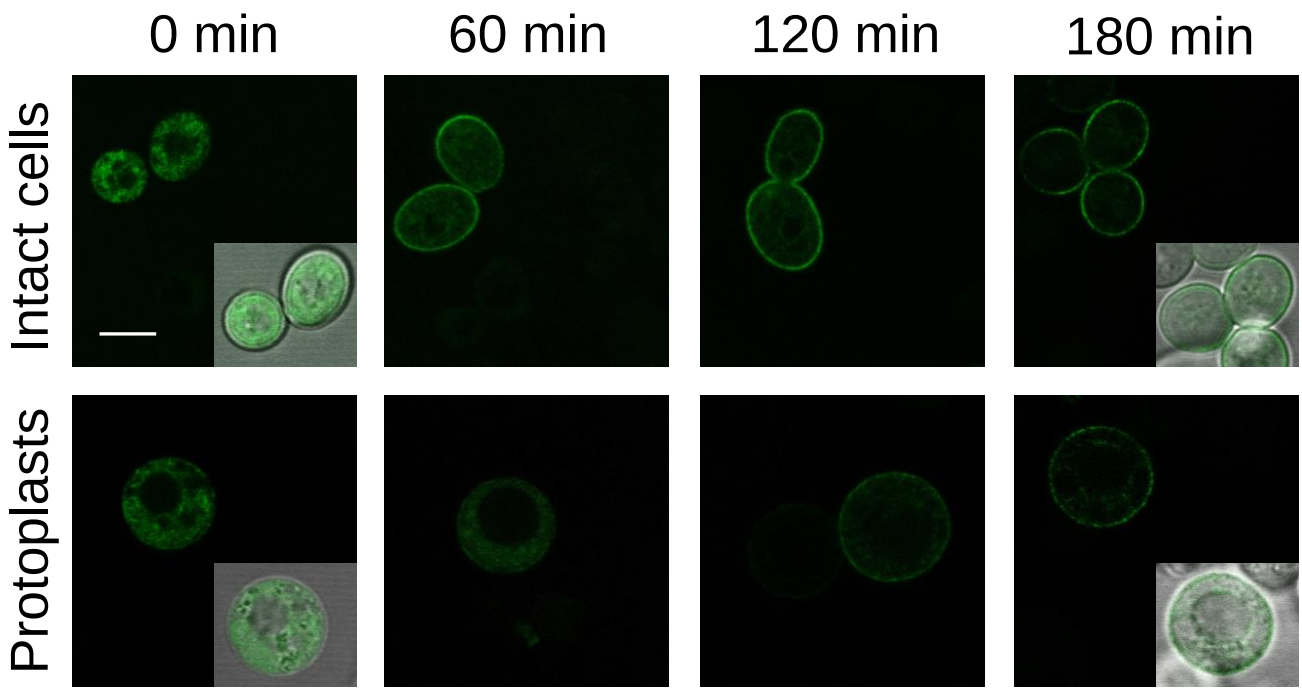

Figure 38: Localization studies of the Tok1-Gfp fusion protein in the *sec6-4* mutant to visualize the trafficking of the Gfp–tagged potassium channel Tok1 from the cytoplasm to the plasma membrane.
The Gfp signal is relocated from the cytoplasm to the plasma membrane. Cells from an overnight culture (SD-Ura) were shifted to galactose containing media incubated for 3 h at 37 °C to allow expression of Tok1-Gfp and accumulation of secretory vesicles in the cytoplasm. After incubation half of the intact cells were washed and transferred to a glucose containing media and the other half was used for protoplast preparation. Protoplasts were stored in a buffer also containing glucose. Pictures were taken with the CLSM every hour over a period of three hours. In both preparations the relocation of the Gfp-signal from the cytosol to the cytoplasm is clear after 120 min. Scale bar, 5 µm.

In addition to figure 38 the relative fluorescence was determined for 0, 60, 120 and 180 minutes after the shift, for intact cells (Fig. 39) and protoplasts (Fig. 40). For both the relocalization of the Gfp-signal

in the plasma membrane was clearly visible after 180 min. In intact cells the membrane was also visible after 60 min. These results show that most secretory vesicles with the Tok1-Gfp were transported to the plasma membrane after the shift within the first 3 h, in both preparations.

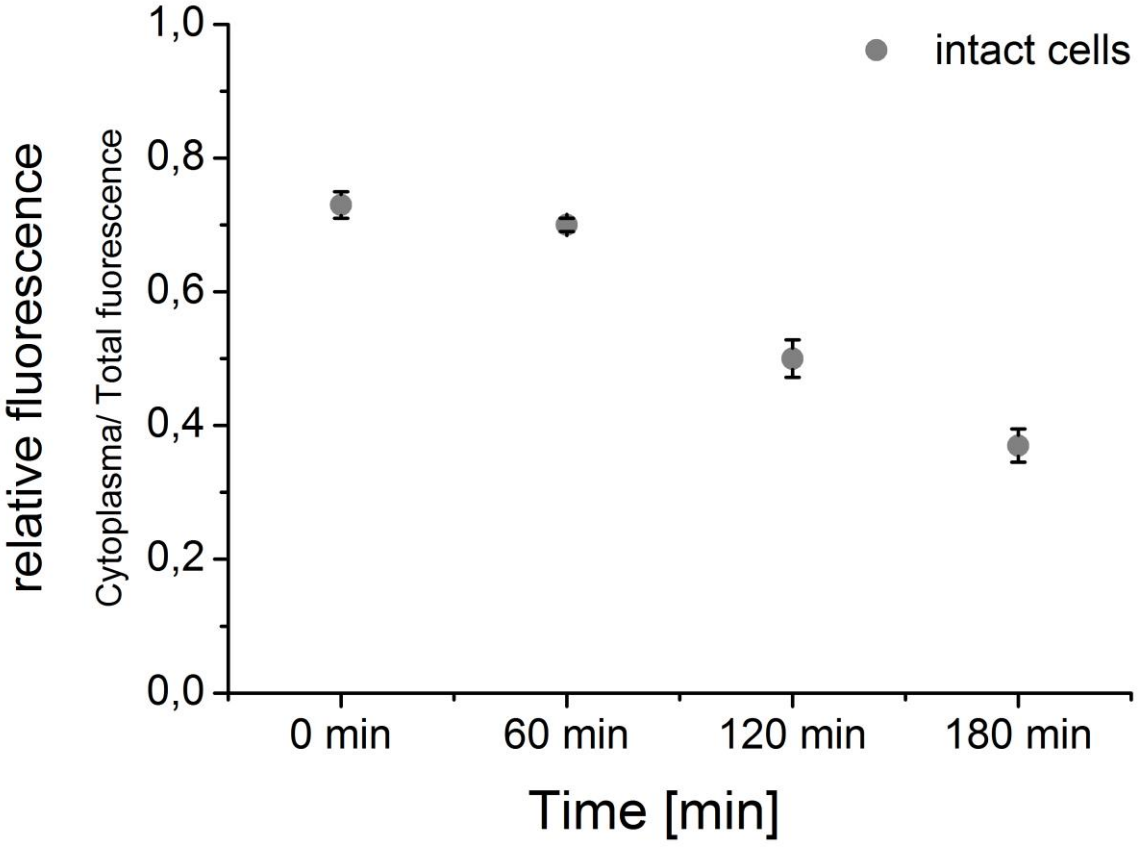

Figure 39: Relative fluorescence of intact cells.

Cells were incubated at 37 °C with galactose for gene expression and vesicle accumulation and transferred to room temperature and glucose containing medium. Relative fluorescence was calculated for 0, 60, 120 and 180 min after the shift. The fluorescence inside of the cell was determined in relation to the total fluorescence of the cell. Cells maintained at 25 °C provided for the determination of the reference value at 0.4 ± 0.01 (control sample). Error bars represent (SEM).

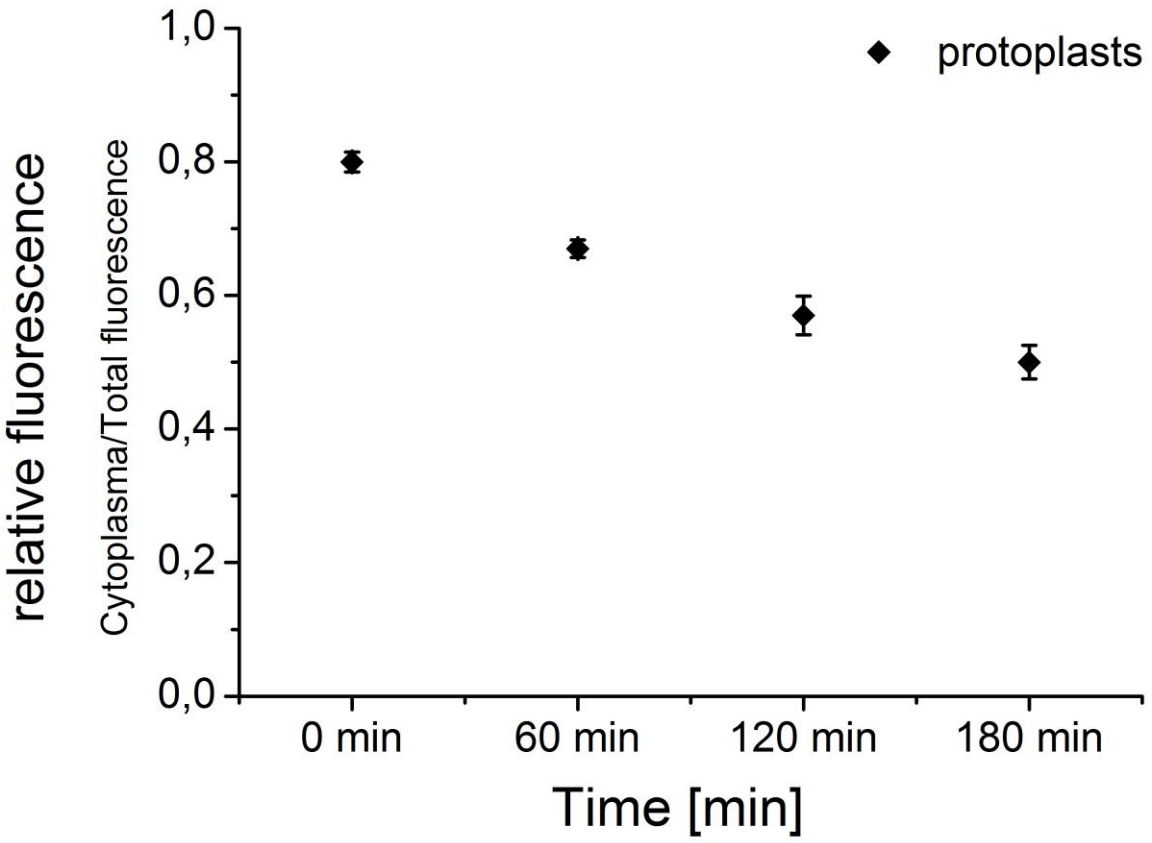

Figure 40: Relative fluorescence of protoplasts.

Cells were incubated at 37 °C with galactose for protein expression and vesicle accumulation. After incubation protoplasts were isolated and shifted to room temperature and incubated in a stabilizing buffer supplemented with glucose. The relative fluorescence was calculated for 0, 60, 120 and 180 minutes after the shift. The fluorescence inside the cell was set in relation to the total fluorescence of the cell. Protoplasts maintained at 25 °C provided for the determination of the reference value at 0.43 ± 0.02 (control sample). Error bars represent SEM.

The relation between exocytotic activity and the capacitance changes of the electrophysiological recordings of chapter 6.4 was demonstrated by performing capacitance measurements with the strain SY1. Through the accumulation of secretory vesicles at 37 °C in the 3 h before measuring, the exocytotic activity should be significantly higher. For reference, cells maintained at 25 °C were also measured. The frequency in SY1 cells (25 °C) was approximately the same as in wild type cells (BY4741, Fig. 41). Eleven cells were measured under the same conditions and only five cells showed exo- and endocytotic activity by a total recording time of 5.9 h (in average 0.5 h per measurement). In the other preparation cells were incubated at 37 °C for 3 h before measuring in order to accumulate secretory vesicles. After incubation cells were shifted to 25 °C. At this temperature the blockade relieved and exocytosis takes place. This preparation showed higher frequencies, as expected. In 9

protoplasts changes in membrane capacitance were measured. The recording time was on average 50 min. Only 8 of 9 protoplasts showed exo- and endocytotic activity. Consistent with the expectation of a higher exocytotic activity, we observed a high frequency of capacitive events in SY1 protoplasts. Especially the frequency of transient exocytotic events was higher than in cells of the reference strain and cells incubated at 25 °C. Regarding permanent events we can also observe a clear increase (Fig 41).

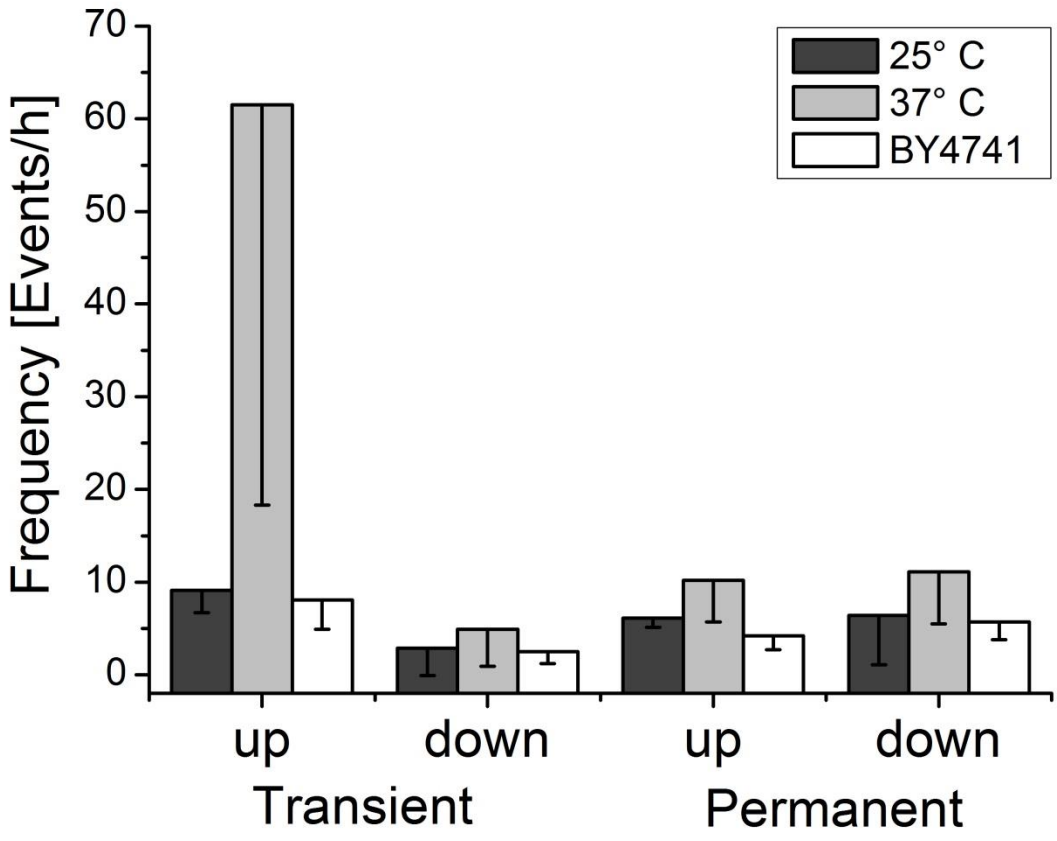

Figure 41: Frequencies of capacitive events in the yeast strains SY1 and BY4741.
SY1 protoplasts were incubated 3 h at 25 °C and 37 °C before measuring. The latter incubation was performed to accumulate secretory vesicles in yeast protoplasts. Protoplasts were measured at room temperature in a bath solution supplemented with 1 % glucose. In SY1 cells (37 °C) a total of 252 events, 150 transient events, and 102 permanent events were detected corresponding to a total frequency of 87.6 events/h. In SY1 cells (25 °C) a total of 91 events, 73 transient events, and 18 permanent events were recorded corresponding to a total frequency of 24.4 events/h. Numbers for the strain BY4741 are documented in chapter 6.4.2.

High frequencies of capacitive events were observed over a time period of 120 min (60 to 180 min after temperature shift; Fig. 42). After 160 min the frequency of capacitive events dropped to the base level (Fig. 42, dotted line). Note that these recordings started 60 min after the temperature shift, owing the rather long time required to successfully establish a tight seal.

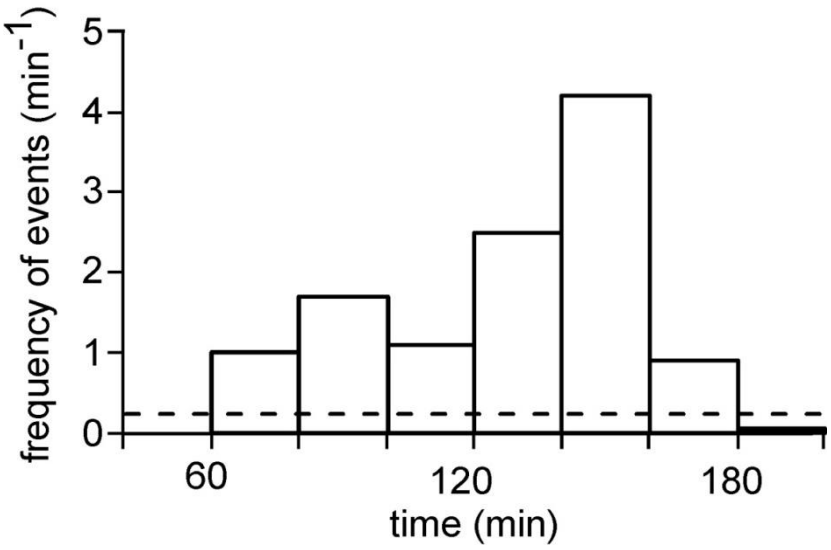

Figure 42: Time course of the frequency of capacitance changes recorded at 25 °C from SY1 protoplasts.

Cells were pre-incubated at the restrictive temperature 37 °C, resulting in accumulation of secretory vesicles. The bars represent the averaged frequencies over 20 min intervals. The dotted line indicates the background frequency recorded from SY1 protoplasts at 25 °C without pre-incubation at 37 °C. The time denotes the time after the temperature change, whereas the recordings started 60 min after the temperature shift.

The vesicle size distribution in SY1 is depicted in figure 43. A comparable size distribution of endo-/exocytotic events to the wild type is observed. 65 % of the capacitance changes are in the range of 0.25 - 1 fF, corresponding to vesicle sizes ranging from 100 to 200 nm with a median value of 0.65 fF or 165 nm (Fig. 43). In comparison with the wild type (BY4741, Fig. 33) larger vesicles with a diameter up to 510 nm were measured (6.5 fF). The large size of these vesicles can be explained by two possible mechanisms: The fusion of multiple vesicles to a giant vesicle before merging with the membrane or the simultaneous fusion of diverse vesicles with the membrane (Lollike *et al*., 2002; Toyooka *et al*., 2009; Goto *et al*., 2009; Wu *et al*., 2014).

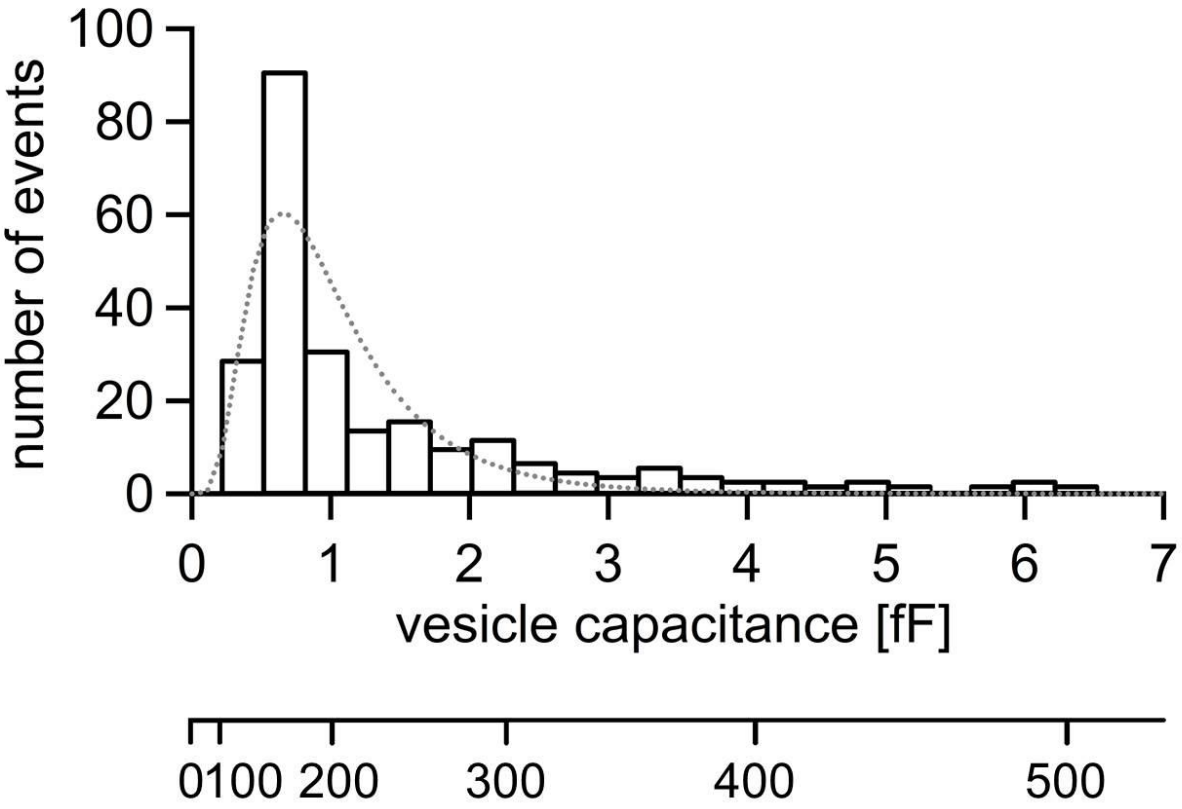

Figure 43: Vesicle size distribution of endo- and exocytotic events in SY1 (37 °C).

Summary of all capacitance steps collected from 9 different protoplasts with a total of n = 253 events (endocytotic and exocytotic), recorded in the cell-attached configuration. The data are described by a lognormal-distribution (solid grey curve), which centers at C_0 = 0.65 fF or 165 nm with a width of w = 0.8, which is defined as ln (C/C_0) at n = 1/e. The corresponding vesicle diameters were calculated assuming a specific membrane capacitance of C = 8 mF/m^2, as determined from whole cell patch-clamp recordings (Homann & Tester 1998).

7. Conclusions

The processes of exo- and endocytosis have been investigated extensively in yeast, as a model system facilitating in-depth understanding of the molecular and biochemical mechanisms of both phenomena (Finger & Novick, 1998; Grote *et al.*, 2000; Delic *et al.*, 2013; Liu *et al.*, 2009). In the present study, capacitance measurements were applied to study the aforementioned processes in yeast protoplasts. The experimental approach enabled for the first time in yeast, the detection of exo- and endocytotic events at high temporal and spatial resolution *in vivo*. Various analyses demonstrated that protoplasts are able to perform exo- and endocytosis with the dynamics similar to that characteristic of intact cells (with microscopic capacitance measurements and macroscopic growth data providing coherent outcomes). These results suggest that the electrophysiological data represents the physiological activity in membrane dynamics of these cells well, even though the measured frequencies were low. A possible explanation for this result is that cell-attached recordings only represent 1 % of the whole cell membrane. Therefore the recording data is not always representative for what is happening throughout the cell. It is interesting to see that the major modes of exo- and endocytosis with permanent and transient fusion/fission events, which were also detected in mammalian cells and plant cells, are already present in yeast, a much simpler eukaryote. This suggests that the different modes of membrane dynamics are an inherent property of the common set of proteins, which are used for these processes in eukaryotes. The *sec6-4* mutant demonstrated clearly that capacity changes in the plasma membrane are caused by exo- and endocytosis. The different frequencies measured at each temperature showed that a block of exocytosis leads to modulation of the frequencies of exo- and endocytotic events. The effect of the modulation, or rather the mutation, was also clear to see in protoplast growth experiments, CLSM recordings and EM recordings. Altogether the data of this work suggests that yeast is a good system for investigating the basic structure/function correlations of complex exo- and endocytosis by using the patch-clamp capacity measurement technique.

8. References

1) Aalto, M.K., Ronne, H. & Keränen, S. (1993). Yeast syntaxins Ssol p and Sso2p belong to a family of related membrane proteins that function in vesicular transport. *The EMBO Journal, 12*, 4095-4104.
2) Albillos, A., Dernick, G., Horstmann, H., Almers, W., Toledo, G.A. & Lindau, M. (1997). The exocytotic event in chromaffin cells revealed by patch amperometry. *Nature, 389,* 509-512.
3) Alés, E., Tabares, L., Poyato, J.M., Valero, V., Lindau, M. & Toledo, G.A. (1999). High calcium concentrations shift the mode of exocytosis to the kiss-and-run mechanism. *Nature Cell Biology, 1,* 40-44.
4) Bagnat, M., Chang, A., & Simons, K. (2001). Plasma Membrane Proton ATPase Pma1p Requires Raft Association for Surface Delivery in Yeast. *Mol Biol Cell, 12,* 4129-4138.
5) Bagnat, M. & Simons, K. (2002). Lipid Rafts in Protein Sorting and Cell Polarity in Budding Yeast *S.c*. *Biol Chem, 383,*1475-1480.
6) Bandmann, V., Kreft, M. & Homann, U. (2011). Modes of Exocytotic and Endocytotic Events in Tobacco BY-2 Protoplasts. *Molecular Plant, 4,* 241-251. doi:10.1093/mp/ssq072
7) Bandmann V., Müller, J.D., Köhler, T. & Homann, U. (2012). Uptake of fluorescent nano beads into BY2-cells involves clathrin-dependent and clathrin-independent endocytosis. *FEBS Letters, 586,* 3626-3632. doi: 10.1016/j.febslet.2012.08.008
8) Bertl, A. & Slayman, C.L. (1990). Cation-selective channels in vacuolar membrane of *Saccharomyces*: Dependence on calcium, redox state, and voltage. *Proc. Natl. Acad. Sci. USA, 87,* 7824-7828.
9) Bertl, A., Blumwald, E., Coronado, R., Eisenberg, R., Findlay, G., Gradmann, D., Hille, B., Köhler, K., Kolb, H.A., MacRobbie, E., Meissner, G., Miller, C., Neher, E. & Palade, P. (1992). Electrical Measurements on Endomembranes. *Science, 258,* 873-874.
10) Bertl, A. & Slayman, C.L. (1992). Complex modulation of cation channels in the tonoplast and plasma membrane of *Saccharomyces cerevisiae* single channel studies. *J.exp. Biol, 172,* 271-287.
11) Bertl, A., Bihler, H., Kettner, C. & Slayman, C.L. (1998). Electrophysiology in the eukaryotic model cell S.c.. *Pflugers Arch - Eur J Physiol, 436,* 999-1013.
12) Bertl, A., Ramos, J., Ludwig J., Lichtenberg-Fraté, H., Reid, J., Bihler, H., Calero, F., Martinez, P. & Ljungdahl, P.O. (2003). Characterization of potassium transport in wild-type and isogenic yeast strains carrying all combinations of trk1, trk2 and tok1 null mutations. *Molecular Microbiology, 47,* 767-780.
13) Betz, W.J., Mao, F. & Smith, C.B. (1996). Imaging exocytosis and endocytosis. *Current Opinion Neurobiology, 6,* 365-371.

14) Bittner, M.A., Habig, W.H. & Holz, R.W. (1989). Isolated Light Chains of Botulinum Neurotoxins Inhibit Exocytosis. *The Journal of Biological Chemistry,264,* 10354-10360.

15) Borisovska, M., Zhao, Y., Tsytsyura, Y., Glyvuk, N., Takamori, S., Matti, U., Rettig, J., Südhof, T. & Bruns, D. (2005). v-SNAREs control exocytosis of vesicles from priming to fusion. *The EMBO Journal, 24,* 2114-2126. doi: 10.1038/

16) Botstein, D. & Fink, G.R. (2011). Yeast: An Experimental Organism for the 21st Century Biology. *Genetics, 189,*695-704. doi: 10.1534/genetics.111.130765

17) Breckenridge, L.J. & Almers, W. (1987). Currents through the fusion pore that forms during exocytosis of a secretory vesicle. *Nature, 328,* 814-817.

18) Brennwald, P., Kearns, B., Champion, K., Keränen, S., Bankaitis, V. & Novick, P. (1994). Sec9 Is a SNAP-25like Component of a Yeast SNARE Complex That May Be the Effector of Sec4 Function in Exocytosis. *Cell, 79,* 245-258.

19) Brennwald, P. & Rossi, G. (2007). Spatial Regulation of Exocytosis and Cell Polarity: Yeast as a Model for Animal Cells. *FEBS Letters, 581,* 2119-2124.

20) Brodsky, F.M. (1988). Living with Clathrin: Its Role in Intracellular Membrane Traffic. *Science, 242,* 1396-1402.

21) Brown, D.A. & London, E. (1998). FUNCTIONS OF LIPID RAFTS IN BIOLOGICAL MEMBRANES. *Annu Rev Cell Dev Biol, 14,* 111-136.

22) Brown, D.A. & London, E. (1998). Stucture and origin of ordered lipid domains in biological membranes. *J Membr Biol, 164,* 103-114.

23) Burgoyne, R.D. & Morgan, A. (1995). Ca^{2+} and secretory-vesicle dynamics. *Trends Neuroscience, 18,* 191-196.

24) Carr, C.M., Grote, E., Munson, M., Hughson, F.M. & Novick, P. (1999). Sec1p Binds to SNARE Complexes and Concentrates at Sites of Secretion. *The Journal of Cell Biology, 146,* 333-344.

25) Carrillo, L., Cucu, B., Bandmann, V., Homann, U., Hertel, B., Hillmer, S., Thiel, G. & Bertl, A. (2015). High-resolution membrane capacitance measurements for studying endocytosis and exocytosis in yeast. *Traffic, 16,* 760-772. doi: 10.1111/tra.12275

26) Ceccarelli, B., Hurlbut, W.P. & Mauro, A. (1972). Depletion of vesicles from frog neuromuscular junctions by prolonged tetanic stimulation. *The Journal of Cell Biology, 54,* 30-38.

27) Ceccarelli, B., Hurlbut, W.P. & Mauro, A. (1973). Turnover of transmitter and synaptic vesicles at the frog neuromuscular junction. *The Journal of Cell Biology, 57,* 499-524.

28) Clarke, B.L. & Weigel, P.H. (1985). Recycling of the Asialoglycoprotein Receptor in Isolated Rat Hepatocytes. *The Journal of Biological Chemistry, 260,* 128-133.

29) Dancourt, J. & Barlowe, C. (2010). Protein sorting receptors in the early secretory pathway. *Annu Rev Biochem, 79,* 777-802. doi: 10.1146/annurev-biochem-061608-091319

30) Debus, K. & Lindau, M. (2000). Resolution of Patch Capacitance Recordings and Fusion Pore Conductances in Small Vesicles. *Biophysical Journal, 78*, 2983-2997.

31) Delic, M., Valli, M., Graf, A.B., Pfeffer, M., Mattanovich, D. & Gasser, B (2013). The secretory pathway: exploring yeast diversity. *FEMS Microbiology Review, 37*, 872-914. doi: 10.1111/1574-6976.12020

32) Elhamdani, A., Azizi, F. & Artalejo, C.R. (2006). Double patch clamp reveals that transient fusion (kiss-and-run) is a major mechanism of secretion in calf adrenal chromaffin cells: high calcium shifts the mechanism from kiss-and-run to complete fusion. *J neurosci, 26,* 3030-3036. doi:10.1523/JNEUROSCI.5275-05.2006

33) Eliasson, L., Renström, E., Ding, W.-G., Proks, P. & Rorsman, P. (1997). Rapid ATP-dependent priming of secretory granules precedes Ca^{2+}-induced exocytosis in mouse pancreatic B-cells. *Journal of Physiology, 503.2,* 399-412.

34) Emans, N., Zimmermann, S. & Fischer, R. (2002). Uptake of a Fluorescent Marker in Plant Cells Is Sensitive to Brefeldin A and Wortmannin. *The Plant Cell Online, 14,* 71-86. doi: 10.1105/tpc.010339

35) Fernandez, J.M., Neher, E. & Gomperts, B.D. (1984). Capacitance measurements reveal stepwise fusion events in degranulating mast cells. *Nature, 312,*453-455.

36) Ferro-Novick, S. & Jahn, R. (1994). Vesicle Fusion from Yeast to Man. *Nature, 370,* 191-193.

37) Finger, F.P., Hughes, T.E. & Novick, P. (1998)a. Sec3p Is a Spatial Landmark for Polarized Secretion in Budding Yeast. *Cell, 92,* 559-571.

38) Finger, F.P. & Novick, P. (1998)b. Spatial Regulation of Exocytosis: Lessons from Yeast. *The Journal of Cell Biology, 142,* 609-612.

39) Flasker, A., Jorgacevski, J., Calejo, A. I., Kreft, M. & Zorec, R. (2013). Vesicle size determines unitary exocytic properties and their sensitivity to sphingosine. *Mol Cell Endocrinol, 376,* 136-147. doi: 10.1016/j.mce.2013.06.012

40) Funato, K. & Riezman, H. (2001). Vesicular and nonvesicular transport of ceramide from ER to the Golgi apparatus in yeast. *J Cell Biol, 155*, 949-959. doi:10.1083/jcb.200105033

41) Gaffield, M. A. & Betz, W. J. (2006). Imaging synaptic vesicle exocytosis and endocytosis with FM dyes. *Nat Protoc, 1,* 2916-2921. doi: 10.1038/nprot.2006.476

42) Gentet, L.J., Stuart, G.J. & Clements, J.D. (2000). Direct Measurement of Specific Membrane Capacitance in Neurons. *Biophysical Journal, 79,* 314-320.

43) Goode, B.L., Eskin, J.A. & Wendland, B. (2015). Actin and Endocytosis in Budding Yeast. *Genetics, 199,* 315-358. doi:10.1534/genetics.112.145540

44) Govindan, B., Bowser, R. & Novick, P. (1995). The Role of Myo2, a Yeast Class V Myosin, in Vesicular Transport. *The Journal of Cell Biology, 128,* 1056-1068.

45) Grossmann, G., Malinsky, J., Stahlschmidt, W., Loibl, M., Weig-Meckl, I., Frommer, W. B., Opekarova, M. & Tanner, W. (2008). Plasma membrane microdomains regulate turnover of transport proteins in yeast. *J Cell Biol, 183,* 1075-1088. doi: 10.1083/jcb.200806035

46) Grote, E., Carr, C. M. & Novick, P. (2000). Ordering the Final Events in Yeast Exocytosis. *The Journal of Cell Biology, 151,* 440-451.

47) Guo, W., Roth, D., Walch-Solimena, C. & Novick, P. (1999). The exocyst is an effector for Sec4p, targeting secretory vesicles to sites of exocytosis. *The EMBO Journal, 18,* 1071-1080.

48) Gustin, M.C., Martinac, B., Saimi, Y., Culbertson, M.R. & Kung, C. (1986). Ion Channels in Yeast. *Science, 233,* 1195-1197.

49) Hamill, O.P., Marty, A., Neher, E., Sakmann, B. & Sigworth, F.J. (1981). Improved Patch-Clamp Techniques for High-Resolution Current Recording from Cells and Cell-Free Membrane Patches. *Pflügers Arch, 391,* 85-100.

50) Hanson, P.I., Heuser, J.E. & Jahn, R. (1997). Neurotransmitter release- four years of SNARE complexes. *Current Opinion in Neurobiology, 7,* 310-315.

51) Heidelberger, R. (2001). ATP Is Required at an Early Step in Compensatory Endocytosis in Synaptic Terminals. *The Journal of Neuroscience, 21,* 6467-6474.

52) Henkel, A.W. & Betz, W.J. (1995). Staurosporine Acetylcholine Blocks Evoked Release of FMI-43 but Not from Frog Motor Nerve Terminals. *The Journal of Neuroscience, 15,* 8246-8258.

53) Henkel, A.W., Kang, G. & Kornhuber, J. (2001). A common molecular machinery for exocytosis and the "kiss-and-rin" mechanism in chromaffin cells is controlled by phosphorylation. *Journal of Cell Science, 114,* 4613-4620.

54) Henkel, A.W., Meiri, H., Horstmann, H., Lindau, M. & Almers, W. (2000). Rhythmic opening and closing of vesicles during constitutive exo- and endocytosis in chromaffin cells. *The EMBO Journal, 19,* 84-93.

55) Heuser, J.E. & Evans, L. (1980). Three-dimensional visualization of coated vesicle formation in fibroplasts. *The Journal of Cell Biology, 84,* 560-583.

56) Heuser, J.E. & Reese T.S. (1973): Evidence for recycling of synaptic vesicle membrane during transmitter release at the frog neuromuscular junction. *The Journal of Cell Biology, 57,* 315-344.

57) Holz, R.W., Bittner, M.B., Peppers, S.C., Senter, R.A. & Eberhard, D.A. (1989). MgATP-independent and MgATP-dependent Exocytosis. *The Journal of Biological Chemistry,264,*5412-5419.

58) Homann, U., Meckel, T. Hewing, J. Hutt, M. T. & Hurst, A.C. (2007). Distinct fluorescent pattern of KAT1::GFP in the plasma membrane of *Vicia faba* guard cells. *Eur J Cell Biol, 86,*489-500. doi: 10.1016/j.ejcb.2007.05.003

59) Homann, U. & Tester, D. J. (1998). Patch-clamp measurements of capacitance to study exocytosis and endocytosis. *Trends in Plant Science, 3,* 110-114.

60) Hou, J., Tyo, K.E.J., Liu, Z. Petranovic, D. & Nielsen, J. (2012). Metabolic engineering of recombinant protein secretion by *Saccharomyces cerevisae*. *FEMS Yeast, 12,* 491-510. doi: 10.1111/j.1567-1364.2012.00810.x

61) Jansen, G., Wu, C., Schade, B., Thomas, D. Y. & Whiteway, M. (2005). Drag & Drop cloning in yeast. *Gene, 344,* 43-51. doi: 10.1016/j.gene.2004.10.016

62) Jonsdottir, G.A. & Li, R. (2004). Dynamics of yeast Myosin I: evidence for a possible role in scission of endocytic vesicles. *Current Biology, 14,* 1604-1609. doi: 10.1016/j.cub.2004.08.055

63) Jorgacevski, J., Fosnaric, M., Vardjan, N., Stenovec, M., Potokar, M., Kreft, M., Kralj-Iglic, V., Iglic, A. & Zorec, R. (2010). Fusion pore stability of peptidergic vesicles. *Mol Membr Biol, 27,* 65-80. doi: 10.3109/09687681003597104

64) Jorgacevski, J., Kreft, M., Vardjan, N. & Zorec, R. (2012). Fusion pore regulationin peptidergic vesicles. *Cell Calcium, 52,* 270-276. doi: 10.1016/j.ceca.2012.04.008

65) Jorgacevski, J., Potokar, M., Grilc, S., Kreft, M., Liu, W., Barclay, J. W., Buckers, J., Medda, R., Hell, S. W., Parpura, V., Burgoyne, R. D. & Zorec, R. (2011). Munc18-1 tuning of vesicle merger and fusion pore properties. *J Neurosci, 31,* 9055-9066. doi: 10.1523/JNEUROSCI.0185-11.2011

66) Jorgacevski, J., Stenovec, M., Kreft, M., Bajic, A., Rituper, B., Vardjan, N., Stojilkovic, S. & Zorec, R. (2008). Hypotonicity and peptide discharge from a single vesicle. *Am J Physiol Regul Integr Comp Physiol, 295,* 624-631. doi: 10.1152/ajpcell.00303.2008.-Neuroendocrine

67) Kabaso, D., Jorgacevski, J., Calejo, A. I., Flasker, A., Gucek, A., Kreft, M. & Zorec, R. (2013). Comparison of unitary exocytic events in pituitary lactotrophs and in astrocytes: modeling the discrete open fusion-pore states. *Front Cell Neurosci, 7,* Article 33 1-6. doi: 10.3389/fncel.2013.00033

68) Kaksonen, M., Sun Y. & Drubin, D.G. (2003). A Pathway for Association of Receptors, Adaptors, and Actin during Endocytic Internalization. *Cell, 115,* 475-487.

69) Kaksonen, M., Toret, C.P. & Drubin, D.G. (2005). A Modular Design for the Clathrin- and Actin-mediated Endocytosis Machinery. *Cell, 123,* 305-320. doi: 10.1016/j.cell.2005.09.024

70) Katz, B. & Miledi, R. (1969). Spontaneous and Evoked Activity of Motor Nerve Endings in Calcium Ringer. *J Physiol, 203,* 689-706.

71) Kelly, R.B. (1985). Pathways of Protein Secretion in Eukaryotes. *Science, 230,* 25-32.

72) Ketchum, K.A., Joiner, W.J., Sellers, A.J., Kaczmarek, L.K. & Goldstein, S.A.N. (1995). A new family of outwardly rectifying potassium channel proteins with two pore domains in tandem. *Nature, 376,*690-695.

73) Kim, J.-S., Yoon, T.-J., Yu, K.-N., Noh, M. S., Woo, M., Kim, B.-G., Lee, K.-H., Sohn, B.-H., Park, S.-B., Lee, J.-K. & Cho, M.-H. (2006). Cellular uptake of magnetic nanoparticle is mediated through energy-dependent endocytosis in A549 cells. *J Vet Sci, 7,* 321-326.

74) Kollár, R., Reinhold, B.B., Petráková, E., Yeh, H.J.C., Ashwell, G., Drgonová, J., Kapteyn, J.C., Klis, F.M. & Cabib, E. (1997). Architecture of the Yeast Cell Wall. *The Journal of Biological Chemistry, 272,* 17762-17775.

75) Kreft, M., Stenovec, M., Rupnik, M., Grilc, S., Krzan, M., Potokar, M., Pangrsic, T., Haydon, P. G. & Zorec, R. (2004). Properties of $Ca^{(2+)}$-dependent exocytosis in cultured astrocytes. *Glia, 46,* 437-445. doi: 10.1002/glia.20018

76) Lamping, E., Tanabe, K., Niimi, M., Uehara, Y., Monk, B. C. & Cannon, R. D. (2005). Characterization of the *Saccharomyces cerevisiae* sec6-4 mutation and tools to create S. cerevisiae strains containing the sec6-4 allele. *Gene, 361,*57-66. doi: 10.1016/j.gene.2005.07.014

77) Lev, S. (2010). Non-vesicular lipid transport by lipid-transfer proteins and beyond. *Nat Rev Mol Cell Biol, 11,* 739-750. doi: 10.1038/nrm2971

78) Lew, D.J. & Simon, S.M. (1991). Characterization of Constitutive Exocytosis in the Yeast *Saccharomyces cerevisiae*. *The Journal of Membrane Biology, 123*, 261-268.

79) Lin, R.C. & Scheller, R.H. (1997). Structural Organization of the Synaptic Exocytosis Core Complex. *Neuron, 19*, 1087-1094.

80) Lindau, M. (1991). Time-resolved capacitance measurements: monitoring exocytosis in single cells. *Quarterly Reviews of Biophysiks, 24,* 75-101.

81) Lindau, M. (2012). High resolution electrophysiological techniques for the study of calcium activated exocytosis. *Biochimica et Biophysica Acta 1820, 8,* 1234-1242. doi: 10.1016/j.bbagen.2011.12.011

82) Lindau, M. & Alvarez de Toledo, G. (2003). The Fusion Pore. *Biochimica et Biophysica Acta (BBA)-Molecular Cell Research, 1641,* 167-173. doi: 10.1016/s0167-4889(03)00085-5

83) Liu, J., Kaksonen, M., Drubin, D. G. & Oster, G. F. (2006). Endocytotic vesicle scission by lipid phase boundary forces. *PNAS, 103,* 10277-10282. doi: 10.1073/pnas.0601045103

84) Liu, J., Sun, Y., Drubin, D. G. & Oster, G. F. (2009). The Mechanochemistry of Endocytosis. *PLoS Biol, 7,* 1-16. doi: 10.1371/journal.pbio.1000204.

85) Liu, J., Sun, Y., Oster, G. F. & Drubin, D. G. (2010). Mechanochemical crosstalk during endocytic vesicle formation. *Current Opinion Cell Biology, 22,* 1-13. doi: 10.1016/j.ceb.2009.11.009

86) Liu, W. & Parpura, V. (2010). SNAREs: Could they be the Answer to an Energy Landscape Riddle in Exocytosis? *Scientific World Jornal, 10,* 1258-1268. doi: 10.1100/tsw.2010.137

87) Llinás, R.R. & Heuser, J.E. (1977). Depolarization-release coupling systems in neurons. *Neurosciences Res. Program Bull, 15,* 556-687.

88) LoGiudice, L. & Matthews, G. (2006). The Synaptic Vesicle Cycle: Is kissing Overrated? *Neuron, 51,* 676-677. doi: 10.1016/j.neuron.2006.09.004; 10.1016/j.neuron.2006.08.020

89) Lollike, K., Lindau, M., Calafat, J. & Borregaard, N. (2002). Compound exocytosis of granules in human neutrophils. *Journal of Leukocyte Biology, 71,* 973-980.

90) Luo, T., Fredericksen, B.L., Hasumi, K., Endo & Garcia, J. V. (2001). Human Immunodeficiency Virus Type 1 Nef-Induced CD4 Cell Surface Downregulation Is Inhibited by Ikarugamycin. *Journal of Virology, 75,* 2488-2492. doi: 0.1128/JVI.75.5.2488–2492.2001

91) Malhotra, V. & Mayor, S. (2006). Golgi grows up. *Nature, 441,* 939-940.

92) Malínská, K., Malinsky, J., Opekarová, M. & Tanner, W. (2003). Visualization of protein compartmentation within the plasma membrane of living yeast cells. *Mol. Biol. Cell, 14,* 4427-4436. doi: 10.1091/mbc.E03-04-0221

93) Manfredi, J.P., Klein, C., Herrero, J.J., Byrd, D.R., Trueheart, J., Wiesler, W.T., Fowlkes, D.M. & Broach, J.R. (1996). Yeast alpha mating factor structure-activity relationship delivered from genetically selected peptide agonists and antagonists of Ste2p. *Mol Cell Biol, 16*, 4700-4709.

94) McDonald, K.L. & Webb, R.I. (2011). Freeze substitution in 3 hours or less. *J Microsc, 243,* 227-233. doi: 10.1111/j.1365-2818.2011.03526.x

95) Mouritsen, O.G. & Jorgensen, K. (1997). Small-scale lipid membrane structure: simulation versus experiment. *Current Opinion in Structural Biology, 7,* 518-527.

96) Mullholland, J., Preuss, D., Moon, A., Wong, A., Drubin, D. G. & Botstein, D. (1994). Ultrastructure of the Yeast Actin Cytoskeleton and Its Association with the Plasma Membrane. *The Journal of Cell Biology, 125,* 381-391.

97) Munro, S. (2003). Lipid Rafts: Elusive or Illusive? *Cell, 115,* 377-388.

98) Nakamoto, R.K., Rao, R. & Slayman, C.W. (1991). Expression of the Yeast Plasma Membrane [H^+]ATPase in Secretory Vesicles. *The Journal of Biological Chemistry, 266,* 7940-7949.

99) Neher, E. & Marty, A. (1982). Discrete changes of cell membrane capacitance observed under conditions of enhanced secretion in bovine adrenal chromaffin cells. *Proc. Natl. Acad. Sci. USA, 79,* 6712-6716.

100) Neher, E. & Sakmann, B. (1976). NOISE ANALYSIS OF DRUG INDUCED VOLTAGE CLAMP CURRENTS IN DERIVATED FROG MUSCLE FIBERES. *J Physiol, 258,* 705-729.

101) Novick, P., Field, C. & Schekman, R. (1979). Secretion and cell-surface growth are blocked in a temperature-sensitive mutant of *S.c.*. *Proc. Natl. Acad. Sci. USA, 76,* 1858-1862.

102) Novick, P., Field, C. & Schekman, R. (1980). Identification of 23 Complementation Groups Required for Post-translational Events in Yeast Secretory Pathway. *Cell, 21,* 205-215.

103) Pearse, B.M. (1976). Clathrin: A unique protein associated with intracellular transfer of membrane by coated vesicles. *Proc. Natl.Acad. Sci. USA, 73,*1255-1259.

104) Prosser, D.C. & Wendland, B. (2012). Conserved roles for yeast Rho1 and mamalian RhoA GTPases in clathrin-independent endocytosis. *Small GTPases, 3,* 229-235. doi: 10.4161/sgtp.21631; 10.1083/jcb.201104045

105) Protopopov, V., Govindan, B., Novick, P. & Gerst, J.E. (1993). Homologs of the Synaptobrevid/VAMP Family of Synaptic Vesicle Proteins Function on the Late Secretory Pathway in *S. cerevisiae*. *Cell, 74,* 855-861.

106) Rituper, B., Flasker, A., Gucek, A., Chowdhury, H. H. & Zorec, R. (2012). Cholesterol and regulated exocytosis: a requirement for unitary exocytotic events. *Cell Calcium, 52,* 250-258. doi: 10.1016/j.ceca.2012.05.009

107) Rituper, B., Gucek, A., Jorgacevski, J., Flasker, A., Kreft, M. & Zorec, R. (2013)a. High resolution membrane capacitance measurements for the study of exocytosis and endocytosis. *Nature Protocols, 8,* 1169-1183. doi: 10.1038/nprot.2013.069

108) Rituper, B., Chowdhury, H.H., Jorgacevski, J., Coorssen, J.R., Kreft, M. & Zorec, R. (2013)b. Cholesterol-mediated membrane surface area dynamics in neuroendocrine cells. *Biochimi Biophys Acta, 7,* 1228-1238. doi: 10.1016/j.bbalip.2013.04.007

109) Robinson, L.J. & Martin, T.F.J. (1998). Docking and fusion in neurosecretion. *Cell Biology, 10,* 483-492.

110) Rothman, J.E. & Warren, G. (1994). Implications of the SNARE hypothesis for intracellular membrane topology and dynamics. *Current Biology, 4,* 220-233.

111) Scheller, R.H. (1995). Membrane Trafficking in Presynaptic Nerve Terminal. *Neuron, 14,* 893-897.

112) Schmid, S.L. & Carter, L.L. (1990). ATP is required for receptor-mediated endocytosis in intact cells. *The Journal of Cell Biology, 111,* 2307-2318.

113) Schott, D., Ho, J., Pruyne, D. & Bretscher, A. (1999). The COOH-Terminal Domain of Myo2p, a Yeast Myosin V, Has a Direct Role in Secretory Vesicle Targeting. *The Journal of Cell Biology, 147,* 791-807.

114) Sedwick, C. (2009). Wrapping Our Heads around Endocytosis. *PLoS Biol, 7,* 1-1. doi: 10.1371/journal.pbio.1000207.g001

115) Shaw, J. D., Cummings, K. B., Huyer, G., Michaelis, S. & Wendland, B. (2001). Yeast as a model system for studying endocytosis. *Exp Cell Res, 271,* 1-9. doi: 10.1006/excr.2001.5373

116) Simons, K. & Ikonen, E. (1997). Functional rafts in cell membranes. *Nature, 387,* 569-572.

117) Sivaram, M. V., Furgason, M. L., Brewer, D. N. & Munson, M. (2006). The structure of the exocyst subunit Sec6p defines a conserved architecture with diverse roles. *Nat Struct Mol Biol, 13,* 555-556. doi: 10.1038/nsmb1096

118) Söllner, T., Bennett, M.K., Whiteheart, S.W., Scheller, R.H. & Rothman, J.E. (1993). A Protein Assembly-Disassembly Pathway In Vitro That May Correspond to Sequential Steps of Synaptic Vesicle Docking, Activation, and Fusion. *Cell, 75,* 409-418.

119) Stenovec, M., Kreft, M., Poberaj, I., Betz, W.J. & Zorec, R. (2004). Slow spontaneous secretion from single large dense-core vesicles monitored in neuroendocrine cells. *The FASEB Journal,* 1-18.

120) Sun, Y., Martin, A.D. & Drubin, D.G. (2006). Endocytic internalization in budding yeast requires coordinated actin nucleation and myosin motor activity. *Dev Cell, 11,* 33-46. doi: 10.1016/j.devcel.2006.05.008

121) Sutter, J. U., Campanoni, P., Blatt, M. R. & Paneque, M. (2006). Setting SNAREs in a different wood. *Traffic, 7,* 627-638. doi: 10.1111/j.1600-0854.2006.00414.x

122) Sutter, J. U., Campanoni, P., Tyrrell, M. & Blatt, M. R. (2006). Selective mobility and sensitivity to SNAREs is exhibited by the *Arabidopsis* KAT1 K+ channel at the plasma membrane. *Plant Cell, 18,* 935-954. doi: 10.1105/tpc.105.038950

123) Sutton, R.B., Fasshauser, D., Jahn, R. & Brunger, A.T. (1998). Crystal structure of a SNARE complex involved in synaptic exocytosis at 2.4A˚ resolution. *Nature, 395,* 347-353.

124) TerBush, D.R., Maurice, T., Roth, D. & Novick, P. (1996). The Exocyst is a multiprotein complex required for exocytosis in *S.c..The EMBO Journal, 15,* 6483-6494.

125) TerBush, D.R. & Novick, P. (1995). Sec6, Sec8, and Secl5 Are Components of a Multisubunit Complex Which Localizes to Small Bud Tips in S.c.. *The Journal of Cell Biology, 130,* 299-312.

126) Theander, S., Lew, D.P. & Nüße, O. (2002). Granule-specific ATP requirements for Ca^{2+}-inducedexocytosis in human neutrophils. Evidence for substantial ATP-independent release. *Journal of Cell Science, 115,* 2975-2983.

127) Thiel, G., Kreft, M. & Zorec, R. (2009). Rhythmic kinetics of single fusion and fission in a plant cell protoplast. *Ann N Y Acad Sci, 1152,* 1-6. doi: 10.1111/j.1749-6632.2008.03996.x

128) Toyooka, K., Goto, Y., Asatsuma, S., Koizumi, M., Mitsui, T. & Matsuoka, K. (2009). A mobile secretory vesicle cluster involved in mass transport from the Golgi to the plant cell exterior. *Plant Cell, 21,* 1212-1229. doi: 10.1105/tpc.108.058933

129) van Meer, G., Voelker, D. R. & Feigenson, G. W. (2008). Membrane lipids: where they are and how they behave. *Nat Rev Mol Cell Biol, 9,* 112-124. doi: 10.1038/nrm2330

130) Vardjan, N., Jorgacevski, J. & Zorec, R. (2013). Fusion pores, SNAREs, and exocytosis. *Neuroscientist, 19,* 160-174. doi: 10.1177/1073858412461691

131) Vardjan, N., Stenovec, M., Jorgacevski, J., Kreft, M., Grilc, S. & Zorec, R. (2009). The fusion pore and vesicle cargo discharge modulation. *Ann N Y Acad Sci, 1152,* 135-144. doi: 10.1111/j.1749-6632.2008.04007.x

132) Walch-Solimena, C., Collins, R.N. & Novick, P. (1997). Sec2p Mediates Nucleotide Exchange on Sec4p and Is Involved in Polarized Delivery of Post-Golgi Vesicles. *The Journal ofCell Biology, 137,* 1495-1509.

133) Weinberg, J. & Drubin, D.G. (2012). Clathrin mediated endocytosis in budding yeast. *Cell, 22,* 1-13. doi: 10.1016/j.tcb.2011.09.001

134) Weise, R., Kreft, M., Zorec, R., Homann, U. & Thiel, G. (2000). Transient and Permanent Fusion of Vesicles in *Zea mays* Coleoptile Protoplasts Measured in the Cell-attached Configuration. *J Membrane Biol, 174,* 15-20.

135) Wolfe, J. & Steponkus, P.L. (1983). Mechanical Properties of the Plasma Membrane of Isolated Plant Protoplasts. *Plant Physiol, 71,* 276-285.

136) Wu, L. G., Hamid, E., Shin, W. & Chiang, H. C. (2014). Exocytosis and endocytosis: modes, functions, and coupling mechanisms. *Annu Rev Physiol, 76,* 301-331. doi: 10.1146/annurev-physiol-021113-170305

137) Yoshida, H. (2007). ER stress and diseases. *FEBS J, 274,* 630-658. doi: 10.1111/j.1742-4658.2007.05639.x

138) Young, M.E., Karpova, T.S., Brügger B., Moschenross, D.M., Wang, G.K., Schneiter, R., Wieland, F.T. and Cooper, J.A. (2002). The Sur7p family defines novel cortical domains in *Saccharomyces cerevisiae*, affects sphingolipid metabolism, and is involved in sporulation. *Mol. Cell. Biol., 22,* 927-934. doi: 10.1128/mcb.22.3.927-934.2002

139) Zanetti, G., Pahuja, K.B., Studer, S., Shim, S. & Schekman, R. (2012). COPII and the regulation of protein sorting in mammals. *Nature Cell Biology, 14,* 20-29. doi: 10.1038/ncb2390

140) Zimmermann, R., Eyrisch, S., Ahmad, M. & Helms, V. (2011). Protein translocation across the ER membrane. *Biochim Biophys Acta, 1808,* 912-924. doi: 10.1016/j.bbamem.2010.06.015

9. List of Equations

Eq 1: relative fluorescence 19

Eq 2: standard error of the mean (SEM) 20

Eq 3: total current across a membrane 21

Eq 4: command voltage 22

Eq 5: The total current at a biological membrane 22

Eq 6: calculation for vesicle capacitance 27

Eq 7: calculation for conductance of the fusion pore 27

Eq 8: calculation of vesicle diameter 27

Eq 9: surface area of a sphere 27

Eq 10: calculation of the radius of the fusion pore 29

Eq 11: gauss function 48

Eq 12: lognormal distribution 55

10. List of Figures

Figure 1: An overview of the secretory and retrograde pathway in yeast cells. 6

Figure 2: An overview of the transport components of secretory vesicles that are carried from the TGN to the plasma membrane. 8

Figure 3: Overview of the endocytotic pathway in yeast. 11

Figure 4: A model to describe the first steps of clathrin-medited endocytosis and vesicle fission (Liu *et al*., 2009). 13

Figure 5: The equivalent circuit of a plasma membrane with a resistance (ion channel (blue)/ R_m) and a capacitance (lipid-bilayer/ C_m) compared with a plate capacitor. 15

Figure 6: Image of a protoplast expressing Tok1-Gfp, recorded with the confocal laser scanning microscope. 20

Figure 7: Overview of a Lock-In amplifier. Adapted from (http://www.physik.uni-regensburg.de/studium/praktika/a2/download/versuch5a.pdf) 22

Figure 8: (A) The reference voltage. In B the output signal represents the resulting current (blue, I_m) which can be separated in the capacitive component (black line/I_C) and the resistive component (red line/I_R) of the output signal. 23

Figure 9: The resulting signals after passing the multiplier. 24

Figure 10: An illustration of the ac signals after being low-pass filtered and converted into dc signals. 25

Figure 11: The minimal electrical circuit of whole-cell and cell-attached configuration. 26

Figure 12: The equivalent circuits of a membrane patch including the conductance of a fusion pore in the cell-attached configuration. 28

Figure 13: Example for the simultaneous change of the membrane capacitance and the membrane conductance. 29

Figure 14: Characterization of events. 31

Figure 15: Characterization of transient events. 32

Figure 16: Representative responses of membrane conductance and capacitance during calibration with the test pulse. 33

Figure 17: The capacitance trace of a transient (A) and a permanent (B) exocytotic event are represented. 34

Figure 18: A: Growth of yeast protoplasts observed during an incubation period of 96 h. 37

Figure 19: Transmission electron microscopic image of the temperature sensitive sec6-4 mutant (strain SY1). 38

Figure 20: Protoplast growth of the strain SY1 during an incubation period of 72 h. 39

Figure 21: Growth of yeast protoplasts with and without glucose. 40

Figure 22: Internalization of the fluorescent endocytosis marker FM4-64 in yeast protoplasts.....42

Figure 23: Relative Fluorescence of FM4-64 in yeast protoplasts. 43

Figure 24: Inhibition of the internalization of the fluorescent endocytosis marker FM4-64 by IKA in intact yeast cells (BY4741).....44

Figure 25: Inhibition of the internalization of the fluorescent endocytosis marker FM4-64 in yeast protoplasts by IKA.....45

Figure 26: Internalization of fluorescent beads.....46

Figure 27: Examples of capacitance recordings from protoplasts of the yeast strain BY4741 in the cell-attached recording configuration. 48

Figure 28: This represents the amplitude histogram of an *Im* current trace. 49

Figure 29: Correlation between amplitudes of the upward and the downward step of the transient membrane capacity changes. 50

Figure 30: Examples of more complex capacitance changes in yeast protoplasts.....51

Figure 31: Frequency of the different modes of endo-/exocytotic events recorded from yeast protoplasts from the yeast strain BY4741 in the presence of glucose.....53

Figure 32: Frequencies of endo-/exocytotic events recorded from yeast protoplasts in the cell–attached patch-clamp configuration. 55

Figure 33: Vesicle size distribution of endo- and exocytotic events in BY4741.....56

Figure 34: Examples for capacitance changes (ΔC_m) in the membrane with simultaneous changes in the conductivity of the membrane (ΔG_m). 58

Figure 35: Distribution of fusion pore conductance calculated from transient changes in the patch conductance (transient changes in the *Re* signal trace) from 40 exocytotic and 2 endocytotic events.....59

Figure 36: Distribution of fusion pore conductance calculated from permanent changes in the patch conductance (permanent changes in the *Re* signal trace) from 11 exocytotic and 15 endocytotic events.....60

Figure 37: Growth-assay of yeast strains BY4741 and SY1 in complex media YPD 62

Figure 38: Localization studies of the Tok1-Gfp fusion protein in the *sec6-4* mutant to visualize the trafficking of the Gfp–tagged potassium channel Tok1 from the cytoplasm to the plasma membrane. 63

Figure 39: Relative fluorescence of intact cells. 64

Figure 40: Relative fluorescence of protoplasts.....65

Figure 41: Frequencies of capacitive events in the yeast strains SY1 and BY4741.....66

Figure 42: Time course of the frequency of capacitance changes recorded at 25 °C from SY1 protoplasts. 67

Figure 43: Vesicle size distribution of endo- and exocytotic events in SY1 (37 °C).....68

11. Abbreviations

A	area
ac	alternating current
ATP	adenosine triphosphate
BAR	Bin/Amphiphysin/Rvs
BDP	BAR Domain Proteins
BSA	bovine serum albumin
°C	degree Celsius
C_0	capacitance with most events
Ca^{2+}	calcium
CaCl	calcium chloride
CIM	clathrin independent endocytosis
CLSM	confocal laser scanning microscopy
C_m	plasma membrane capacitance
CME	clathrin mediated endocytosis
COP I/II	cytoplasmatic coat protein complex I/II
cos	cosine
C_{pa}	patch capacitance
C_s	stray capacitance
C_{spec}	specific capacitance
C_v	vesicle capacitance
d	diameter
dc	direct current
EE	early endosome
e.g.	for example
EM	electron microscopy
ER	endoplasmatic reticulum

etc.	etcetera
F-actin	filamentous actin
fF	femto farad
FM4-64	N-(3-Triethylammoniumpropyl)-4-(6-(4-(Diethylamino) Phenyl)Hexatrienyl)Pyridinium Dibromide)
g	(gravitational) force of weight
G_a	access conductance
Gal	galactose
GFP	green fluorescent protein
Glc	glucose
G_m	membrane conductance
G_P	pore conductance
G_{pa}	patch conductance
h	hour
His	histidine
Hz	hertz
I_C	capacity current
IKA	ikarugamycin
Im	imaginary part of the admittance
I_m	membrane total current
I_R	resistive current
KCl	potassium chloride
KH_2PO_4	potassium hydrogen phophat
KHz	kilo hertz
KOH	potassium hydroxide
kV	kilo Volt
LE	late endosome
Leu	leucin
ln	natural logarithm

m^2	square meters
Mat	mating
MES	2-(*N*-morpholino)ethanesulfonic acid
Met	methionine
mF	mill farad
mg	milligram
$MgCl_2$	magnesium chloride
Min	minutes
mL	milliliters
mM	mill molar
ms	milliseconds
MVB	multi vesicular body
mV	millivolt
Myo2	Type V myosin motor
MΩ	mega Ohm
n	number (of)
nm	nanometers
NSF	N-ethylmaleimide-sensitive factor
OD	optical density
OsO_4	Osmium
ρ	resistivity of saline
PIP_2	Phosphatidylinositol-4,5-bisphosphat
$PI(4,5)P_2$	Phosphatidylinositol-4,5-bisphosphat
pS	pico simens
PVC	pre-vacuolar compartment
Re	real part of the admittance
r_{FP}	radius of the fusion pore

R_m	membrane resistance
rms	root mean square
rpm	rounds per minute
SD	synthetic dextrose
SD	standard deviation
Sec	Secretory
SEM	standard error of the mean
SGal	synthetic galactose
Sin	sinus
SNARE	*s*oluble *N*-ethylmaleimide-sensitive-factor *a*ttachment protein *re*ceptor
SNAP	*s*oluble *N*-ethylmaleimide-sensitive-factor attachment protein
SNR	signal-to-noise ratio
TGN	trans-Golgi network
ts	temperature sensitive
t-SNARE	target-SNARE
µL	microliters
µm	micrometers
µs	microseconds
Ura	uracil
V	volt
V_0	amplitude of the command voltage V
vs	versus
v-SNARE	vesicle-SNARE
ω	frequency
w	width
YPD	yeast extract peptone dextrose
λ	wavelength

12. Acknowledgements

An dieser Stelle möchte ich mich bei allen Personen bedanken, die mich bei dieser Arbeit begleitet haben und zum Gelingen beigetragen haben.

Vor allem bedanken möchte ich mich bei:

Herrn Professor Dr. Adam Bertl, für seine Unterstützung bei dieser Arbeit und die Freiheit zu Forschen und dem nachzugehen was mich interessiert hat. Weiterhin möchte ich mich dafür bedanken, dass ich die Möglichkeit hatte auf zahlreiche Konferenzen und Seminare zu gehen und für die Möglichkeit diese Arbeit in seiner AG zu schreiben.

Herrn Professor Dr. Gerhard Thiel, für die Übernahme des Koreferats und für seine guten Ratschläge und sein Talent einen zu motivieren.

Dr. Timo Greiner, Dr. Agata Staniek und Kerry Kukuvetz für das Korrekturlesen.

Dr. Indra Schröder für die Hilfe beim Material und Methoden Teil und für die zahlreichen Antworten auf die Zahlreichen Fragen.

Byram und Daniel für eure Hilfsbereitschaft.

AG Thiel bestehend aus Charlotte von Chappius, Christian Braun, Vera Bandmann, Bastian Roth, Fenja Siotto, Manuela Gebhard, Patrick Becker, Sebastian Fuck, Christine Gibhardt, Anne Berthold und Thomas Guthmann für die total tolle Zeit mit euch und den vielen, vielen tollen Erlebnissen

Ganz besonders bedanke ich mich hier bei Vera, Timo und Basti, für die tollen Trips die in allen Richtungen immer nur 30 min dauerten und weil ihr immer da wart, sowohl bei tollen spaßigen Zeiten, als auch bei schwierigen nicht so tollen Zeiten. Danke für eure wunderbare Freundschaft!

An Silvia Haase für die tollen und vielen Gesprächen und die kleinen Überraschungen auf meinen Schreibtisch! An Brigitte Hertel für deine Ratschläge und deine beruhigende Wirkung.

An meine Mitbewohner Kiki und Kilian für eure Unterstützung und euer Verständnis!

Meine Freundinnen Sabine und Maria für eure Unterstützung und eure Tipps und dafür, dass ihr da seid.

An meine Freunde Marcel, Dennis, Cora, Cristina, Steffi, Sarah und Florian für eure Unterstützung.

Ein ganz besonderer Dank geht an einen ganz besonderen Menschen meinen Liebsten und Freund Christian Braun, weil du mir immer zu Seite stehst, mich unterstützt und mir auch manchmal humorvoll zeigst, dass ein anderer Weg manchmal auch besser ist. Danke für deine Liebe und deine Freundschaft.

An meine Schwestern Jimena, Maricruz, Mariana und Andrea und meine Mutter dafür, dass ihr an meiner Seite seid seitdem ich denken kann und mich unterstützt.

13. Ehrenwörtliche Erklärung

Ich erkläre hiermit ehrenwörtlich, dass ich die vorliegende Arbeit entsprechend den Regeln guter wissenschaftlicher Praxis selbstständig und ohne unzulässige Hilfe Dritter angefertigt habe.

Sämtliche aus fremden Quellen direkt oder indirekt übernommenen Gedanken sowie sämtliche von Anderen direkt oder indirekt übernommenen Daten, Techniken und Materialien sind als solche kenntlich gemacht. Die Arbeit wurde bisher bei keiner anderen Hochschule zu Prüfungszwecken eingereicht.

Darmstadt, den ……

.....

14. Own Work

Chapter 4.7 „Capacity Measurements to Study Exo- and Endocytotic Events" was already published in a similar way in Carrillo et al., 2015

Chapter 5 "Material and Methods" some passages were already published in Carrillo *et al*., 2015

Chapter 6.1 "Yeast protoplasts grow" was already published in a similar form in Carrillo *et al*., 2015

Chapter 6.2 "Internalization of FM4-64" was already published in a similar form in Carrillo *et al*., 2015

Chapter 6.4.1 "Modes of exo- & endocytosis in yeast" was already published in a similar form in Carrillo *et al*., 2015

Chapter 6.4.2 "Frequencies of exo- and endocytotic events" was already published in a similar form in Carrillo *et al*., 2015

Chapter 6.4.3 "Energy requirement of exo- and endocytosis in yeast protoplasts" was already published in a similar form in Carrillo *et al*., 2015

Chapter 6.4.4 "Vesicle size distribution" was already published in a similar form in Carrillo *et al*., 2015

Chapter 6.6 "Modulation of exo- and endocytotic frequencies via the SY1 sec6-4 Mutant" was already published in a similar form in Carrillo *et al*., 2015

The grow-assay of chapter 6.6 "Modulation of exo- and endocytotic frequencies via the SY1 sec6-4 Mutant" was made in the Bachelor Thesis of Daniela Nietz 2012.

15. Curriculum Vitae

Personal Data

Dipl. Biol. Lucia Carrillo

Born the 26.12.1986 in Freiburg
Nationality: French
Landgraf-Georg-Straße 66
64283 Darmstadt, Germany

Academic Career

Since 11/ 2011	PhD thesis in the yeast membrane biology group of Professor Adam Bertl at the Technische Universität Darmstadt
03/ 2011 - 10/ 2011	Diploma thesis “Electrophysiological characterization of a novel mutation R883W in hERG C-Terminus” at the plant membrane biophysics group of Professor Gerhard Thiel at the Technische Universität Darmstadt. Grade: very good, with distinction
10/ 2006 - 10/ 2011	Field of Study: Biology with an emphasis in microbiology, plant physiology, electrophysiology and ecology at the Technischen Universität Darmstadt
08/2008 - 12/2008	Stay abroad at the University of Costa Rica

Education

08/ 2003 - 07/ 2006	Landrat-Gruber-Schule, Dieburg (Grade: Abitur 1,8)

Conferences and Publications

02/ 2015	High-resolution capacity measurements for studying endocytosis and exocytosis in yeast. (Publication in Traffic: tra 12275)
02/ 2014	Biophysical Society 58th Annual Meeting. San Francisco, USA. (Poster presentation)
08/ 2013	26th International Conference on Yeast Genetics and Molecular Biology. Frankfurt am Main, Germany. (Poster presentation)
09/ 2012	3rd International Workshop on Expression, Structure and Function of Membrane Proteins. Florence, Italy.